Aus dem Interfakultären Institut für Zellbiologie
der Universität Tübingen
Ärztlicher Direktor: Professor Dr. H.-G. Rammensee
in Zusammenarbeit mit der
Medizinischen Universitätsklinik und Poliklinik
Abteilung Innere Medizin II
Ärztlicher Direktor: Professor Dr. L. Kanz
und der
Universitätsklinik für Urologie
Ärztlicher Direktor: Professor Dr. A. Stenzl

A surface marker study to identify epithelial and mesenchymal stromal progenitor cells in human prostate

Inaugural-Dissertation
zur Erlangung des Doktorgrades
der Humanwissenschaften

der Medizinischen Fakultät
der Universität Tübingen

vorgelegt von

Neli Petkova

aus

Jambol, Bulgarien

2014

Dekan: Professor Dr. I. B. Autenrieth
1. Berichterstatter: Professor Dr. S. Stevanović
2. Berichterstatter: Professor Dr. A. Nordheim

ERKLÄRUNG

Hiermit erkläre ich, dass ich die Arbeit selbständig und nur mit den angegebenen Hilfsmitteln angefertigt habe und dass alle Stellen, die im Wortlaut oder dem Sinne nach anderen Werken entnommen sind, durch Angaben der Quellen kenntlich gemacht sind.

Tübingen, 2014

Neli Petkova

ABSTRACT

Prostate cancer is the most frequently diagnosed male cancer in the Western world and a leading cause of cancer-related death in men. In the search for novel markers for diagnosis and selective targeting of prostate cancer cells, tumor-specific surface antigens need to be identified, which discriminate between cancer and benign stem/progenitor cells. The discovery of cell surface markers in prostate cancer in prostate assists in the discrimination between benign and malignant stem/progenitor cells at different levels of differentiation. Of particular interest is the analysis of the precise phenotype of a progenitor subset, termed Transit-Amplifying Cells (TACs), as both prostate hyperplasia and prostate cancer are supposed to develop from these cells. The main goal of this study is the isolation and characterization of prostate stem/progenitor cells with particular emphasis on TACs in order to distinguish between benign and malignant cells. The results showed that prostate stem/progenitor cells could be isolated at high purity in the $CD49f^{+}Trop\text{-}2^{+}$ fraction. Moreover, TACs could be enriched in the $CD49f^{+}Trop\text{-}2^{+}CD24^{+}$ population. These findings provide a basis for future research in the field of prostate hyperplasia and cancer biology.

ZUSAMMENFASSUNG

Prostatakrebs ist die am häufigsten diagnostizierte Krebserkrankung bei Männern in der westlichen Welt und eine Hauptursache der durch Krebs verursachten Todesfälle. Auf der Suche nach neuen Markern für die Diagnose und für das Targeting von Prostata-Krebszellen müssen tumorzell-spezifische Oberflächenantigene identifiziert werden, die möglichst selektiv auf Krebszellen, jedoch nicht auf gutartigen Prostata-Stammzellen/Vorläuferzellen exprimiert sind. Für die Unterscheidung von malignen und benignen Zellen ist jedoch die Kenntnis des Expressionsmusters on gesunden Zellen Voraussetzung für ein spezifisches Tumor-Targeting. Von besonderem Interesse ist die Analyse des genauen Phänotyps einer Progenitorpopulation von Prostatazellen, die die so genannten Transit-Amplifying Cells (TACs) enthält, da angenommen wird, dass sich sowohl die Prostatahyperplasie als auch der Prostatatkrebs aus diesen Zellen entwickeln. Das Hauptziel dieser Arbeit ist daher die Isolierung und Charakterisierung von Stamm/Progenitorzellen aus Prostata mit Schwerpunkt auf die Charakterisierung von TACs, um gutartige von malignen Zellen unterscheiden zu können. Die Ergebnisse zeigen, dass Stamm/Progenitorzellen hochrein in der CD49f^{+}Trop-2^{+} Population angereichert werden können. Zusätzlich konnten TACs in der CD49f^{+}Trop-2^{+}CD24^{+} Fraktion isoliert werden. Diese Ergebnisse bilden eine Basis für zukünftige Forschungen auf dem Gebiet der Tumoren und der Hyperplasie bei der Prostata.

Satisfaction of one's curiosity is one of the greatest sources of happiness in life.

— Dr. Linus Pauling

ACKNOWLEDGMENTS

Foremost, I would like to express my sincere gratitude to my advisors, Professor Dr. A. Nordheim and Prof. Dr. Christian Schwentner, for the continuous support during my Ph.D. studies and research, for their patience, motivation, enthusiasm and immense knowledge. My special gratitude goes to Professor Dr. S. Stevanović for his ideas and supervision.

I am also grateful to Jörg Hennenlotter, Prof. Stenzl, Jülian Heinkele and Ursula Kuehs from the department of Urology for all the great support and ideas, provided tissue samples and clinical data during the studies of the human prostate.

My sincere thanks go to my laboratory colleagues: Dr. Malgorzata Sobiesiak, Flavianna Cerabona, Susanne Schumann, Sabrina Grimm, Daniela Lehnen, Kavitha Sivasubramanyan and Abhishek Harichandan for their great support and help during my time in the Laboratory for Stem Cell Research.

I would like to thank Ivan Kalev and Pavel Nikolov who helped me with the proofreading, as well as my family and friends for their great support.

CONTENTS

LIST OF FIGURES

LIST OF TABLES

LISTINGS

ACRONYMS

BPH	Benign prostate hyperplasia
CaP	Prostate cancer
TA	Transit-amplifying cells
EMT	Epithelial-mesenchymal transition
AR	Androgen receptor
PCR	Polymerase chain reaction
CSC	Cancer stem cell
ECM	Extracellular matrix
CAM	Cell adhesion molecule
CFU	Colony forming unit
MCS	Mesenchymal stem cell

1

INTRODUCTION

Prostate cancer (CaP) is one of the most prevalent neoplastic diseases among men and a leading cause of cancer-related death next to lung cancer. After surgical removal of the prostate or androgen deprivation therapy, the tumor often turns into a hormone-independent neoplasia and metastasizes to local or distant lymph nodes and bone tissues.

Existing theories propose that the cause of androgen independence of CaP is a rare subpopulation of stem-like cells, capable of cancerous growth. However, it has been established that normal prostate epithelial stem cells exhibit similar androgen independence. Identifying the cancerous subset of cells — and most importantly, distinguishing them from the normal cells — is therefore a major goal in cancer biology.

The ability to discriminate between normal and cancer stem cells of the prostate has been a major challenge in recent years. The subset of stem-like cells in normal or benign tissues is characterized by expression of identical surface molecules with a matching expression pattern in comparison to malignant tissues. One goal of these experiments is therefore to distinguish normal prostate epithelial and mesenchymal stem cells and to provide a definition of prostate cancer stem cells in terms of surface marker expression. In this study, we aim at establishing the best isolation procedure for normal prostate stem and progenitor cell subsets and verify their stem and progenitor cell features by colony-forming assays, western blot, flow cytometry and RT-PCR analysis.

2 BACKGROUND

2.1 ANATOMY OF THE HUMAN PROSTATE

The human prostate is an exocrine gland, located in the pelvis and surrounding the urethra beneath the bladder (Figure 2.1). Its function is to secrete and store slightly alkaline seminal fluid, which constitutes around 30% of semen. The seminal fluid is generally composed of simple sugars and two proteolytic enzymes — prostate-specific antigen (PSA) and prostatic acid phosphatase (PAP) — both of which are secreted by this gland. According to the McNeal model [79], the human prostate is anatomically divided into peripheral, central and transitional zones. Benign prostate hyperplasias usually originate in the transitional zone, whereas cancer typically develops in the peripheral zone [103]. The gland opens into elongated channels which are gathered out from 12 to 20 small excretory ducts.

Histologically, the prostate exhibits tubuloalveolar gland architecture composed of pseudo-stratified epithelium. The prostate epithelium is embedded in a connective tissue matrix and organized in ducts that branch out from the urethra and end in the secretory acini. The epithelium forms a bilayer, consisting of a basal layer of undifferentiated cells close to the basal lamina and a luminal layer of terminally differentiated, column-shaped secretory cells, which are facing the lumen. Three epithelial cell types can be distinguished: proliferative basal, secretory luminal (both residing in the aforementioned layers) and a small subset of rare neuroendocrine (NE) cells, scattered throughout the basal membrane.

The basal cells are immature, highly proliferative cells that express high molecular weight cytokeratins (CK) 5 and 14, bcl-2, CD44, Ki67, p63, PCNA, MIT 1 at high levels and CK18 at very low levels. These cells are androgen independent.

The luminal cells exhibit a strong expression of low molecular weight CK8 and CK18, as well as PSA (prostate specific antigen), AR (androgen receptor) and PAP (prostatic acidic phosphatase). The keratin expression patterns change upon differentiation and location. The luminal cells are androgen-responsive and they require androgens for their growth and survival [63].

The neuroendocrine (NE) cells are characterized by expression of chromogranin A, synaptophysin and NSE (neuro-specific enolase). In addition, they produce various neuropeptides as serotonin, bombesin, neurotensin and parathyroid hormone-related proteins [99]. The proteins secreted by NE cells support epithelial growth and viability.

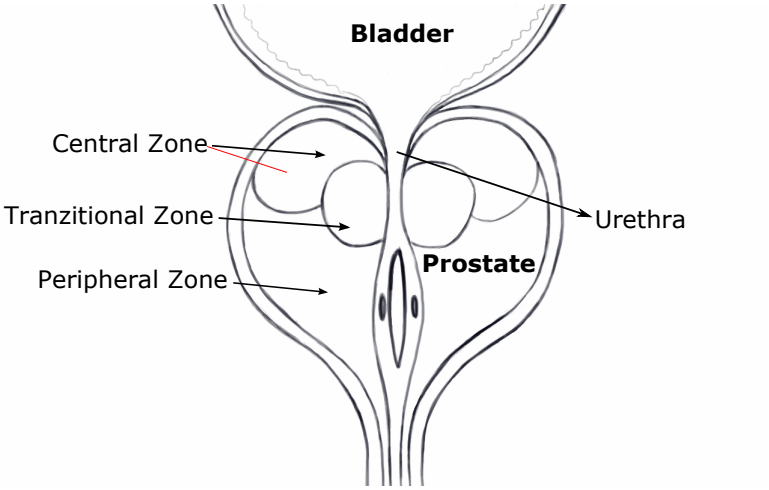

Figure 2.1: Anatomy of the prostate gland.

They are terminally differentiated, but androgen-insensitive and distributed throughout the basal epithelium, often transversing to luminal layer.

2.2 EVIDENCE FOR PROSTATE STEM CELLS AND MARKERS

Evidence for the existence of a stem cell population within the human prostate has been presented in the 1980s [24, 25]. Experiments with murine prostate tissues demonstrate the presence of a small number of androgen-independent cells, able to reconstitute the whole functional prostate gland. Later experiments showed that both basal and luminal cells have a common origin [45].

The putative prostate stem cell niche is found in the proximal region (the region closest to the urethra) [124]. BrdU pulse-chase experiments in mice showed that long term label-retaining cells are localized proximally to the urethra and revealed the first evidence of tissue-specific stem cell localization. This region is known to consist of morphologically distinct stromal cells, which are able to secrete high levels of TGF-β — a soluble factor, which promotes stem cell quiescence [96].

Within the prostate epithelium, stem cells were found to be localized in the basal layer [25]. These experiments showed that only cells from the basal layer preferentially survive androgen ablation. Additionally, p63-null mice are born without prostate or mammary glands [62, 103, 104, 65, 25].

When placed in appropriate culturing conditions, prostate epithelial stem/progenitor cells are able to form different colony types. Hudson et al. proposed two types of 2D colonies — large dense (type I) colonies and small/intermediate loose (type II) colonies [44]. Guzmán-Ramírez et al. distinguished 3 types of colonies — holoclones (type I, i.a. Hudson), paraclones (type II, i.a. Hudson), and

mesoclones — (intermediate type) [37]. Colonies were grown under 2D (low attachment) and under 3D conditions (Matrigel or Costar low-attachment plate). The anchorage-independent (3D) growth kept the cells to maintain their stem cell potential [37, 31, 102]. Recently, 3-dimensional growth of epithelial colonies co-cultured with stromal cells was reported [136].

Basal layer epithelial stem cells express specific stem/progenitor cell markers such as Ki67, p63 and bcl-2. p63 encodes two main isoforms, transcribed using alternative promoters (TAp63 and ΔNp63). ΔNp63 has multiple functions during skin development and in adult stem/progenitor cell regulation. It is predominantly expressed in the basal prostate cells when cultured. The prostate basal cells, but not the secretory or neuroendocrine cells, express p63 [103, 104, 62]. P63 dimers and tetramers are described in dependence to their activity and function. The p63 dimers exist in two forms: inactive (dephosphorylated) and active (phosphorylated) [21].

Bcl-2 is an anti-apoptotic protein, which is expressed in cells with long lifespan [1].

CD44 is a single-pass trans-membrane glycoprotein involved in cell-cell and cell-matrix adhesion and in cell signalling. It is present in the basal compartment of the prostate epithelium [36, 50]. Its CD44s splice isoform is present in benign epithelium, while cancer cells overexpress the novel splice variant (v) isoform, CD44v7-10 [47]. There is a great body of evidence regarding the role of CD44 in different human cancers and normal tissues. CD44 correlates with stem cell development and tumor formation in breast cancer [81, 70, 43, 2], pancreatic cancer [140], colorectal [23], gastric [38], head and neck [58], ovarian [101] cancer. In mouse, a single $CD44^+$ cell is sufficient to generate a complete prostate *in vivo* [68]. There are contradictory evidences about CD44 as a stem cell marker in human prostate. Some data show correlation between $CD44^+$ cells and stemness and tumorigenicity in prostate cancer cell lines and tumor xenografts [46, 88, 86]. Moreover, in human prostate cancer and prostate cancer cell lines, CD44 is associated with cells of neuroendocrine phenotype [117]. However, there is an evidence that CD44-negative cells are cells with clonogenic capacities in human prostate [134].

CD164 is a 80–90 kD sialomucin molecule, highly glycosylated by both O- and N-linked glycans. The transmembrane forms of CD164 are considered to mediate adhesion and are believed to regulate hematopoiesis by facilitating the adhesion of human $CD34^+$ cells to the bone marrow stroma [132, 131]. There is an evidence that CD164 participates in the localization of prostate cancer cells to the bone marrow [41]. It is known that mucin expression also influences tumor progression and metastasis [78]. As most prostate cancer metastases are located in the bone, the role of this molecule is of interest for

further investigation. CD164 is reported to be expressed by luminal cells and subsequently in prostate cancer of luminal origin [73].

Several candidate markers have been reported to isolate stem/progenitor cells in the human prostate — integrin alpha2/beta1 [16, 87], CD133 [94], CD44 [15, 46, 85], CD49f [34, 134], Trop-2 [34], CD44 and Ep-CAM [36]. Using immunohistochemical profiling, many authors have reported the existence of an intermediate phenotype between basal and secretory epithelial cells [12, 129]. In a recent study by Goldstein et al., two fractions of basal cells were identified using the cell surface marker Trop-2 (Trop-2^{hi} and Trop-2^{low}). They could demonstrate that only Trop-2^{hi} cells co-expressing CD49f were able to give rise to high-grade spheres (3-D colonies) [34]. CD49f (integrin α6 subunit) is an adhesion molecule involved in cell-matrix interaction and together with CD29 functions as a subunit for laminin receptor. In murine and human prostate Trop-2 is expressed only by the basal cells of the epithelial compartment [36, 66]. Trop-2, also called tumor-associated calcium signal transducer 2 (TACSTD2), is a single-pass type I trans-membrane protein of the Ep-CAM family. However, its ligand has not yet been identified. Trop-2 is involved in the regulation of the cell-cell adhesion and is supposed to have similar functions as Ep-CAM (Trop-1), another molecule from the same family. Trop-2 is associated with stem cells in human and mouse prostate [34, 31] as well as in mouse liver (hepatic oval cells) [83]. It is highly expressed in many tumors including colorectal cancer [56, 133], oral squamous-cell carcinoma [28] and pancreatic cancer [27].

An additional molecule investigated in prostate biology is CD24. CD24 was firstly discovered in 1978, when Springer et al. raised rat anti-mouse antibodies against leucocytes (M1/69 and M1/75) and later discovered their target molecule. It was named heat-stable antigen, due to its heat resistance [113]. This a cell surface molecule, which contains a mucin-type glycosylphosphatidylinositol (GPI)-anchored region [114]. It is a subject of heavy glycosylation — a process, which is highly variable in different tissues and cell types and leads to varied molecular weight of CD24 in the range of 20 to 70 kDa [26, 54]. The mature protein is only 27 to 30 amino acids long, nearly half of which are serine and threonine residues. They are potential sites for N- and O-linked glycosylation [4].

CD24 is found to be expressed on various cell types and to conduct many functions [26]. The molecule was initially revealed to be a marker for B-cells. Later it was found to be expressed in neutrophils and B-cell precursors but not in T-cells or monocytes. On the neutrophil surface, CD24 acts as an adhesion molecule by binding to P-selectin and facilitating the rolling on endothelial cells during the process of inflammation (as a primary immune response to inflammation).

Later, CD24 was found to be expressed in neuronal tissue and in certain types of epithelial cells, for example keratinocytes, renal, prostate and breast epithelium [8, 97, 59]. More recently, CD24 was described as a marker for luminal epithelial cells of the human prostate [107, 35, 72], as well as a marker of the basal layer of the murine counterpart [66]. Thus, murine colony forming cells are 6-fold enriched in the $CD24^{+}CD49f^{+}$ population [66]. CD24 is also expressed by both basal and luminal epithelial cells of mouse and human mammary glands [107]. In prostate cancer cells lines CD24 was reported to be a negative marker for cancer stem cells, whereas it is a marker for cancer stem cells in ovarian cancer [30], colorectal cancer [138], liver cancer [67], and pancreatic cancer [69]. We show that $CD49f^{+}Trop\text{-}2^{+}CD24^{+}$ cells in human BPH and cancer have colony forming and proliferative potential, which raises the question about the function and ontogeny of these cells within human prostate epithelium. The role of CD24 in benign diseases has not been identified. In prostate and breast cancer $CD44^{+}CD24^{-}$ subset shows phenotype closer to stem cells. Nevertheless, $CD24^{+}$ cells are associated with poor prognosis in cancer for prostate [61], breast [2, 81], and other epithelial malignancies [60]. Moreover, recent studies identified $CD24^{+}$ tumor-initiating cells in cancer [30], colorectal cancer [138], liver cancer [67] and pancreatic cancer [69].

CD24 mediates signal transduction by recruiting Src-family protein tyrosine kinases (PTK) — c-fgr, lyn and lck, and activates the mitogen-activated protein (MAP) kinase, recruiting membrane rafts [26]. CD24 is shown to increase the motility and to alter adhesion of several cells; some of the processes are connected with rearrangement of integrins [9, 125, 8].

2.3 CELL ADHESION MOLECULES

The cell adhesion molecules, known as CAMs, are divided into four major categories: cadherins, integrins, selectins and members of the immunoglobulin superfamily. The adhesion molecules mediate the process of cell adhesion through cell-matrix or cell-cell interactions. Several integrins and cadherins are reported to be expressed in human epithelium.

2.3.1 *Cell-matrix AM (Integrins)*

The integrins are a family of transmembrane glycoprotein receptors that mediate cell-matrix interactions. In humans, 18α and 8β subunits are present [33]. Each β subunit binds to one of several α subunits to form a heterodimeric receptor, which is able to detect proteins in the extracellular matrix. Virtually every cell expresses integrins. Epithelial cells in adult tissues are generally stationary cells; neverthe-

less they do express several integrins. Integrins function as signaling molecules as they detect attachment, detachment, and changes in the local compositions of ligands. Signals initiated by integrins can modulate epithelial proliferation, differentiation, survival and gene expression.

2.3.2 *Cell-Cell AM (Cadherins)*

The classical cadherins are transmembrane adhesion glycoproteins, which provide homotypic interactions between cells and are used to maintain cell-cell adhesion or mediate cell migration [118]. These are calcium-dependent molecules, which intracellularly link to the actin cytoskeleton with the participation of several molecules (catenins, p120).

EMT is characterized by reduced E-cadherin and increased N-cadherin expression and these changes in the adhesion properties increase the cell motility and invasion capabilities of the cells. Such expression profile is reported for some tumors and proposed in prostate cancer. Prostate carcinoma EMT is not well-defined in terms of molecular profiling and expression pattern in the cells. P-cadherin (Plancental cadherin) is expressed mostly on basal and proliferating layers of epithelia and its expression decreases during cellular differentiation. In breast carcinoma, an increased expression is observed and one is related to a worse prognosis [91]. In benign prostate, P-cadherin is reported as novel basal cell marker [49], having variability of expression patterns in different CaP [110].

2.3.3 *Stage-specific embryonic antigens*

Stage-specific embryonic antigens (SSEA) SSEA-3 and SSEA-4 are epitopes on related glycosphingolipids, which are termed GL-5 and GL-7 respectively [51]. Glycosphingolipids consist of a carbohydrate moiety or chain linked to ceramide. SSEA-3 and SSEA-4 have been described as markers for pluripotency and they are expressed on putative embryonic stem cells [42]. Recently, however, SSEAs have been described on variety of tissues on different levels of differentiation. In human ovaries, small SSEA-4 positive epithelial stem cells have been identified. SSEA-4 is used to isolate mesenchymal stem cells [29] and dental pulp stem cells [53] in human, as well as to enrich neuronal progenitors [7]. It is also expressed on epithelial cells of human cornea, where it is a negative marker for enrichment for stem/progenitor cells [123].

2.3.4 *SUSD2 (W5C5)*

SUSD2 stands for Sushi domain containing 2. Its gene is located in chromosome 22 and encodes an 822-amino acid protein containing a transmembrane domain and domains with a function close to cell-to-cell and cell-to-matrix adhesion: somatomedin B, AMOP, von Willebrand factor type D and Sushi domains. Its function is not well known. SUSD2 has been recently identified as a novel and specific marker for prospective isolation of bone marrow-derived mesenchymal stem/stromal cells.[105].

2.4 MODELS OF PROSTATE EPITHELIUM DIFFERENTIATION

Prostate epithelial stem cells are able to differentiate into luminal (secretory) cells. According to an existing theory, the differentiation process links the basal and the luminal cells in a hierarchical manner, which is confirmed by the identification of immunophenotipically intermediate cell types. The process passes through several stages of differentiation to these intermediate cell types, which reside in the basal or the luminal layer and express markers typical for both layers. Immunohistological analyses of human prostate tissue have identified two intermediate phenotypes based upon cytokeratin expression patterns that are thought to represent cells of intermediate differentiation stages between basal and luminal cells and possibly resemble progenitor or transit populations [74]. These rare cells co-express CK5, CK14, and CK18. Some intermediate cells express CK19 and/or PSCA [122].

Different models for the development of intermediate cells and their localization exist. Tokar et al. propose a model to distinguish cells of the basal compartment (PS/P cells and mature basal cells) and the luminal compartment (luminal cells and intermediate cells) [120]. In this model, the more mature basal cells play a crucial role in maintaining the integrity of the prostate and the luminal cell differentiation [11, 62]. Isaacs propose a model of differentiation, in which putative stem cells divide and differentiate into transit-amplifying (TA) progenitor cells that give rise to intermediate cells of the luminal compartment. These cells possess both basal and luminal characteristics [48]. According to this view, the luminal intermediate cells are the direct progenitors of terminally differentiated secretory luminal cells. Therefore, intermediate cells are supposed to reside in both compartments, in dependence to their differentiation level. The differentiation from the basal to the luminal compartment is associated with the loss of basal markers and the acquisition of luminal markers.

Lawson et al. build upon this hypothesis, proposing an additional hierarchical differentiation of prostate epithelial cells including different intermediate progenitors [66]. The classical linear hierarchical

model, described in the work of Isaacs and Litvinov, is supported by the evidence that the intermediate cells express both basal and luminal markers [71, 48]. Prostate stem cells, which reside in the basal layer, divide and give rise to transit-amplifying (TA) cells, which express basal markers and start acquiring luminal markers during their maturation. These cells, depending on their level of maturation, may reside in both layers, possess transient self-renewal capacity and produce terminally differentiated secretory luminal cells. In the bifurcated hierarchical model, proposed by Lawson, basal and luminal cells represent separate epithelial cell lineages. These are supported by the TA cells or the lineage-restricted basal and luminal cell progenitors. Subsequently, the layer-dependant progenitors differentiate into basal or luminal terminally mature cells, respectively.

2.5 BENIGN PROSTATE HYPERPLASIA

The characterization of prostate epithelial stem/progenitor cells of benign prostate hyperplasia (BPH) may provide clues about the etiology and pathophysiology of prostate cancer. Epithelial stem cells are thought to be involved in the etiology of both BPH and prostate cancer. BPH is one of the most frequent concomitant anomalies in elderly men suffering from prostate cancer and is characterized by a progressive hyperplasia of glandular and stromal tissues mainly in the transitional zone. As the stromal compartment is reported to be about two-fold enlarged compared to the epithelial tissue, it is commonly regarded as a proliferative stromal disease. Recently, it has been proposed that BPH stroma is directly influenced by the epithelium via epithelial-mesenchymal transition (EMT) of the basal cells, which lose their attachment within the epithelial basal layer and their epithelial phenotype and acquire a mesenchymal phenotype [5].

Inflammation of the prostate is very common in BPH patients and inflammatory cell infiltrates are confirmed in pathologies in many patients. Inflammatory infiltrate such as macrophages and lymphocytes are known to produce growth factors (bFGF, cytokines IL-1 and IL-6) and pro-inflammatory cytokines in BPH. COX-2, an enzyme, which converts arachidonic acid to prostaglandins, plays a role in BPH and has an increased role in the development of the disease. [57]. Moreover, the prostaglandins, which are products of this reaction, play various roles in mediating and moderating inflammation and are associated with the progression of BPH [57].

There are many assumptions concerning the aetiology of BPH: alteration of stem cell homeostasis [48], embryological reawakening [55], interaction between epithelium and stroma, inducing cell growth and prostate-specific differentiation [6], changes of the hormonal levels of androgens and estrogens [40] and inflammation [82].

2.6 PROSTATE CANCER (CAP) AND CANCER METASTASES

Prostate cancer (CaP) is the most commonly diagnosed cancer among men. CaP is a malignant tumor of epithelial origin (carcinoma), considered to be a heterogenous disease. The most common treatment of prostate cancer is hormonal therapy, which includes androgen ablation and/or employing androgen antagonists for inhibition of the androgen action [128]. It is very common that after such treatments the cancer enters a hormone-refractory (androgen-independent) stage. This evidence prompts the hypothesis that androgen-independent cancer stem cells may have a key role in the recurrence of prostate cancer.

It is known that around 30% of the human prostate cancers show neuroendocrine differentiation [39]. However, the role of neuroendocrine cells in cancer development remains unclear to date. These cells secrete neuropeptides that may contribute to hormone-refractory prostate cancer and metastasis through paracrine mechanism.

Prostate cancer (CaP) metastasizes preferentially into the skeleton, causing severe clinical problems: hypercalcemia, bone fractures, and pain. The metastasizing process goes through a number of steps, which include detachment of cancer cells from the primary tumor, migration, adhesion and invasion of cancer cells into the blood or lymphatic vessels, extravasations out of the vessel and interactions with the target tissue. In osseous tissues, the cancer cells interact mainly with bone-resorbing osteoclasts, feeding them with various stimulatory growth factors, such as parathyroid hormone-related peptide, which leads to disruption of the bone tissue and release of stroma-bound growth factors. One such factor is transforming growth factor-β, which in turn stimulates the growth of cancer cells.

Up to 70% of the patients with breast cancer or prostate cancer, and 15 to 30% of all patients with lung, colon, bladder or kidney cancer develop osseous metastasis. Once the tumors progress to the bone, they are incurable [95]. Osseous (bone) metastasis causes severe bone pain and can result in fractures without any injury, as well as other life-threatening conditions [137]. There are two major types of osseous metastasis, one in which bone destruction is the predominant feature, and another in which new bone formation is predominant.

2.6.1 *Role of adhesion molecules in prostate cancer invasion and metastasis*

Metastasis requires the interaction of malignant cells with three distinct microenvironments: (i) the primary organ, (ii) the circulation, and (iii) the target organ where metastatic lesions will develop. Both soluble and insoluble stromal elements are involved in the metastatic cascade [17].

The extracellular matrix (ECM) is a complex network of proteins surrounding cells, serving as a structural foundation in tissues. The interaction of cells with the extracellular matrix is essential for the organization and maintenance of the tissue architecture and function. The ECM provides the cells with information about the environment and in this way influences cell and tissue development. Epithelial tissues are surrounded by basal lamina (BL), which is a highly structured form of ECM. The basal lamina is responsible for the compartmentalization of the tissue and acts as a barrier stopping cell migration and invasion. It is built mainly from collagens, elastins, proteoglycans; as well as proteins which serve as attachment sites for the epithelial cells: fibronectin, laminin, vitronectin and entactin.

The ECM of the bone consists of many non-collagenous molecules such as bone sialoprotein (BSP), osteopontin (OPN), osteonectin, osteocalcin, vitronectin and thrombospondin [32]. The basal membrane of most epithelial tissues is composed of laminin and collagen type IV (col IV), as well as other collagen subtypes. The prostate epithelial extracellular matrix is known to consist of collagen I and laminin [115, 126].

Epithelial-mesenchymal transition (EMT) is a process, in which epithelial cells lose their epithelial phenotype and acquire mesenchymal characteristics. These changes involve the loss of E-cadherin-mediated cell-cell adhesion, as well as the cell-to-matrix adhesion. The cells lose their apical-basal polarity and acquire a motile behaviour with concomitant reorganization of the cytoskeleton. EMT plays role in the development and the formation of the body and in the differentiation of multiple tissues and organs. EMT also contributes to tissue repair. Via still unknown mechanisms, EMT can adversely cause tissue fibrosis or cancerous processes. Therefore, it is of interest for cancer research and therapy to gain insight into this process. According to the stem cell hypothesis, it is believed that stem/progenitor cells are involved in this process. Therefore, deciphering the role of stem/progenitor cells would provide key insights to understanding the pathophysiology of this process.

Down-regulation of E-cadherin is considered as a hallmark in the course of EMT. The concomitant increase of vimentin expression is considered as a reliable marker combination to determine the fate of EMT. Different E-cadherin repressors are involved directly or indirectly in the process: Snail, Zeb, E47, KLF8 (which repress the activity of the E-cadherin promoter [90, 130]) and Twist, Goosecoid, E2.2, FoxC2 (repressing it indirectly) [135, 109]. The loss of apico-basal polarity is another crucial step in EMT. In epithelial cells, three protein complexes participate in the establishment and maintenance of polarity: Par, Crubms and Scribble and their expression is regulated by EMT inducers [80]. Zeb1 directly represses the transcription of cell po-

larity genes, like Crumbs3 and Pals1-associated tight junction protein (PATJ) [3, 112].

There is a growing body of evidence that EMT is an important step in the pathological processes of benign prostate hyperplasia (BPH) and prostate cancer formation [5, 98]. The molecules involved are cell surface marker N-cadherin and intracellular markers such as PDGF-D, NF-kB, Notch-1 and ZEB1. In prostate cancer, the expression of these molecules is upregulated during EMT. There is an increasing evidence that androgen deprivation (currently employed in cancer therapy) causes EMT in prostate cancer [116], supporting the hypothesis that stem/progenitor cells (which are androgen responsive) are involved in the process. An important question in this regard is to investigate at which level of progenitor differentiation the disease is initiated and whether suitable markers exist to monitor malignant transformation.

2.6.2 *Adhesion molecule changes in cancer*

The $\alpha 6\beta 4$ protein (CD49f/CD104) is an integrin, whose extracellular ligand is laminin [100]. This molecule facilitates the linkage between the cytoskeleton and the extracellular collagen VII network and is important for maintaining the tissue architecture. It is essential for the assembly of hemidesmosomes — multiprotein complexes formed in basal epithelial cells, located close to the basal lamina and functioning as anchors between the intracellular cytokeratin network and the extracellular matrix. The expression of $\alpha 6\beta 4$ integrins can be affected positively or negatively during epithelial tumor progression. The loss of this integrin is considered to correlate with loss of hemidesmosomes by the basal cells, which enables tumor migration and metastasis. Moreover, loss of the $\alpha 6\beta 4$ integrin is associated with invasive prostate carcinoma [19]. Furthermore, alterations of $\alpha 6\beta 4$ integrins are evident in early, precancerous PIN lesions. However, the $\alpha 6$ (CD49f) subunit is upregulated in prostate cancer.

2.7 EVIDENCE FOR CANCER STEM CELLS

The cancer stem cells hypothesis says that heterogeneous tumors contain a small subset of stem-like cells of cancer origin, which have the capacity to retain cancer growth and to allow the cancer to survive any chemotherapy treatments. These cells are called CSCs (cancer stem cells), because they possess properties of the normal stem cells, as self-renewal and differentiation. Stem cells in tumors were firstly identified in acute myeloid leukemia and described as expressing the phenotype $CD34^+$ $CD38^-$ [13]. CSCs have been subsequently discovered in tumors of different origin, such as breast, prostate, pancreas or melanoma.

Epithelial stem cells are of interest due to their capacity to restore a certain organ and for their potential role in cancer initiation. Epithelial cancer stem cells are pointed out as target populations in sarcomas. Normal prostate epithelial stem cells share the property of androgen independence with the cancer stem cells, which in turn are capable of developing the lethal phase of CaP, termed *hormone refractory CaP*. The identification of this subset of cells, and most importantly — distinguishing these cells from the normal ones, is a concern of primary importance in cancer biology.

2.8 STROMAL CELLS

The stromal layer of the prostate gland consists of fibroblasts and smooth muscle cells, mixed with intermediate myofibroblasts. All stromal cells express vimentin, smooth muscle cells and myofibroblasts also express α-smooth muscle actin (α-SMA). Smooth muscle myosin and desmin are expressed only by smooth muscle cells. Most of the stromal cell nuclei *in vivo* are positive for androgen, suggesting that the stromal layer is androgen-dependent.

Prostate stromal progenitor cells are able to differentiate into fibroblasts and smooth muscle cells. Transforming growth factor-β (TGF-β) promotes the differentiation into smooth muscle cells, which is associated with the elevated expression of α-SMA and desmin [106]. In absence of TGF-β, the cells express mainly vimentin and fibronectin, which corresponds to a fibroblastoid phenotype. Vimentin belongs to the intermediate filament family. It is highly expressed in mesenchymal cells and has been used as a specific mesenchymal marker. The differentiation of cultured prostatic stromal cells is modulated by adrenergic receptor antagonists [108, 10], estradiol, dexamethasone and androgen [139]. During human fetal development we have previously shown that the prostate undergoes changes mimicking both cancer as well as benign prostatic hyperplasia. Starting from the second trimester there is distinct growth of the fetal prostate exhibiting an identical histology as seen in the elderly [75]. The same is true for prostate cancer. 5-α reductase 1 and 2 are key enzymes in prostate cancer development and both are over-expressed during fetal development similar to prostatic neoplasia [76].

3

METHODS

3.1 MATERIALS

3.1.1 *Laboratory instruments*

List of equipment used:

1. BD FACS Aria^{TM} Ilu sorter (Becton Dickinson, Heidelberg, Germany)
2. BD FACS Canto flow cytometry analyser (Becton Dickinson, Heidelberg, Germany)
3. Bio-Rad SmartSpec^{TM} 3000
4. PerkinElmer Gene Amp. PCR System 2400
5. Roche PCR Light Cycler (Roche, Basel, Switzerland)
6. Microscope Zeiss Axiovert 40C
7. Microscope Zeiss equipped with Sony 3CCD-Iris camera
8. Centrifuge

3.1.2 *Software*

1. FlowJo software (Tree Star Inc., OR, USA)
2. BD FACSDiva v6.1.3 software (Becton Dickinson, Heidelberg, Germany)
3. FCS Express 4
4. IrfanView
5. Adobe Photoshop CS2

3.1.3 *Laboratory Chemicals*

1. Methanol (VWR International, Radnor, Pennsylvania)
2. Ethanol (Merck, Darmstadt, Germany)
3. Roti-Histol (Roth, Cat No 6640.4)

4. Phosphate Buffered Saline (LONZA, Basel, Switzerland, Cat No BE17-516F)
5. Ammonium Chloride (STEMCELL Technologies, Vancouver, British Columbia, Canada, Cat No 07850)
6. Tris-Glycine buffer (10X) BioChemica (Applichem, Gatersleben, Germany, Cat No A1418)
7. Nonfat dried milk powder (Applichem, Gatersleben, Germany, Cat No A0830)
8. SDS Solution, 10% (Promega, , Manheim, Germany, Cat No V6553)
9. Tween-20 ((Sigma-Aldrich, St. Louis, MO, USA, Cat No A1379)
10. Pedrogen 30% H_20_2 ((Sigma-Aldrich, St. Louis, MO, USA, Cat No 31642)
11. Formaldehyde 37% (ROTH, Cat No CP10.1)
12. Precision Plus Protein Dual Standards, (Bio-Rad Laboratories, Hercules, California, USA, Cat N 161–0374)
13. SIGMA FAST BCIP/NBT (Sigma-Aldrich, St. Louis, MO, USA, Cat N B5655)
14. DAPI (Sigma-Aldrich, St. Louis, MO, USA,)
15. FDA (Fluorescein diacetate) (Invitrogen, Darmstadt, Germany, Cat No F1303)
16. Anexin-V-FLUOS (Roche Diagnostics, Mannheim, Germany, Cat No 11 828 681 001)
17. Target Retrieval Solution (Dako, Glostrup, Denmark, Cat No S1699)
18. Fluorescent Mounting Medium (Dako, Glostrup, Denmark, Cat No S3023)
19. Protease inhibitor cocktail tablets, EDTA-free (Roche Diagnostics, Mannheim, Germany, Cat No 11 873 580 001)
20. Bio-Rad Dc Protein Assay Kit, (Bio-Rad Laboratories, Hercules, CA, USA, Cat No 500-0113)
21. Mini-PROTEAN TGX^{TM} (Bio-Rad Laboratories, Hercules, CA, USA, Cat No 456-1024)
22. 5-Bromo-2'-deoxyuridine (Applichem, Darmstadt, Germany, Cat No A2139)

23. Rhodanile Blue ((Sigma-Aldrich, St. Louis, MO, USA, Cat No 121495)
24. VECTASTAIN ABC Kit Elite (Vector laboratories, Burlingame, CA, USA, Cat No PK-6200)
25. Avidin/Biotin Blocking Kit(Vector laboratories, Burlingame, CA, USA, Cat No SP-2001)
26. Peroxidase Substrate Kit (Vector laboratories, Burlingame, CA, USA, Cat No SK-4100)
27.

3.1.4 *Antibodies*

3.1.4.1 *Antibodies for FACS*

See Table 3.1 and Table 3.2.

3.1.4.2 *Antibodies for immunohistochemistry*

See Table 3.1.

3.1.4.3 *Antibodies for western blot*

See Table 3.4.

3.1.4.4 *Secondary antibodies used in immunohistochemistry and flow cytometry*

See Table 3.5.

3.1.5 *Materials for methods is molecular biology*

3.1.5.1 *Primers*

See Table 3.6.

3.1.5.2 *Reagents*

1. Nuclease-Free Water, 1000 ml (Qiagen, Hilden, Germany, Cat No 129115)
2. RT-PCR Grade water (Life Technologies, Carlsbad, CA, USA, Cat No AM9935)
3. RNaseZap Rnase Decontamination Solution (Applied Biosystems, Darmstadt, Germany, Cat No 9892G)
4. Deoxyribonuclease I, Amplification Grade (Invitrogen, Darmstadt, Germany, Cat No 18068-015)

Target	Fluorochr.	Company	Host	IG class	Clone
CD10	PE	BD Pharmingen	mouse	IgG_1, κ	HI10a
CD13	PE	BD	mouse	IgG_1, κ	L138
CD15	FITC	BD	mouse	IgM, κ	MMA
CD24	PE, APC	Miltenyi Biotec	mouse	IgG_1	32D12
CD26	PE	BD	mouse	IgG_{2a}, κ	L272
CD29	PE	BioLegend	mouse	IgG_1, κ	TS2/16
CD31	PE	BD	mouse	IgG_1, κ	L133.1
CD41	FITC	BioLegend	mouse	IgG_1, κ	HIP8
CD44	FITC	BD	mouse	IgG_1, κ	L178
CD44	FITC, APC	e-Bioscience	rat	IgG_{2b}, κ	IM7
CD49a	PE	BD Pharmingen	mouse	IgG_1, κ	SR84
CD49b	FITC	BD Pharmingen	mouse	IgG_1, κ	AK-7
CD49f	FITC	BD Pharmingen	rat	IgG_{2a}, κ	GoH3
CD51	PE	BioLegend	mouse	IgG_{2a}, κ	NKI-M9
CD61	PE	BioLegend	mouse	IgG_1, κ	VI-PL2
CD90	FITC	Miltenyi Biotec	mouse	IgG_1	DG3
CD90	APC	BD Pharmingen	mouse	IgG_1, κ	5E10
CD104	FITC	BioLegend	mouse	IgG_{2a}, κ	58XB4
CD105	PE	e-Bioscience	mouse	IgG_1	SN6
CD117	PE	N/A	mouse	IgG_1	104D2
CD133	PE	Miltenyi Biotec	mouse	IgG_1	AC133
CD140b	PE	BD Pharmingen	mouse	IgG_{2a}, κ	28D4
CD140b	APC	BioLegend	mouse	IgG_1, κ	18A2
CD144	PE	BeckmanCoulter	mouse	IgG_1	TEA 1/31
CD146	PE	BD Pharmingen	Mouse	IgG_1, κ	P1H12

Table 3.1: Antibodies used in FACS

5. RNase-free DNase Set (Qiagen, Hilden, Germany, Cat No 79254)
6. RNAsy Mini Kit (Qiagen, Hilden, Germany, Cat No 74104)
7. RNeasy Plus Micro Kit (Qiagen, Hilden, Germany, Cat No 74034)
8. RNA Clean and Concentrator^{TM}-5 (Zymo Research, Irvine, CA, USA, Cat No R1015)
9. ImProm-II^{TM} Reverse Transcription System (Promega, Manheim, Germany, Cat No A3800)
10. Recombinant RNasin®Ribonuclease Inhibitor (Promega, Manheim, Germany, Cat No N2511)

Target	Fluorochr.	Company	Host	IG class	Clone
CD164	PE	BD Pharmingen	mouse	IgG_{2a}, κ	N6B6
CD200	PE	BD Pharmingen	mouse	IgG_1, κ	MRC OX-104
CD271	APC	Miltenyi Biotec	mouse	IgG_1	ME20.4-1.H4
CD324	Alexa 488	Biolegend	mouse	IgG_1, κ	67A4
CD325	APC	e-Bioscience	mouse	IgG_1, κ	8C11
CD326	Alexa 488	Biolegend	mouse	IgG_{2b}, κ	9C4
CDCP1	PE	BD Pharmingen	mouse	IgG_1, κ	cub1
Her-2	PE	BD	mouse	IgG_1, κ	Neu 24.7
Her-3	APC	Biolegend	mouse	IgG_1, κ	1B4C3
SSEA-3	PE	BD Pharmingen	rat	IgM	MC-631
SSEA-4	PE	BD Pharmingen	mouse	Ig_{G3}	MC813-70
TRA-1-60	PE	BD Pharmingen	rat	IgM,κ	TRA-1-60
TRA1-81	PE	BD Pharmingen	mouse	IgM,κ	TRA-1-81
TROP-2	FITC, APC	R&D Systems	mouse	IgG_{2a}	77220
CD344	PE	Biolegend	mouse	IgG_1, κ	CH3A4A7
SUSD2	PE	Miltenyi Biotec	mouse	IgG_1, κ	W5C5
TNAP	PE	Miltenyi Biotec	mouse	IgG_1	W8B2

Table 3.2: Antibodies used in FACS (cont.)

Target	Company	Host	IG class	Clone	Cat N
CD24	BD Pharmingen	mouse	IgG_2a, κ	ML5	555426
CD24	Thermo Scientific	mouse	IgM,κ	SN3b	MS1279P1
CD49f	BD Pharmingen	rat	IgG_2a, κ	GoH3	555734
ALDHA1	Proteintech	rabbit	IgG	Poly	15910-1-AP
CK17	Proteintech	rabbit	IgG	Poly	10164-2-AP
AR	Cell Signaling Tech.	rabbit	IgG	D6F11	5153S
CK5	Thermo Scientific	rabbit	IgG	SP27	MA5-16372
CK18	AbD Serotec	mouse	IgG_1	CY90	MCA1864HT
Trop-2	R&D Systems	goat	IgG	Poly	AF650

Table 3.3: Antibodies used in immunohistochemistry

11. qPCR Master Mix Plus for SYBR®Green I (Eurogentec, Cat No RT-SN2X-03+)

12. LightCycler®480 SYBR Green I Master (Roche, Basel, Switzerland, Cat No 04707516001)

13. FastStart SYBR Green Master (Roche, Basel, Switzerland, Cat No 04673484001)

Target	Company	Host	IG class	Clone
beta-tubulin	Cell Signaling technologies	rabbit	IgG	9F3
beta-actin	Cell Signaling technologies	mouse	IgG2b	8H10D10
GAPDH	Sigma-Aldrich	rabbit	IgG	Poly
CD24	BD Pharmingen	mouse	IgG_2a, κ	ML5
p63	Biolegend	rabbit	IgG	Poly6190
p63	Sigma-aldrich	mouse	IgG_2a	4A4
bcl-2	Dako	mouse	IgG_1, κ	124
CK5	Thermo-Scientific	rabbit	IgG	SP27

Table 3.4: Antibodies used in Western blot

Antibody	Host	Company	Cat N
a-mouse IgG (H+L) Alexa 488	goat	Invitrogen	A11029
a-mouse Cy3	rabbit	Chemicon	N/A
a-rabbit IgG (H+L) Cy3	goat	Invitrogen	A10520
a-rabbit Cy3	goat	Invitrogen	A10520
a-rabbit IgG (H+L) Alexa 488	goat	Invitrogen	A11034
a-rat IgG (H+L) Alexa 488	rabbit	Invitrogen	A21210
a-goat Alexa 488	rabbit	Invitrogen	A-11078
a-mouse IgM FITC	goat	N/A	N/A
a-mouse IgM+IgG (H+L) Cy3	goat	Millipore	AP130C
a-rat IgG Cy3	goat	Abcam	N/A

Table 3.5: Secondary antibodies used in immunohistochemistry and flow cytometry

14. MessageBOOSTER^{TM} cDNA Synthesis from Cell Lysates Kit (Epicentre Biotechnologies, Cat No MBCL90310)
15. CD24 siRNA, Trilencer-27 (Origene, USA, Cat No SR311132)
16. Lipofectamine RNAiMAX Reagent (Invitrogen, Darmstadt, Germany, Cat No 13778-150)
17. Opti-MEM Medium (Gibco, Paisley, UK, Cat No 31985)

3.1.6 *Materials for cell culture*

1. RPMI-1640 (PAA, Pasching, Austria, Cat No E15-840)
2. Hank's BSS (1x) (PAA, Pasching, Austria, Cat No H15-007)
3. Fetal Calf Serum (PAA, Pasching, Austria, Cat No A15-151)

4. KnockOut Serum Relpacement (Gibco, Paisley, UK, Cat No 10828-028)
5. CnT12 (CellNTec, Basel, Switzerland, Cat No CnT12)
6. CnT52 (CellNTec, Basel, Switzerland, Cat No CnT52)
7. Trypsin-EDTA (PAA, Pasching, Austria, Cat No L11-003)
8. Amino acids 50X (PAA, Pasching, Austria, Cat No M11-002)
9. Non-essential Amino acids (Gibco, Paisley, UK, Cat No 11140)
10. Accutase (PAA, Pasching, Austria, Cat No L11-007)
11. L-Glutamine 200 mM (PAA, Pasching, Austria, Cat No M11-004)
12. Penicilin/Streptomicin (PAA, Pasching, Austria, Cat No P11-010)
13. Gentamicin (PAA, Pasching, Austria, Cat No P11-004)
14. Sodium Pyruvate Solution, 100 mM (PAA, Pasching, Austria, Cat No S11-003)
15. Gelatine (Biochrom, Berlin, Germany, Cat No L 7230)
16. Gamunex 10% (Telecris Biotherapoietics, Frankfurt am Mein, Germany, Cat No T100113)
17. Collagenase, from Clostridium histolycum (Sigma, Cat No C9891)
18. Dispase II (Neutral Protease , grade II) (Roche Diagnostics, Mannheim, Germany, Cat No 11089700)
19. Insulin solution, human (Sigma, Cat No I9278)
20. Androstanolone (Fluka, Netherlands, Cat No 100952529)
21. Cryo-defined Freezing Medium (CellNTec, Basel, Switzerland, Cat No CnT-CRYO-50)
22. 2-Mercaptoethanol (Sigma, Cat No M-7522)
23. NH OsteoDiff Medium (Miltenyi Biotec, Bergisch Gladbach, Germany, Cat No 130-091-678)
24. NH AdipoDiff Medium (Miltenyi Biotec, Bergisch Gladbach, Germany, Cat No 130-091-677)

3.1.7 *Other materials*

1. BD Cytofix/Cytoperm^{TM} (Becton Dickinson, Heidelberg, Germany, Cat No 554722)

3.2 PATIENT SELECTION AND TISSUE PROCESSION

This study is based on 100 prostate samples from patients with BPH or prostate cancer, obtained from November 2009 to April 2013 after transurethral (n=56) or transvesical (n=19) resection of the prostate or cystoprostatectomy (n=25). Our work was approved by the local ethics committee (379/2010B02) and all tissue samples were collected after informed consent. The patients ranged from 26 to 89 years old in age. In addition, a representative fraction of every fresh tissue specimen was fixed in formalin, embedded in paraffin, stained with haematoxylin and eosin, and further examined by an uro-pathologist. None of the patients, claimed to suffer from BPH, showed any sign of prostate cancer in routine histological work-up. Initially, 20 samples were used for FAC sorting and subsequent clonogenicity analysis, 80 samples were used for experiments with primary tissues, as well as in preliminary experiments.

For the purpose of our study, freshly obtained samples were gathered in sterile containers with collection medium RPMI-1640 (PAA, Pasching, Austria). Next, the samples were processed mechanically into 1 mm^2 pieces, digested overnight in a medium, containing RPMI-1640 (PAA, Pasching, Austria), 200U Collagenase IA (Sigma-Aldrich, St. Louis, MO US), 0.5 mg/ml Dispase II (Roche, Basel, Switzerland), 1 μg/ml DNAse I (Sigma-Aldrich, St. Louis, MO, USA). The incompletely digested acini were additionally processed through 18G and 20G syringe needles. The cell suspension was passed through a nylon mesh to remove any remaining undigested fragments.

In order to lyse the remaining erythrocytes, the mixture of cells was incubated in 0.8% ammonium chloride solution (Stemcell Technologies, Grenoble, France) for 10min on ice. The resulting cell suspension was washed and any undigested debris was removed using a 40 μm mesh filter. The resulting single-cell suspension was used for further experiments.

3.3 CELL CULTIVATION METHODS

3.3.1 *Epithelial differentiation medium for cultivated epithelial cells*

1. Required stocks:
    - 0,1M $CaCl_2$ (100×) -1.1g $CaCl_2$ salt in 100 ml dH_20
    - 10^{-5}M 5-DHT (1000×) — prepared from 10^{-2} M — 0.00029 g in 10 ml
    - CnT52
2. Final preparation (for 50 ml):
    - 0.5 ml 0.1 M $CaCl_2$

- 0.05 ml 10^{-5} M 5-DHT
- 49.5 ml CnT52

3.3.2 *Differentiation medium for cultivated stromal cells*

NH OsteoDiff Medium (for osteoblastic differentiation) and NH Adipo Diff Medium (for adipocyte differentiation) (Miltenyi Biotec) supplemented with 1% Penicillin/Streptomycin was added to a 24-well plate with confluent stromal cells in passage 3. The medium was exchanged every third day. On the 14^{th} day of the differentiation, Alizarin red and Alkaline phosphatase assays were performed to detect osteoblastic differentiation and on the 21^{th} day — Oil Red O was used for adipocyte differentiation. As a negative control, used to detect spontaneous differentiation, for each experiment one well was left with the normal cultivation medium.

For the Alkaline phosphatase assay, a tablet of SIGMA FAST BCIP/NBT (Sigma-Aldrich, St. Louis, MO, USA) was dissolved in 10 ml dH_20 and filtered. The cells were fixed with ice cold methanol (precooled on -20°C) and incubated in a freezer for 5 min. The remaining methanol was removed with double washing of dH_20 and the cells were incubated with SIGMA FAST for 10 min on RT.

3.3.3 *Clonogenicity*

The colony-forming capacity of primary prostate epithelial cells was determined by plating defined cell numbers into 6-well culture plates. On the 14^{th} day of cultivation, colonies containing more than 32 cells were microscopically scored. Alternatively, the cells were fixed with 3% FA for 10 min and stained with 1% Rhodanile Blue (Sigma-Aldrich, St. Louis, MO, USA) for 30 min. Plating efficiency was calculated as the number of counted colonies, divider by the number of cells plated (500, 1000, 2000) $\times$ 100. Colonies were enumerated in duplicate. Three types of colonies were scored: holoclones, paraclones and mesoclones, which were determined microscopically, based on their morphology and cell number. Paraclones were determined as composed of small, spindle-shaped and scattered cells; the colonies were irregular and loose, with a cell count of 32–100 cells. Mesoclones were larger, irregular and loose, composed of scattered cells with different morphology (spindle-shaped and round) and a count of 100–500 cells. Holoclones were round-shaped and dense, composed of cells with different morphology and good mutual connections; the cell count was greater than 500. The enrichment of colonies after cell sorting was calculated using the following formula:

$$E = \frac{c/S}{c/U} = \frac{U}{S} \tag{3.1}$$

where c is the number of colonies, S are plated cells in the sorted fraction and U are the plated cells in unfractionated cells.

3.4 FLOW CYTOMETRY

3.4.1 *Detection of apoptosis and viability with annexin V*

Annexins are a family of calcium-dependent proteins, which bind preferentially to the phospholipid phosphatidylserine. Under normal physiologic conditions, phosphatidylserine is predominantly located in the inner part of the plasma membrane. When apoptosis is initiated, phosphatidylserine loses its asymmetric distribution across the phospholipid bilayer and gets translocated to the extracellular membrane. This process prepares the cells as a target of phagocytosis. Once the phosphatidylserines are located on the outer surface of the cell membrane, they can be detected by fluorescently labeled Annexin V.

3.4.2 *Fluorescence activated cell sorting (FACS) and flow cytometry analysis*

The primary cells were incubated with 10 mg/ml polyglobin for 15 min on ice to block any non-specific binding to the Fc receptors. Next, the cells were stained with fluorochrome-conjugated antibodies for 15 min on ice (all antibodies are listed in Table 3.1 and Table 3.2). After washing, the cells were stained with 4', 6-diamidino-2-phenylindole (DAPI; Sigma-Aldrich, St. Louis, MO, USA) to exclude non-viable cells from the analysis. Cultured cells were first digested with Accutase (PAA, Pasching, Austria), washed in FACS buffer (fluorescence activated cell sorting buffer) containing Phosphate Buffer Saline (PBS), supplemented with 1% of fetal bovine serum (FBS) and 0.01% of NaN_3 and incubated with polyglobin. Direct staining was performed as described above. For indirect staining, cells were first labeled with the primary antibody (25 μl of culture supernatant). After washing twice in FACS buffer, cells were then stained with goat anti-mouse secondary antibody conjugated with R-phycoerythrin (PE) (Dako Cytomations, Glostrup, Denmark). After washing, the cells were stained with DAPI prior to flow cytometric analysis. At least $1/x104$ cells were analyzed on a BD FACSCanto II flow cytometer (Becton Dickinson, Heidelberg, Germany). Data was processed using the FlowJo software (Tree Star Inc., OR, USA). Cell sorting was performed on a FACSAria-II cell sorter (Becton Dickinson, Heidelberg, Germany). 500–2000 cells from the selected populations were sorted into 6-well plates containing undefined Prostate Epithelial Progenitor cell medium with low pituitary extract (CellNTec, Bern, Switzerland).

3.4.3 *Combined direct and indirect flow cytometry FACS staining*

For co-staining of directly labelled and unlabeled antibodies, an alternative staining procedure was performed. The prostate cells in suspension were initially incubated with 10 mg/ml polyglobin for 15 min on ice to block any non-specific binding to the Fc receptors. Next, the unlabeled antibody was incubated for 15 min (25 μl of culture supernatant with 50 μl of cell suspension). After washing twice with FACS buffer, a secondary antibody was incubated for 15 min. After the indirect staining, additional blocking for 20 min was performed, with plain mouse IgG (20 μl, 1:20 dilution). After the blocking, without washing, the directly labelled antibody was incubated for 15 min, as a fourth step in the staining. All steps were performed on ice. After the last step, the samples were measured with FACS Canto.

3.4.4 *Intracellular staining with BD Cytofix/Cytoperm*

1. Blocking of the cells with PG (15 min on ice)
2. Surface staining of the cells (as mentioned in Section 3.4.2)
3. One-step fixation and permeabilization — 100 μl BD Cytofix/-Cytoperm solution (20 min on ice)
4. Washing with BD saponin-containing buffer (1$\times$ solution in PBS)
5. Primary antibody incubation, 15 min on ice (CK5 1:50)
6. Washing with saponin containing buffer $\times$2
7. Secondary antibody incubation, 15 min on ice (anti-rabbit AF488 1:500, anti-rabbit Cy_3 1:100)
8. Washing with saponin-containing buffer and transfer of the cells to FACS tubes with BD buffer

3.4.5 *Aldefluor assay*

The Aldefluor assay was used to compare the ALDH1A1 activity of the colonies, grown from the two subsets ($CD24^+$ and $CD24^-$). In order to perform the analysis, Aldefluor kit (StemCell Technologies, Grenoble, France) was used as prescribed by the manufacturer. The measurement of specific ALDH1A1 activity was based on the difference between the presence/absence of the Aldefluor inhibitor diethylaminobenzaldehyde (DEAB). For co-expression studies, additional surface staining with the indicated antibodies was performed after treatment of the cells with Aldefluor. The stained cells were analyzed

on a FACSCanto II flow cytometer (Becton Dickinson, Heidelberg, Germany) using the FlowJo software for data analysis.

3.4.6 *Proliferation and cell cycle analysis (BrdU and PI)*

Proliferation of the two subsets of interest was examined on cultivated cells of the two fractions (with BrdU pulsing) or on primary cells after FACS sorting (cell cycle analysis with PI). The cells with or without BrdU pulsing applied (performed for 30 min in the same medium) were fixed in ice cold 70% ethanol and frozen on -20°C. Antibody against the incorporated BrdU (B44 clone, Becton Dickinson, Heidelberg, Germany) was used to visualize the cells in a process of DNA replication. Propidium iodide (Sigma-Aldrich, St. Louis, MO, USA) was used to fluorescently stain the DNA and thus to label the cells in different cell cycle stages. The samples were analysed using BD FACSCanto II flow cytometer (Becton Dickinson, Heidelberg, Germany) and the BD FACSDiva v6.1.3 software.

3.5 DNA AND RNA ANALYSIS METHODS

3.5.1 *Quantitative real-time polymerase chain reaction*

Total RNA from cultivated cells was isolated using RNeasy Kit (Qiagen, Hilden, Germany) and the quantity of the RNA was determined with Nanodrop2000 (Thermo Scientific, Waltham, MA USA).

PCR allows the rapid amplification of specific DNA fragments from complex mixtures of DNA molecules. We used several qPCR protocols for mRNA expression analysis from primary and cultivated cells.

The classical qPCR reaction included two steps: (i) cellular mRNA was reverse transcribed with a reverse transcription kit (ImProm-II^{TM} Reverse Transcription System from Promega, Manheim, Germany) in a thermal cycler (Perkin Elmer GeneAmp PCR System 2400). SYBR Green (qPCR Mastermix Plus for SYBR Green I, Eurogentec, Seraing, Belgium) was used as fluorescent reporter to determine the quantified DNA using the Roche LightCycler 480 System. β-actin and 18S RNA were used as internal controls. The primers and reference sequences are described in Table 3.6. Relative mRNA levels were calculated based on threshold of the cycle values (C_t) corrected for the expression for β-actin and 18S.

The reaction mixture for DNA reverse transcription is:

- 4 μl 5$\times$ Puffer
- 1 μl dNTPs
- 2.4 μl $MgCl_2$
- 1 μl RNase inh.

	Primer	Sequence
1	CK18 Forward	TGATGACACCAATATCACACGA
2	CK18 Reverse	GGCTTGTAGGCCTTTTACTTCC
3	CK8 Forward	AGGGCTGACCGACGAGAT
4	CK8 Reverse	CACCACAGATGTGTCCGAGA
5	SOX9 Forward	GTACCCGCACTTGCACAAC
6	SOX9 Reverse	TCGCTCTCGTTCAGAAGTCTC
7	AR Forward	GCCTTGCTCTCTAGCCTCAA
8	AR Reverse	GGTCGTCCACGTGTAAGTTG
9	CK5 Forward	GAGCTGAGAAACATGCAGGA
10	CK5 Reverse	TCTCAGCAGTGGTACGCTTG
11	CK19 Forward	GCCACTACTACACGACCATCC
12	CK19 Reverse	CAAACTTGGTTCGGAAGTCAT
13	CK17 Forward	TTGAGGAGCTGCAGAACAAG
14	CK17 Reverse	AGTCATCAGCAGCCAGACG
15	TP63 Forward	TTGAGATTAGCATGGACTGTATCC
16	TP63 Reverse	GTTCTGAATCTGCTGGTCCAT
17	PSA Forward	GTGCTTGTGGCCTCTCGT
18	PSA Reverse	AGCAAGATCACGCTTTTGTTC
19	PSCA Forward	AGCTTGAACTGCGTGGATGA
20	PSCA Reverse	TTGCACAAGTCGGTGTCACA
21	SOX2 Forward	GGGAAATGGGAGGGGTGCAAAAGAGG
22	SOX2 Reverse	TTGCGTGAGTGTGGATGGGATTGGTG
23	B-actin Forward	AGTCCTGTGGCATCCACGAAACT
24	B-actin Reverse	CACTGTGTTGGCGTACAGGTCTT
25	18s Forward	CGGCTACCACATCCAAGGAA
26	18s Reverse	GCTGGAATTACCGCGGCT

Table 3.6: PCR primers

- 1 μl Reverse transcriptase
- 1 μl Oligo-dt

The standard protocol used for the Real-time PCR reaction was:

1. 2 min at 95°C (initial denaturation)
2. 45 sec at 95°C (denaturation)
3. 30 sec at variable temperature (60°C to 68°C) (annealing)
4. Variable time (30 sec to 4 min) at 72°C (elongation)

5. Variable time (2 to 16 min) at 72°C (elongation termination)

For qPCR analysis of sorted primary cells, the MessageBOOSTER^{TM} cDNA synthesis kit (Epicentre, Madison, WI, USA) was used. 3000 cells were FACS sorted, lysed and frozen on -80°C. Next, mRNA was reverse transcribed to first strand cDNA synthesis with MMLV reverse transcriptase. Second strand cDNA was synthesized with MessageBOOSTER DNA polymerase. *In vitro* transcription was conducted for four hours using MessageBOOSTER T7 RNA Polymerase. The resulting cRNA was purified and concentrated with RNA Clean & Concentrator™-5 (Zymo Research Corp, Irvine, CA, USA). An additional step of reverse transcription was performed before the Real-time PCR reaction. All Ct values were calculated after normalization to β-actin.

3.5.2 *siRNA Transfection for CD24*

Required reagents:

- CD24 siRNA
- Lipofectamine RNAiMAX Reagent
- Opti-MEM medium

For this method, cultivated epithelial cells derived from BPH were cultivated in a 6-well plate with 2.5 ml of medium (CnT52). One day before the transfection, a medium without antibiotics was added. Preparation of the reagents for the transfection:

1. 5.04 μl (30 μg) from each siRNA (A+B+C = siRNA-mix) + 250 μl Opti-MEM were mixed thoroughly in an Eppendorf tube (for the negative siRNA control, only the scrambled RNA provided by the kit: 5.04 μl)
2. 5 μl Lipofectamine + 250 μl Opti-MEM were mixed in a separate tube
3. (1) and (2) were mixed together and pipetted up and down
4. The mixtures were incubated for 20 min RT
5. 500 μl per well were added

3.6 PROTEIN PURIFICATION AND ANALYSIS

3.6.1 *Protein extraction from cultivated cells*

Protein lysates were prepared from cell lines grown on variable cell culture dish formats, depending on the experiment. The cells were

detached with Trypsin. After stopping the enzyme, the cells were washed with PBS twice. For the purpose of lysate preparation, an NT-40 buffer was used and was supplemented with complete Protease-Inhibitor cocktail tablets (Roche, Basel, Switzerland). Cell lysis was performed on RT for 3 min, after which the lysates were spinned on 4°C on 13000 RPM for 45 min. The supernatants from the NT-40 lysates were subsequently subjected to quantification and frozen on -20°C. The protein concentration was estimated using modified Bradford method, suitable for lysates with high concentration of detergent.

Reagents for preparation of NT-40 buffer:

- 1.5 ml 5M NaCl (150 mM final)
- 2.5 ml 1M Tris-HCl Lsg. pH 8 (50 mM)
- 0.5 ml NP-40
- 45.5 ml dH_20.

3.6.2 *SDS-Polyacrylamide Gel Electrophoresis (SDS-PAGE)*

Separation of proteins by their molecular weight was accomplished via sodium dodecyl sulphate polyacrylamide electrophoresis (principle described by Laemmli). 7.5% precast gels (Mini-PROTEAN® TGX™Bio-Rad Laboratories, Hercules, California, USA) were used. To run the protein samples, 5–25 μg sample/lane (depending on the antibody used) were used, prediluted in Laemmli buffer. Running Chamber system from Bio-Rad was used for SDS-PAGE separations as recommended by the manufacturer. Precision Plus Protein Dual Standards (BIO-RAD Laboratories, Hercules, California, USA) were loaded together with the protein samples as molecular size standards. The separation was performed at 100 V and 50 mA for approximately 2 h.

Preparation of the running buffer:

- 50 ml 10× Tris-Glycine
- 5 ml 10% SDS
- fill up to 500 ml dH_20.

3.6.3 *Transfer of proteins on nitrocellulose membranes*

Transfer and immobilization of proteins from gels onto PVDF membranes was accomplished via electroblotting using a Bio-Rad Transferring Chamber (principle described by Towbin et al.). The transfer

buffer was prepared freshly and used to generously soak all components of the blotting sandwich during assembly. Blotting was performed at 4°C under stirring for 45 min at 100 V and 400 mA.

Transfer buffer:

- 50 ml 10× Tris-Glycine
- 0.5 ml 10%SDS
- 100 ml Methanol
- 500 ml dH_20.

Blocking of unspecific antibody binding to the PVDF membrane was performed using 5% milk powder. For protein detection, antibodies against CK5 (rabbit IgG, Thermo Scientific, Rockford, IL, USA), CK18 (mouse IgG_1, AbD Serotec, Martinsried, Germany) and p63 (mouse IgG, Sigma-Aldrich, St. Louis, MO, USA) were used. Depending on the primary antibody, GAPDH (Glyceraldehyde 3-phosphate dehydrogenase) or β-actin antibodies were used as housekeeping genes (respectively rabbit IgG, Sigma-Aldrich, St. Louis, MO, USA and mouse IgG, Stemcell Technologies, Grenoble, France). Dual color western blot was performed using antibodies, labeled either with IRDye 800CW (green) or IRDye 700CW (red) (LI-COR Biosciences, Lincoln, NE, USA), and the Li-COR Odyssey system (LI-COR Biosciences, Lincoln, NE, USA) was employed for protein band detection and data analysis. The list of antibodies is specified in Table 3.4.

The antibodies were used in the following concentrations:

- Cytokeratin 5 (rabbit Ab): 1:500 dilution
- Cytokeratin 18 (mouse Ab): 1:200 dilution
- Androgen receptor (rabbit Ab): 1:500 dilution
- P63 (mouse Ab): 1:1000 dilution (5 μl in 10 ml suspension)
- Anti-GADPH (rabbit Ab) — 1:5000 (house keeping gene control)
- Anti-β-actin (rabbit Ab) — 1:2000 (house keeping gene control)

3.7 IMMUNOHISTOCHEMISTRY/IMMUNOFLUORESCENCE

The adjacent tissue of each FAC sorting was formalin-fixed and paraffin embedded. Sections of 5 μm were deparaffinized and rehydrated in descending series of ethanol. Antigen retrieval was performed by heating the sections in 10 mM citrate buffer (pH 6.0). Alternatively for unmasking of the CD49f antigen, 1% fucine (Invitrogen, Darmstadt, Germany) treatment was performed. For blocking of any unspecific

staining we used 10% of serum, obtained from the same species, in which the secondary antibody is produced (goat, horse or rabbit). For the purpose of immunofluorescence, secondary Cy_3 or Alexa Fluor 488 labeled antibodies (goat or rabbit) were applied; DAPI was used for nuclei contrastaining.

For DAB immunofluorescence several blocking procedures were performed in addition — blocking of endogenous peroxidases with 1% H_2O_2 and blocking of avidin and biotin. The Vectastain ABC kit (Vector Laboratories, Burlingame, CA, USA) was used for the avidin-biotin complex (ABC) method according to the manufacturer's instructions. Peroxidase activity was visualized with 3,3'-diaminobenzidine (DAB) (Dako Cytomations, Glostrup, Denmark).

3.7.1 *Immunofluorescence protocol*

1. Wash twice with PBS
2. Fix with 1% PFA 30 min, RT
3. Wash twice with PBS
4. Cell permeabilization with 0.1% Triton in PBS (stored on 4°C), for 20 min
5. Wash twice with PBS
6. The cells were blocked with 10% goat serum in PBS, for 20 min
7. Primary antibody 1 h RT or overnight on 4°C, the antibodies were diluted in 0.1% BSA
8. Wash twice with PBS
9. Secondary antibody 1 h RT, Ab in 0.1% BSA and 1:3000 DAPI
10. Wash twice with PBS
11. Mounting with cover slips.

The list of antibodies is specified in Table 3.3. They were used in the following concentrations:

- Cytokeratin 5 (rabbit Ab): 1:100 dilution
- Cytokeratin 18 (mouse Ab): 1:100 dilution
- Cytokeratin 17 (mouse Ab): 1:100 dilution
- Androgen receptor (rabbit Ab): 1:100 dilution
- CD24 (mouse Ab): 1:50 dilution
- ALDHA1 (mouse Ab): 1:50 dilution
- CD24 (mouse Ab): 1:50 dilution

3.8 STATISTICS

The data were described using the mean value of each group, SD (standard deviation) and SEM (standard error of the mean). One-way analysis of variance (parametric ANOVA) and Kruskal-Wallis test (non-parametric ANOVA) were performed for comparison of the colony forming ability of different FAC sorted subsets, as well as to compare different colonies for surface marker expression. P-values <0.05 were considered to represent statistical significance and <0.001 — as highly significant. 18 primary BPH samples were used to compare the colony-forming ability. Additionally, most of the experiments were performed in a triplicate at minimum.

4 EXPERIMENT DESIGN

4.1 DESIGN OF EXPERIMENTS

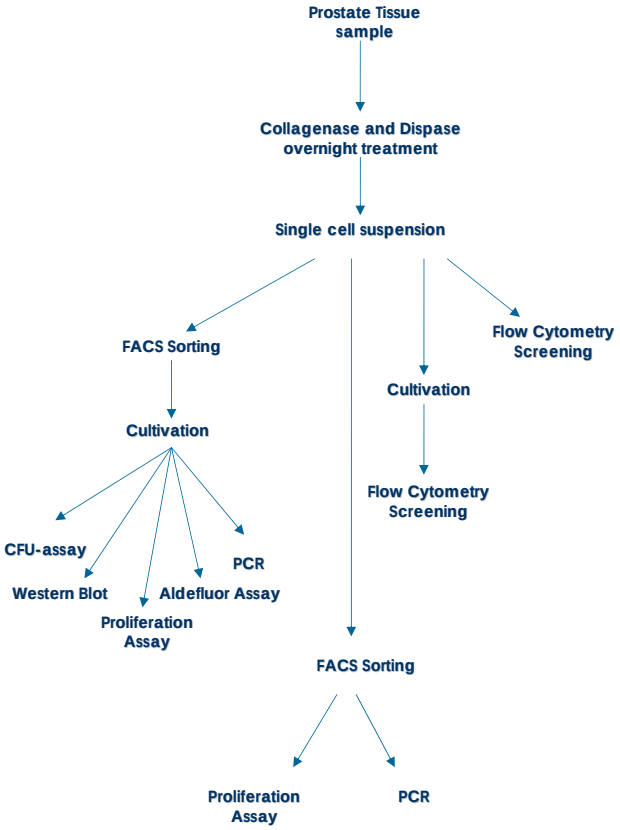

Figure 4.1: Design of experiments (explanation is given on page 34)

Prostate tissue samples were digested overnight and the best conditions were achieved. On the next day, the resulting single-cell suspension was used for various experiments. Parts from all samples were paraffin-embedded for further histochemical and immunohistochemical examination.

4.2 FLOW CYTOMETRY TESTING OF PRIMARY PROSTATES

The cells from single cell suspensions were FACS tested for surface marker expression, co-expression between the surface markers, as well as between the surface markers and intracellular markers.

4.3 EXPERIMENTS ON CULTIVATED UNFRACTIONATED CELLS

Single-cell suspensions (without FACS separation) were brought into culture and depending on the selective medium, epithelial and stromal mesenchymal cell cultures were obtained. When the cells reached confluence, they were replated and after the third passage were tested for expression of a broad range of surface markers. The purpose of this procedure was to confirm the epithelial and mesenchymal character of these cells on one side; and on the other, to discover new potential markers for prostate progenitor cells.

4.4 FACS SORTING AND EXPERIMENTS WITH SORTED CELLS

4.4.1 *Experiments on cultivated cells after FACS sorting*

Different cell subsets have been sorted from single cell suspensions and were further cultivated for 14–21 days in epithelial medium (CnT-52, which is described in Chapter 3). On the 14^{th} day, the cells were examined for their clonogenicity. When confluence was reached (which is around the 21–24^{th} day), the cells from the colonies were tested for surface and intracellular markers with FACS, PCR, western blot and immunofluorescence. Additionally, the cells were examined for ALDHA1 activity, as well as for proliferation, using PI and BrDU.

4.4.2 *qPCR from FACS sorted cells*

Subsets of interest were FACS sorted from primary single-cell suspension and the cells were lysed. Further experiments for intracellular marker expression and comparison between different subsets were performed with qPCR.

5 RESULTS

5.1 CELL VIABILITY ASSESSMENT

BPH and prostate cancer samples were collected after prostate transurethral resection or cystectomy. The samples were first digested overnight at specifically chosen optimal conditions. To select the surviving cells for further examination, we tested the resulting single-cell suspension for cell viability. A viable population was observed, negative for both Annexin V and PI, which was found to be appropriate for further cultivation, functional examination and *in vitro* assays.

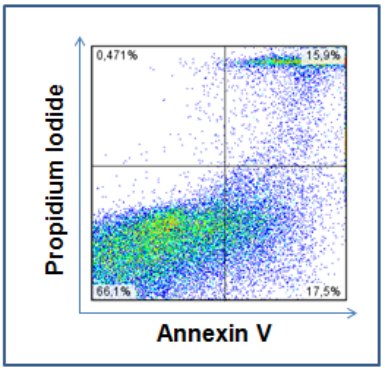

Figure 5.1: Annexin V and PI co-staining for examination of the viability, after surgery, cells negative for Annexin V and PI were considered for viable.

5.2 DIFFERENTIAL GROWTH OF COLONIES

After obtaining single-cell suspensions, the unfractionated cells were plated on different media to separate them by origin. Two media for epithelial cell selection (CnT12 and CnT52) and two media for mesenchymal cell selection (Knock-out serum-free medium and RMPI-1640 with 10% FCS) were used to achieve this goal.

Epithelial-like colonies were found to grow best in a defined serum-free medium (CnT12 and CnT52), rather than a serum-containing one (RPMI-1640 supplemented with 10% FCS). Conversely, mesenchymal-like colony formation was more effective in a serum-containing medium (RPMI-1640 supplemented with 10% FCS) compared to the serum-free setting (KO-DMEM supplemented with human b-FGF) — Figure 5.2.

We have grown the epithelial colonies in 2D (monolayer) and 3D (low attachment) conditions (Figure 5.3). When replated, the epithe-

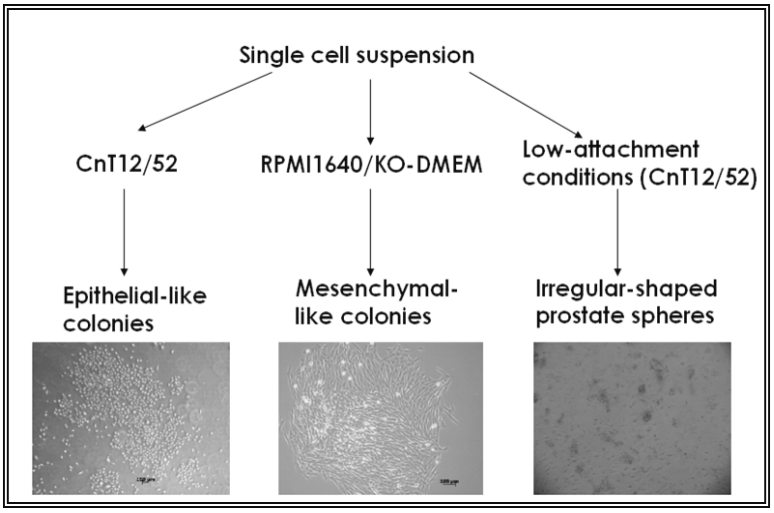

Figure 5.2: Differential outgrowth of primary prostate cells. Cells from primary prostate single-cell suspension showed selective growth serum-free medium: epithelial in CnT12/52, mesenchymal in RPMI-1640 and KO-DMEM. Prostate spheres were able to grow in the CnT12/52 only.

lial mass was maintained without decline of the growth for 5–10 passages. These cells were easy to maintain, freeze and thaw repetitively. Preliminary results showed that the cultured cells expressed the epithelial markers CD324 (E-Cadherin), CD326 (Ep-CAM), CD49f and CD49b and they did not express the mesenchymal markers CD90, CD325 (N-Cadherin). Low expression of the stromal marker CD49a was also observed (Figure 5.4).

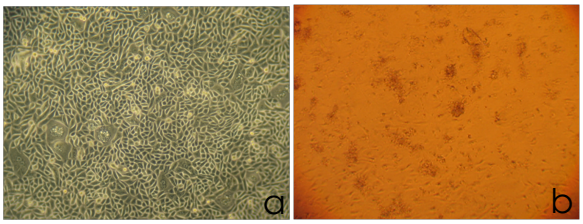

Figure 5.3: Cultivated prostate epithelial cells cells after being replated: cells maintain growth in 2-D conditions (a) and 3-D conditions(b).

The mesenchymal colonies were maintained in monolayer conditions for minimum of 5 passages. They were cultivated in RPMI-1640, supplemented with 10% FCS. Stromal cells possessed a mesenchymal phenotype and a spindle-shaped form. Flow cytometry analysis confirmed the expression of mesenchymal markers (CD90, CD140b, CD71, and CD49a^{hi}) and the absence of epithelial markers (CD324, CD326 and CD49f) — Figure 5.4.

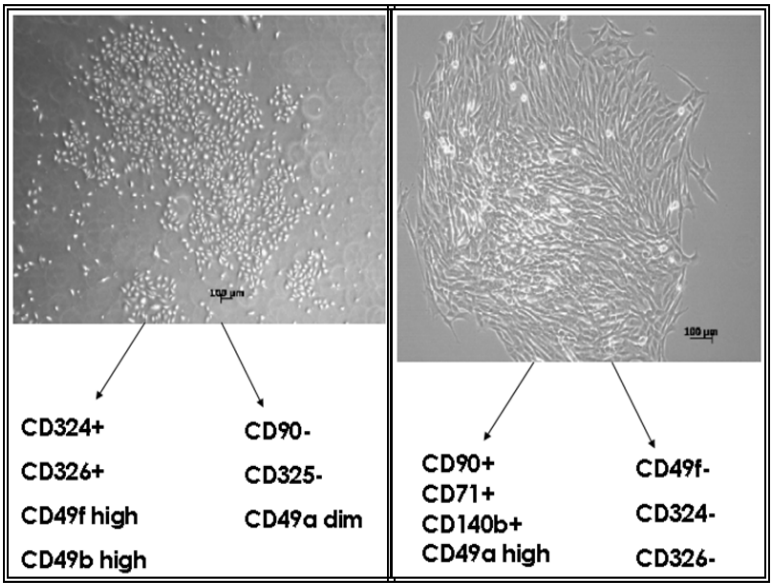

Figure 5.4: Prostate epithelial and mesenchymal colonies: Cells from the epithelial colonies (left) expressed the epithelial markers CD324, CD326,CD49b^{hi},CD49f^{hi}, whereas cells from the mesenchymal colonies expressed the mesenchymal markers CD90, CD140b, CD71, and CD49a^{hi}.

5.3 SURFACE MARKER STUDY OF PRIMARY BENIGN AND CANCER SAMPLES

5.3.1 *Surface marker expression study*

We examined the expression of various surface markers on primary prostate cells in an attempt to distinguish the epithelial from the mesenchymal phenotypes. A wide range of surface markers was studied, including previously known markers for prostate stem cell enrichment, markers known to be present on the prostate cell surface, as well as markers of previously unknown expression on prostate. In search for novel markers having the ability to enrich for stem cells, a panel of in-house-produced antibodies was utilized.

We organized the markers in five groups: integrins, epithelial markers, mesenchymal markers, markers of unknown expression on prostate, and antibodies of unknown specificity (corresponding to in-house antibodies of unknown specificity). The selected integrins were CD49a, CD49b, CD49f, CD29, CD41, CD51, CD61 and CD104. A few of them are known to be expressed in the human prostate (CD49a, CD49b, CD49f and CD104), while others have not been studied yet in such context (CD29, CD41, CD51 and CD61). All chosen integrins were expressed on primary prostate cells but with different patterns. CD29 — the ubiquitous $\beta 1$ integrin — was present in the majority of the prostate cells. The rest of the integrins were expressed only on a subset of all primary prostate cells (originating from patients with

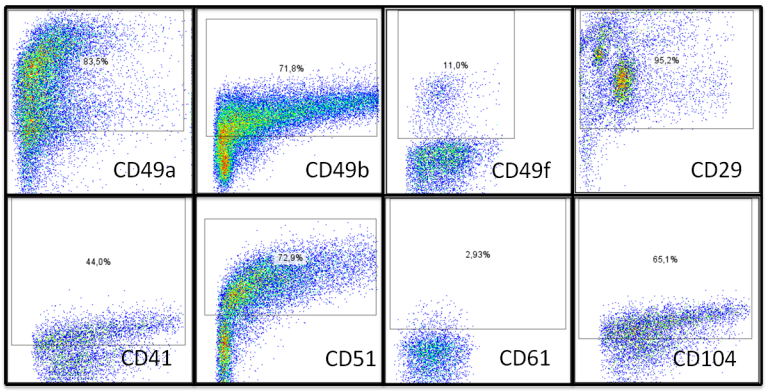

Figure 5.5: Integrin expression on primary prostate cells. The selected integrins were CD49a, Cd49b, CD49f, CD29, CD41, CD51, CD61, CD104. As shown on the figure, all chosen integrins were expressed on primary prostate cells but with different patterns. FCS is shown on the x-axis.

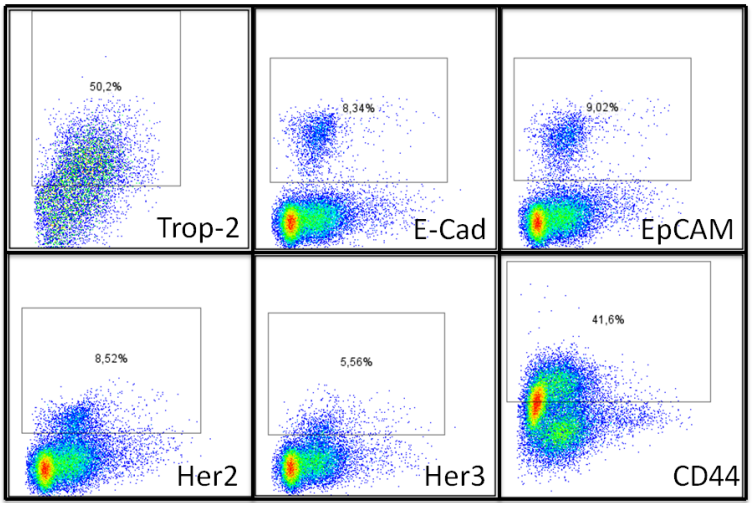

Figure 5.6: Epithelial marker expression on primary prostate cells. The selected markers were CD24, Trop-2, E-cadherin, Ep-CAM, Her2 and Her3. As shown on the figure, all chosen epithelial markers were expressed on primary prostate cells. FCS is shown on the x-axis.

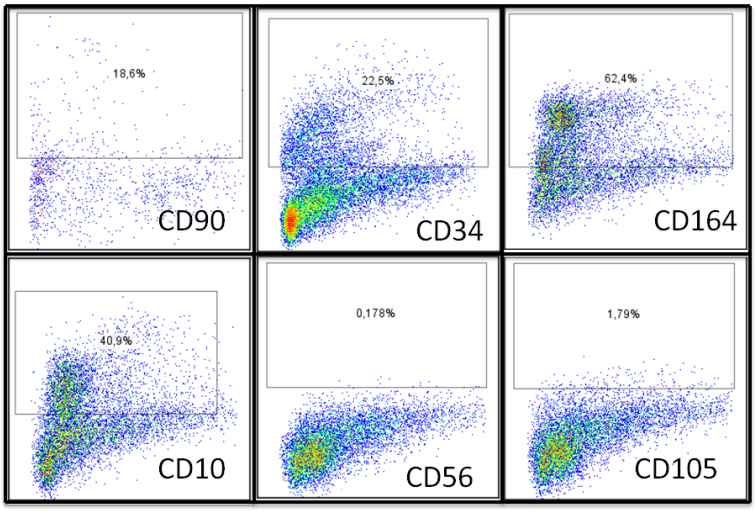

Figure 5.7: Mesenchymal marker expression on primary prostate: the selected markers were CD90, CD34, CD140b, N-CAM, CD10, CD56, CD105. These markers were expressed on primary prostate tissue, except CD56. FCS is shown on the x-axis.

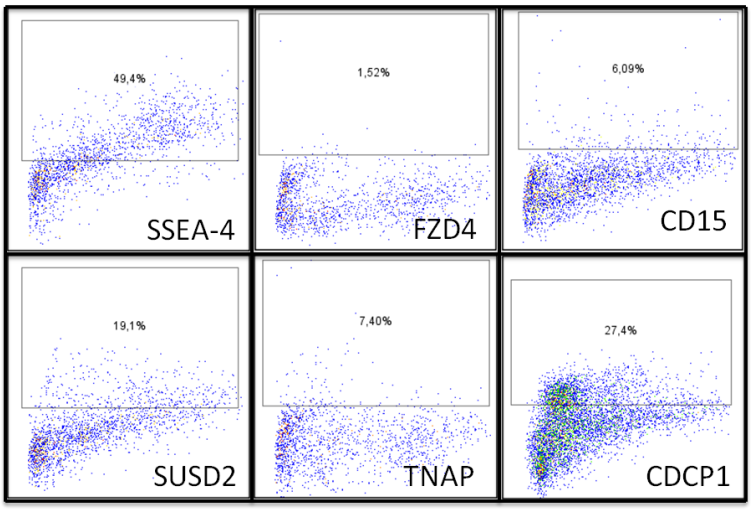

Figure 5.8: Markers of unknown expression on primary prostate cells: SSEA-4, TNAP, SUSD2, Frizzled-4 and CD15. From the examined markers, SSEA-4, TNAP, SUSD2 and CD15 were expressed on primary BPH cells, whereas Frizzled-4 showed no expression.

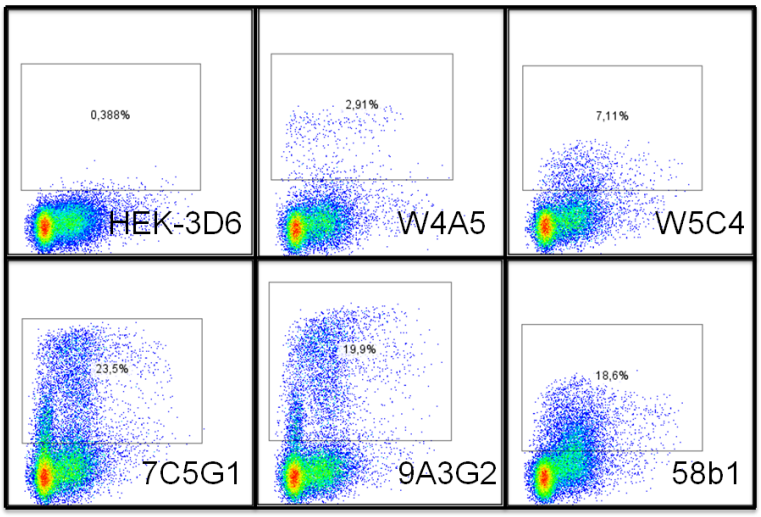

Figure 5.9: Expression patterns of in-house antibodies with unknown antigens on primary prostate cells: HEK-3D3, W4A5, W5C4, 7C5G1, 9A3G2, 58b1. W4A5, W5C4, 7C5G1, 9A3G2 and 58b1 (possibly CD276) were expressed on cell subsets with a different density, whereas HEK-3D3 was not expressed on primary BPH cells. FCS is shown on the x-axis

either BPH or prostate cancer), shown on Figure 5.5. It has been previously reported that CD49b, CD49f and CD104 are expressed on the basal epithelium of the prostate, where the stem/progenitor cells reside. CD49a in contrast is strongly expressed on the stromal compartment cells, which has been demonstrated by subsequent experiments in this study. CD41, CD51 and CD61 were also examined, but as their expression pattern does not correlate with the basal phenotype, they were not considered further. From the list of integrins, CD49f was chosen for selection of epithelial stem/progenitor cells and CD49a — for mesenchymal stem/progenitor cells.

The markers, selected as epithelial, included CD24, Trop-2, E-cadherin, Ep-CAM, Her2 and Her3. They were all expressed on primary human prostate cells (BPH) (Figure 5.6), as well as on cultivated epithelial cells (Figure 5.10).

As mesenchymal markers, CD90, CD34, CD140b, N-CAM, CD10, CD56, CD105 were selected. These markers were expressed on primary prostate tissue, except CD56 (Figure 5.7).

Interestingly, SSEA-4, TNAP, SUSD2 and CD15, which possess unknown expression on prostate, were expressed on primary BPH cells, while Frizzled-4 was not (Figure 5.8).

Using our in-house antibodies targeting unknown antigens, HEK-3D3 was not expressed on primary BPH cells, whereas W4A5, W5C4, 7C5G1, 9A3G2 and 58b1 (possibly CD276) were expressed on cell subsets with a different density (Figure 5.9).

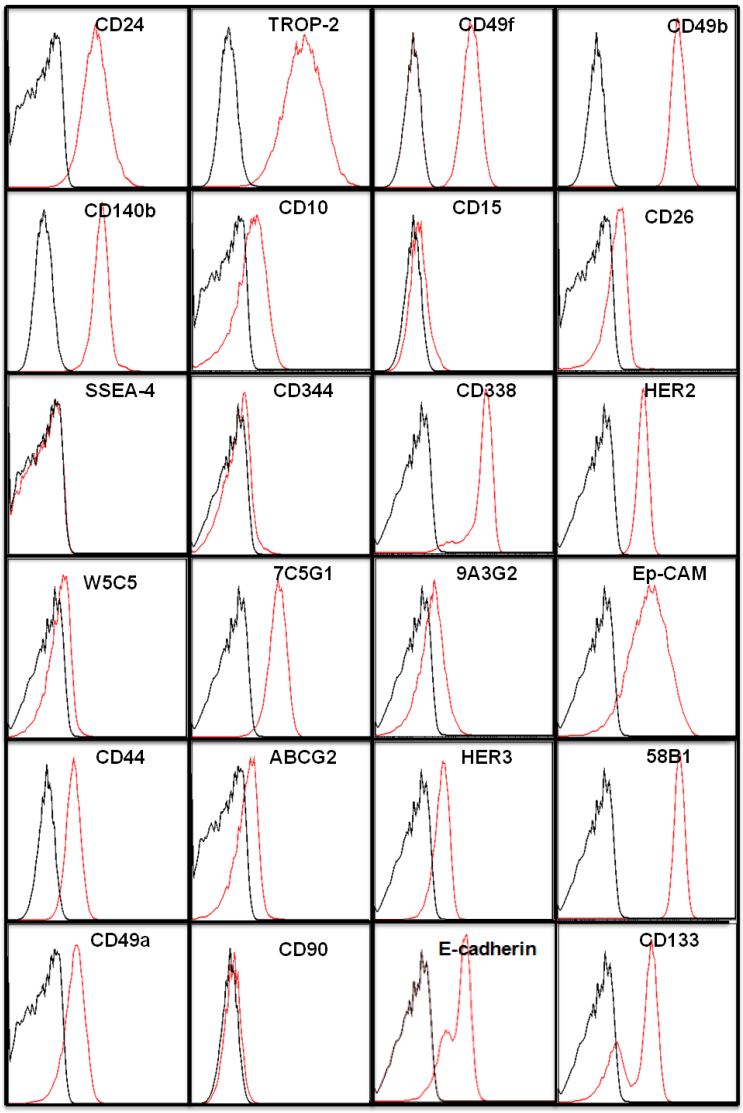

Figure 5.10: Flow cytometry examination of cultivated prostate epithelial cells. Cells were examined for expression of a panel of markers. The epithelial cultivated cells were positive for CD24, Trop-2, CD49f, CD49b, CD44, CD140b, CD10, CD338, Her2, Her3, Ep-CAM, E-Cadherin and the antibodies with unknown antigens 58B1 (possibly CD276), 7C5G1, 9A3G2, expressed CD26 and CD49a at low levels, and showed negativity for CD90, SSEA-4, CD344 and SUSD2(W5C5).

5.3.2 *Study on surface markers of cultivated human prostate epithelial and mesenchymal cells*

In addition, a wide panel of markers have been used to examine the expression on cultivated epithelial and mesenchymal stromal cells. The epithelial cells were positive for CD24, Trop-2, CD49f, CD49b, CD44, CD140b, CD10, CD338, Her2, Her3, Ep-CAM, E-Cadherin and the antibodies with unknown antigens 58B1 (possibly CD276), 7C5G1,

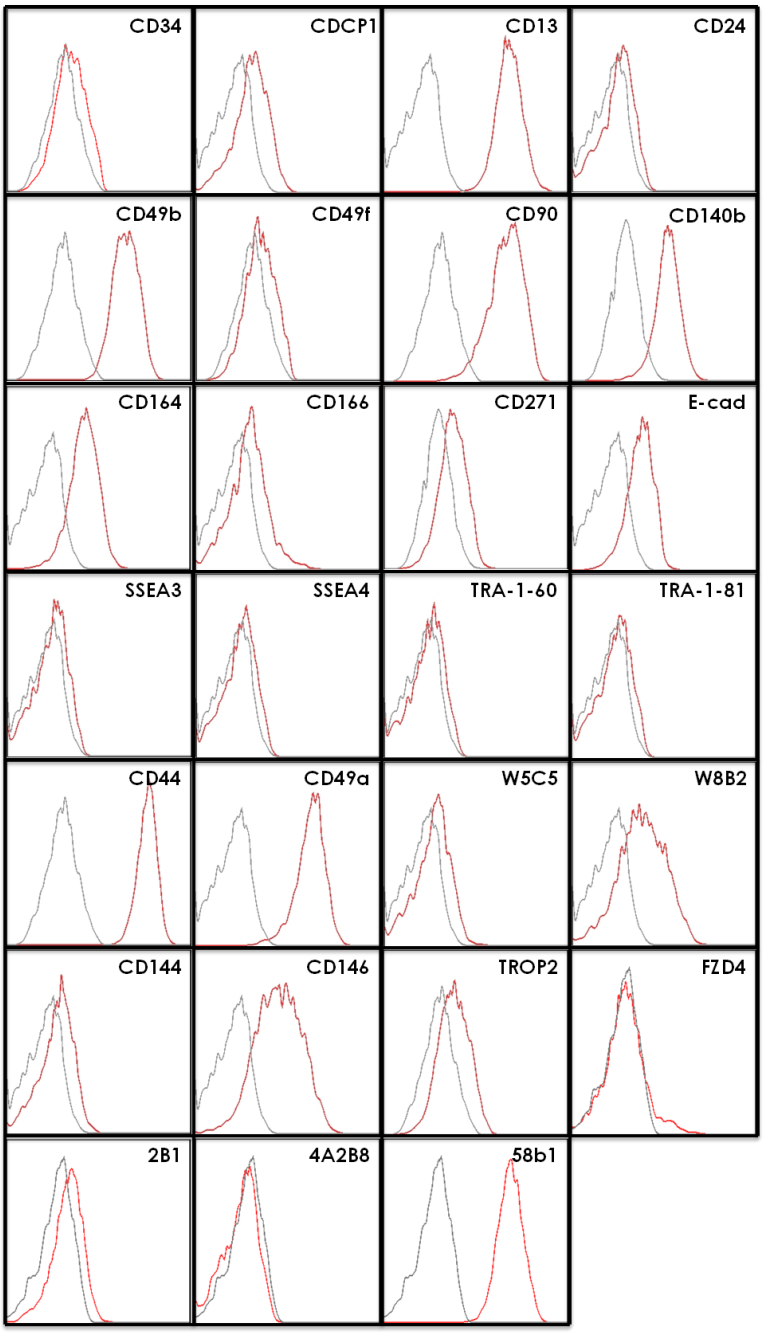

Figure 5.11: Flow cytometry examination of cultivated prostate stromal mesenchymal cells. Cells were examined for expression of a panel of markers. The stromal mesenchymal cultivated cells expressed highly CD13, CD140b, CD44, CD49a, CD146, CD164 and 58b1 (possibly CD276), they did not express the stem cell markers SSEA-3, SSEA-4, TRA-1-60 and TRA-1-81, the epithelial markers CD24, E-cad, Trop-2, as well as CD49f. SUSD2 (W5C5), TNAP (W8B2) and frizzled- 4 were expressed only on specific subsets. FCS is shown on the x-axis.

9A3G2. They also expressed CD26 and CD49a at low levels, but were negative for CD90, SSEA-4, CD344 and SUSD2(W5C5) (Figure 5.10).

The cultivated mesenchymal cells were tested using a large panel of mesenchymal markers, epithelial markers and markers of unknown expression. Figure 5.11 shows that CD13, CD140b, CD44, CD49a, CD-146, CD164 and 58b1 were highly expressed, whereas the stem cell markers SSEA-3, SSEA-4, TRA-1-60 and TRA-1-81 were not expressed. The epithelial markers CD24, E-cad, Trop-2, as well as CD49f, were not expressed on these cells. SUSD2 (W5C5), TNAP (W8B2) and frizzled-4 were expressed on specific subsets only. Interestingly, CD44 was highly expressed on 100% of the mesenchymal cells, although it has been previously reported to be expressed on the basal epithelial cells of the human prostate. Additional markers expressed on both epithelial and mesenchymal cells were CD164 and CD49b (Figure 5.11).

5.3.3 *Coexpression analysis and gating strategy for cell sorting*

Next, coexpression analysis was performed, in order to identify potential subsets of stem/progenitor cells. Several markers have been examined for coexpression with Trop-2 as a known marker for epithelial cells. These experiments showed that CD24, CD26, SSEA-4, CD164 and CD15 were epithelial markers, as they were coexpressed with Trop-2.

CD49f and Trop-2 were used as main surface markers to separate promising subsets. Those subsets, which section the $CD49f^{+}Trop\text{-}2^{+}$ subset, were regarded as promising, as they could potentially be able to separate subpopulations with distinct differentiation capacities. A set of markers was tested in a coexpression experiment with Trop-2 and CD49f. Two of them were considered to be appropriate for sectioning the $Trop\text{-}2^{+}CD49f^{+}$ subset: CD24 and SSEA-4. Markers as TNAP and SUSD2 (W5C5) were excluded, as they do not coexpress with Trop-2 and they were regarded as appropriate for selection of progenitor cells originating from the prostate stroma (Figure 5.13).

Using a negative control for flow cytometry, two major subsets based on CD49f expression were observed: CD49f-positive (corresponds to $CD49f^{hi}$ in the literature) and CD49f-negative (corresponds to $CD49\text{-}f^{low}$). When the antibody clone GoH3 against CD49f was used in conjunction with a bright fluorochrome (for example R-PE), two clear subsets can be distinguished within the positive fraction: $CD49f^{hi}$ and $CD49f^{low}$. After gating on the $CD49f^{+}$ cells, the following plot depicted Trop-2 and one additional marker of interest. CD24 and SSEA-4 (4A2B8) were identified to section the basal $CD49f^{+}Trop\text{-}2^{+}$ subset into two subsets. Different gating strategies were evaluated and compared in order to discriminate epithelial subsets with various differentiation profiles within the human prostate. When gating on Trop-2-positive cells, which comprises the majority of epithelial cells, two epithelial subsets were observed ($CD24^{+}$ and $CD49f^{hi}$). When gating on both CD49f-positive and negative cells, since CD49f is not

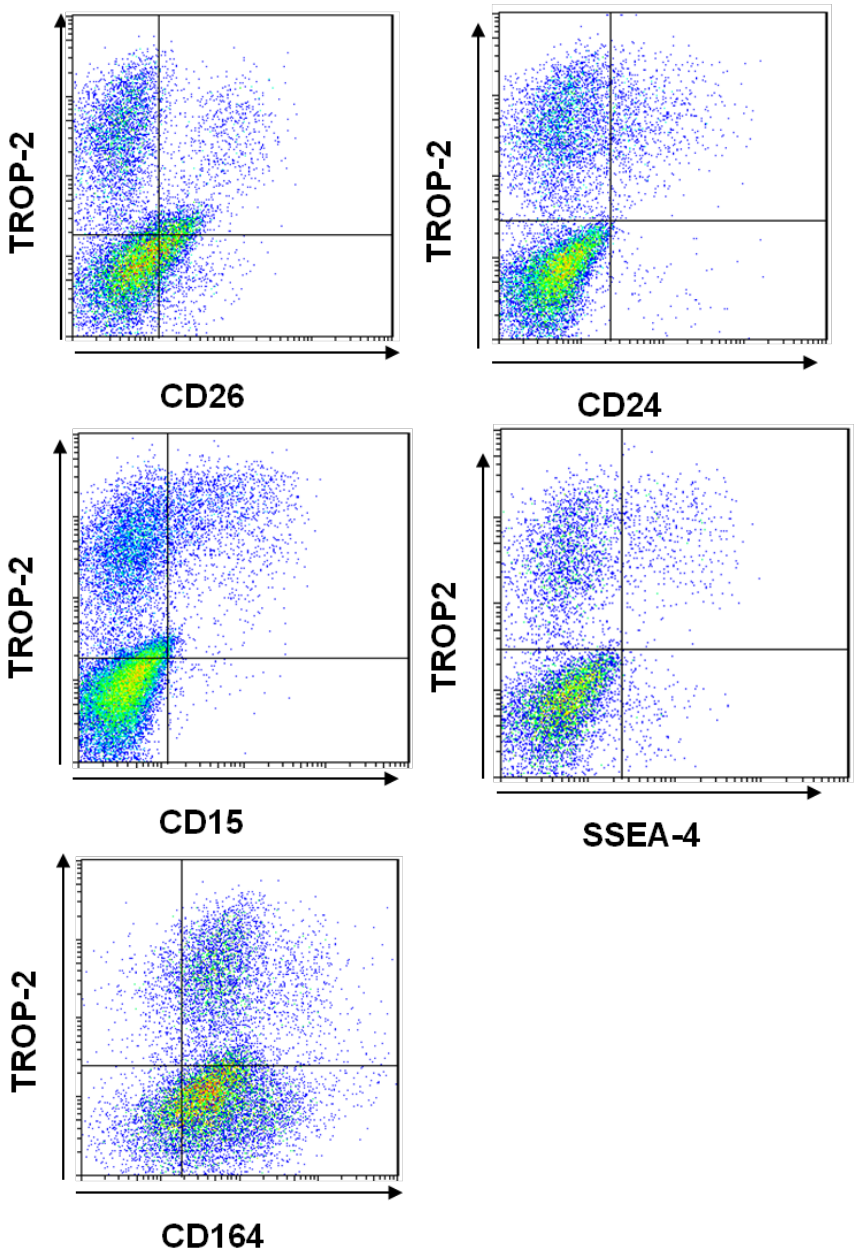

Figure 5.12: Coexpression of markers with Trop-2 on primary prostate. CD24, CD26, SSEA-4, CD164 and CD15 were mostly coexpressed with Trop-2, which can describe them as mainly epithelial markers in prostate tissue.

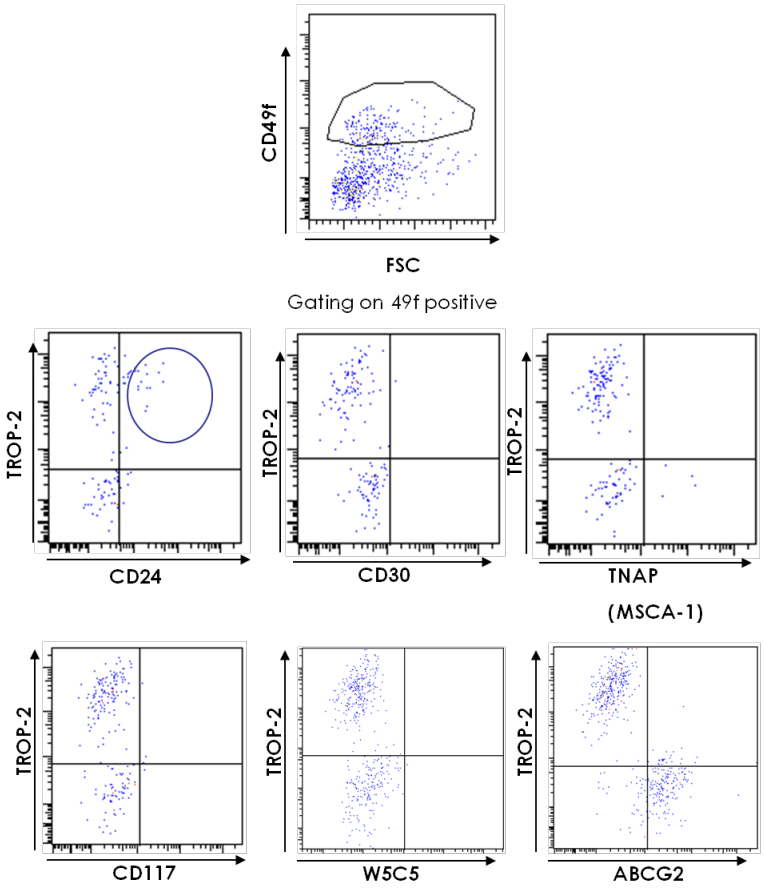

Figure 5.13: Coexpression of markers with Trop-2 and CD49f. The CD49f^{+} subset was selected and further shown as a coexpression window between Trop-2 and another marker. CD24 showed an interesting subset of coexpression of all the markers, whereas the other markers were excluded.

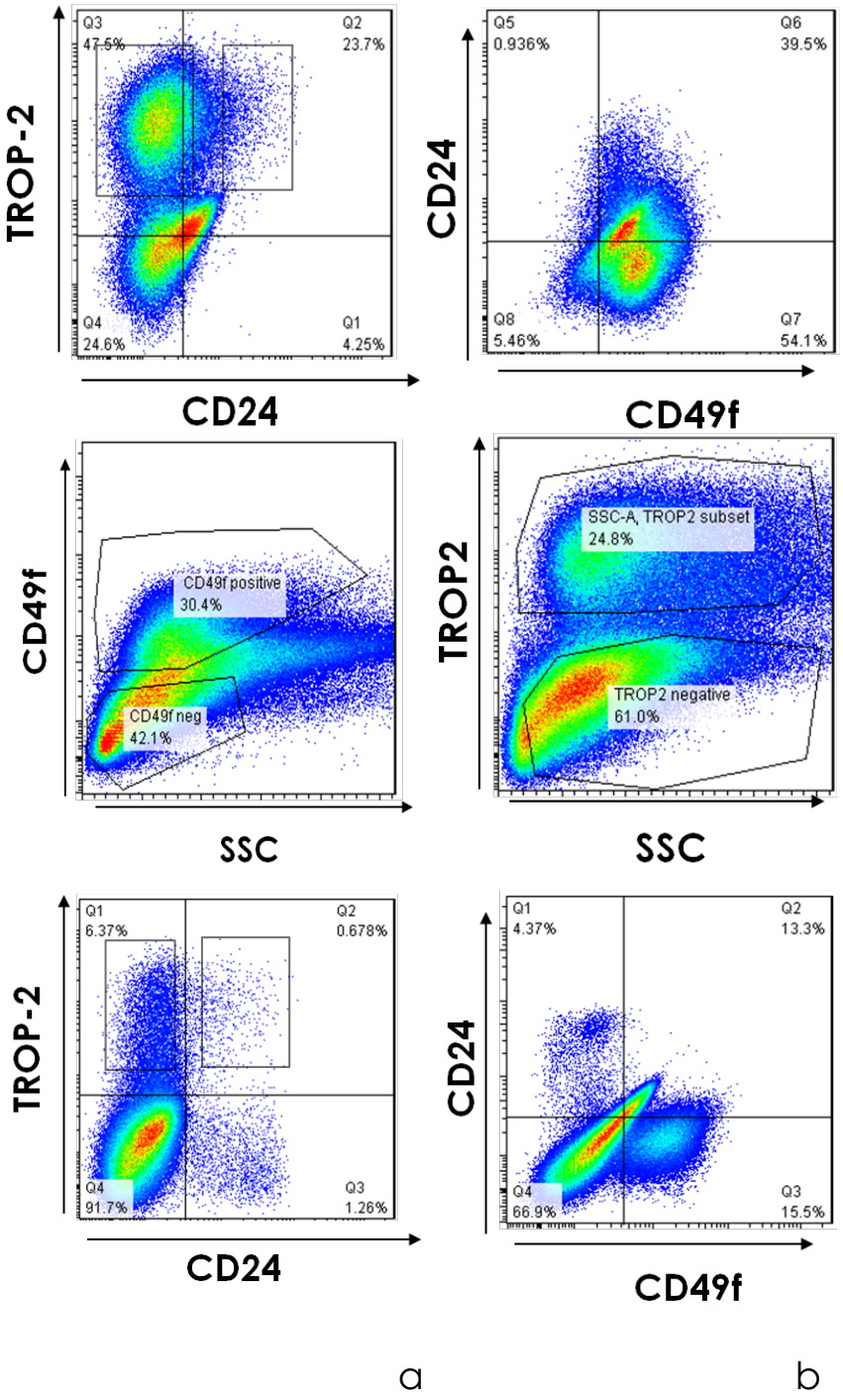

Figure 5.14: Gating on CD49f positive and negative cells shows four different epithelial subsets: CD49f^{+}Trop-2^{+}CD24^{-}, CD49f^{+}Trop-2^{+}CD24^{+}, CD49f^{-}Trop-2^{+}CD24^{-} and CD49f^{-}Trop-2^{+}CD24^{-} (a). Gating on Trop-2 positive cells displays two epithelial subsets (b).

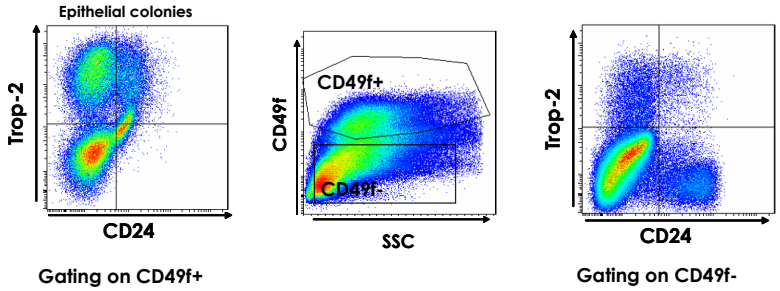

Figure 5.15: Flow cytometry coexpression analysis using the surface markers CD49f, Trop-2 and CD24. When gating on both positive and negative cells, four different epithelial subsets (coexpressed with Trop-2) were found: CD49f$^+$Trop-2$^+$CD24$^-$, CD49f$^+$Trop-2$^+$CD24$^+$, CD49f$^-$Trop-2$^+$CD24$^-$ and CD49f$^-$Trop-2$^+$CD24$^-$.

a selective epithelial marker, four different epithelial subsets were found: CD49f$^+$Trop-2$^+$CD24$^-$, CD49f$^+$Trop-2$^+$CD24$^+$, CD49f$^-$Trop-2$^+$CD24$^-$ and CD49f$^-$Trop-2$^+$CD24$^-$ (Figure 5.14). Within the CD49f$^+$ subset, three distinct cell subsets could be identified: CD49f$^+$Trop-2$^+$CD24$^-$ and CD49f$^+$Trop-2$^+$CD24$^+$ (epithelial) and CD49f$^+$Trop-2$^-$CD24$^-$ (non-epithelial). When further gating on CD49f^{hi} and CD49f^{low} was performed, the same epithelial subsets (in coexpression with CD24 and Trop-2) were found to be available with different density (Figure 5.16).

5.4 FURTHER EXAMINATION OF SURFACE MARKERS

5.4.1 *CD49b*

CD49b is an α_2-integrin subunit, present in the VLA-2 ($\alpha_2\beta_1$) integrin. VLA-2 has been previously reported to enrich prostate epithelial stem/progenitor cells [89, 16]. In our experience, the CD49f$^+$CD49b$^+$ subset enriches colonies, but due to the overlap of their expression, only CD49f was further used to enrich the stem cells in a combination with other markers (Figure 5.17). Another valid reason for excluding CD49b as an epithelial progenitor cell marker was its very high expression on cultivated stromal cells.

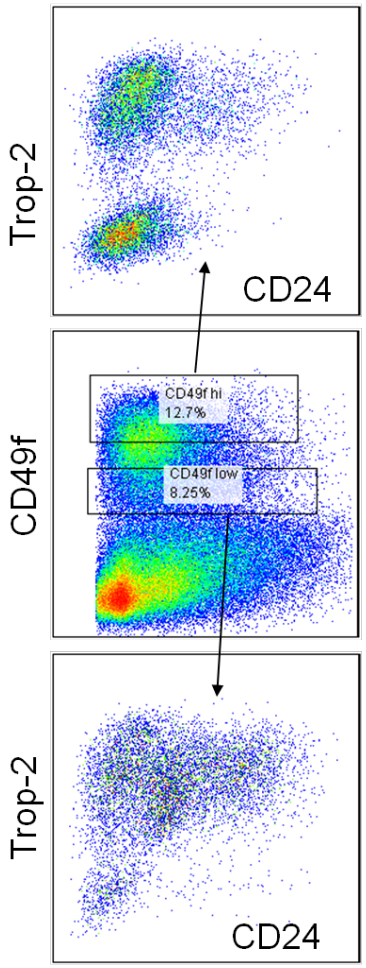

Figure 5.16: Gating on CD49f^{hi} and CD49f^{low} displays CD24^{+} subsets with different density

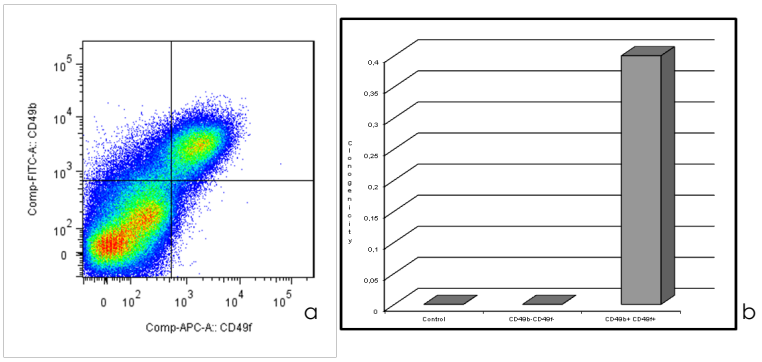

Figure 5.17: Coexpression of CD49b with CD49f (a) and clonogenicity of CD49f^{+}CD49b^{+} subset. the CD49f+ CD49b+ subset enriches the epithelial colonies (b).

5.4.2 *CD117 and CD133*

In line with previous reports [119, 44], the results of this study confirm that CD133 and CD117 are not suitable for prostate epithelial progenitor cell isolation, because they are not consistently expressed on cells of primary BPH or prostate cancer samples Figure 5.18. In addition, both markers were not expressed by cultivated epithelial and stromal cells.

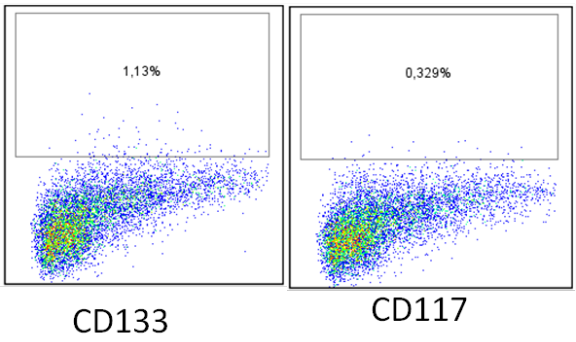

Figure 5.18: Expression of CD133 and CD117. Results showed that both markers were not consistently expressed on cells of primary prostate. FCS is depicted on the x-axis.

5.4.3 *CD44*

The current study shows that CD49f$^+$ cells do not coexpress CD44 in all the examined samples (Figure 5.19). These experiments were performed with two different antibody clones (L178 and IM7). In 6 samples from BPH or prostate cancer patients, coexpression of the two markers was not observed.

CD44 and CD49f were previously described as stem cell markers in human prostate and both of them are expressed in the basal layer. In our experience, only CD49f$^+$ cells, but not CD44$^+$ cells were able to grow into monolayer colonies, suggesting that CD44 is not a marker for stem/progenitor cells in primary prostate. This is in line with the earlier work of Yamamoto et al.. All costaining experiments were performed using the right isotype-matched controls.

Interestingly, CD44 was highly expressed on both epithelial and stromal cultivated cells. As described above, CD44 is a prostate basal epithelial marker, which explains the basal character of the epithelial colonies. On the other hand, CD44 is a mesenchymal stem cell marker in bone marrow. In the current study, CD44 was selectively identified on prostate epithelial and mesenchymal cells, utilizing two different antibodies clones: L178 for the stromal mesenchymal and IM7 for the epithelial cells.

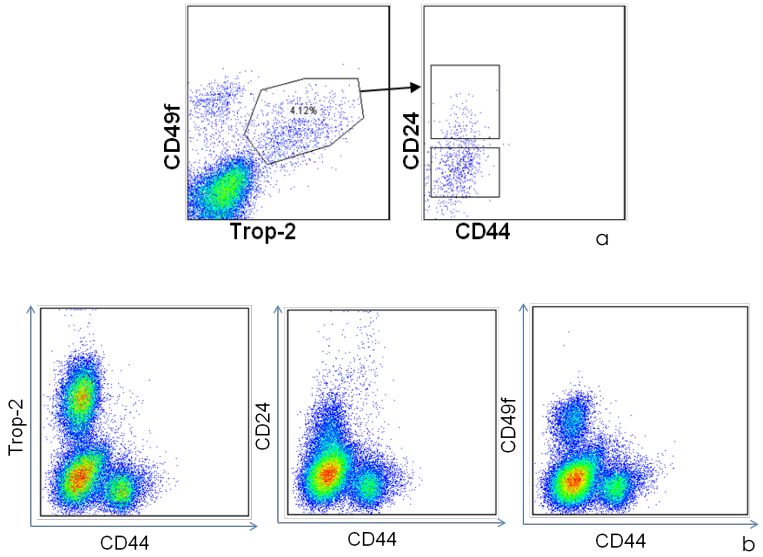

Figure 5.19: Coexpression of CD44 with the basal markers. Gating on CD49f-Trop-2+ cells results in the appearance of CD24+ and CD24- cells, both of which do not coexpress CD44 (a). CD49 and Trop-2 were not coexpressed with CD44, whereas CD24 was coexpressed with CD44 in a very small subset (b).

5.5 FACS SORTING OF THE PROMISING POPULATIONS

After evaluation of the coexpression profiles, promising populations were cell sorted for examination of their clonogenicity. The growth capacity of primary prostate cells from 18 primary BPH samples and 2 prostate cancer samples and their ability to form epithelial colonies was analyzed. Cells plated at a density of 200 cells/cm^2 gave rise to a frequency of clonogenic cells of up to 1/2000. In preliminary experiments, the colonies were able to grow exclusively in the CD49f$^+$CD49b$^+$ subset (Figure 5.17) and in the CD49f$^+$Trop-2$^+$ subset (Figure 5.20), in line with the previously published data [34, 31]. A 12-fold enrichment of epithelial colonies was observed in the CD49f$^+$Trop-2$^+$ subset, which was used as a main subset in the current study (Figure 5.20). To further discriminate between more mature and more primitive progenitors, two additional markers are applied for investigation: CD24 and SSEA-4.

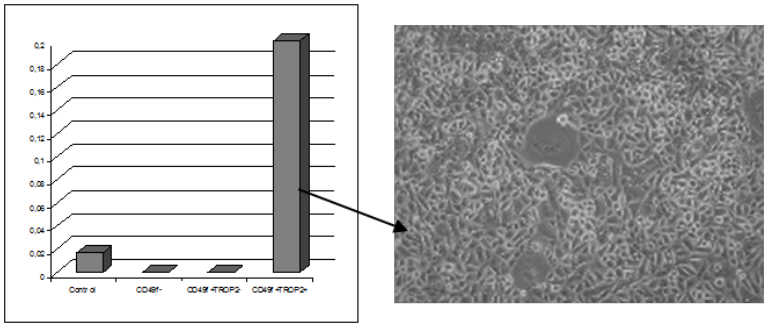

Figure 5.20: Clonogenicity of CD49f and Trop-2 positive cells. The colonies were able to grow exclusively in the CD49f^{+}Trop-2^{+} subset with 12-fold enrichment. The CD49f^{-} and CD49f^{+}Trop-2^{-} subsets did not show any epithelial growth.

With regards to the expression of the markers of interest on primary prostate cells, Table 5.1 shows that Trop-2 is expressed on 20.4 $\pm$2.3%, CD49f on 24.7$\pm$3.3%, CD24 on 8.3$\pm$0.8% and SSEA-4 2.6$\pm$2.0% of total cells.

After gating on the CD49f^{+} subset and employing Trop-2 and CD24, three distinct cell subsets could be identified: CD49f^{+}Trop-2^{+}CD24^{-}, CD49f^{+}Trop-2^{+}CD24^{+} and CD49f^{+}Trop-2^{-}CD24^{-}. Of these, only the CD49f^{+}Trop-2^{+} cells were able to give rise to colonies. The average fraction of CD49f^{+}Trop-2^{+}CD24^{-} cells was 9.4$\pm$2.3% of total cells, whereas CD49f^{+}Trop-2^{+}CD24^{+} cells comprised only 1.3$\pm$0.3%.

Further sorting of the CD49f^{hi} and CD49f^{low} depicted epithelial growth in both subsets. Therefore, only the CD49f^{+}Trop-2^{+} cells were able to give rise to colonies (in our experience both CD49f^{hi} and CD49f^{low}). In subsequent studies, the CD24^{+} and CD24^{-} subsets were analyzed in more detail using 3-color immunofluorescence, cell sorting and colony forming assays.

5.5.1 *Localization of the examined markers*

It was previously reported that CD49f and Trop-2 are expressed in the basal epithelium [34, 31], which is confirmed in the current study using a set of immunofluorescence experiments. In all BPH samples examined with flow cytometry analysis, a CD24^{+}-positive subset was found to be coexpressed with CD49f, which is strongly considered to be a marker of the basal layer in human and murine prostates [66, 36]. In the current experiments, the localization of CD49f was confirmed to be within the basal compartment, while of CD24 and Trop-2 — in the basal and luminal layer (Figure 5.21). Within the luminal layer, Trop-2 was highly expressed in the proximal compartment, which corresponds to the luminal intermediate cells, whereas it was not found in the distal compartment, which corresponds to the terminally differentiated luminal secretory cells. SSEA-4 was found to be

sample	% of expr. in BPH CD24	Trop-2	CD49f	Gated on CD49f $CD24^+$	$CD24^-$	% of all viable cells $CD24^+$	$CD24^-$
1	16.0	18.3	4.2	2.9	20.1	0.1	0.8
2	10.6	6.5	10.6	0.8	8.9	0.1	0.9
3	12.6	11.7	25.6	0.4	8.1	0.1	2.1
4	6.1	8.3	1.5	6.6	18.8	0.1	0.3
5	6.8	14.6	20.4	1.1	26.8	0.2	5.5
6	9.3	13.9	28.3	5.3	22.4	1.5	6.3
7	3.2	14.9	19.8	1.0	25.9	0.2	5.1
8	3.4	22.5	26.6	2.2	36.5	0.6	9.7
9	9.6	30.7	29.9	7.0	52.4	2.1	15.7
10	6.5	34.7	12.3	6.7	30.1	0.8	3.7
11	11.3	26.0	19.9	6.2	21.8	1.2	4.3
12	4.7	5.9	5.6	11.5	12.6	0.6	0.7
13	13.5	25.3	34.5	7.9	28.0	2.7	9.7
14	9.5	33.8	36.9	3.3	48.2	1.2	17.8
15	13.2	13.7	24.4	16.9	15.3	4.1	3.7
16	8.9	9.4	22.6	9.9	22.0	2.2	5.0
17	2.8	31.0	8.0	3.8	59.6	0.7	10.7
18	7.8	46.0	54.9	7.7	65.8	4.2	36.1
19	3.6	24.3	54.6	3.2	54.2	1.7	29.6
20	2.5	24.9	51.1	2.4	60.9	1.2	31.1
21	11	11.5	30.9	6.7	14.3	2.1	4.4
Mean	8.3	20.4	24.7	5.3	30.6	1.3	9.4
SEM	0.8	2.3	3.3	0.9	3.9	0.3	2.3

Table 5.1: Marker expression on total unfractionated cells

expressed by the prostate gland epithelium and visualized in the region between the basal and luminal layer (Figure 5.21). CD164 was expressed strongly by the luminal compartment of human prostate (Figure 5.21).

In addition, bcl-2, CK5 and p63 were localized in the basal compartment, while androgen receptor (AR) — in the luminal compartment (Figure 5.22). CK17 was a trans-epithelial marker (Figure 5.22). ALDHA1 was expressed in the basal layer of the epithelial compartment, as well as in the stromal cells, directly surrounding the epithelial acini (Figure 5.24).

5.6 CD24 AS A MARKER OF TRANSIT-AMPLIFYING CELLS

5.6.1 *$CD49f^+Trop\text{-}2^+CD24^-$ cells are more clonogenic than $CD49f^+Trop\text{-}2^+CD24^+$ cells*

Eighteen primary BPH and two cancer samples were utilized to perform cell sorting in combination with CD24, Trop-2 and CD49f. The clonogenic capacity of the cells from the resulted subsets was mi-

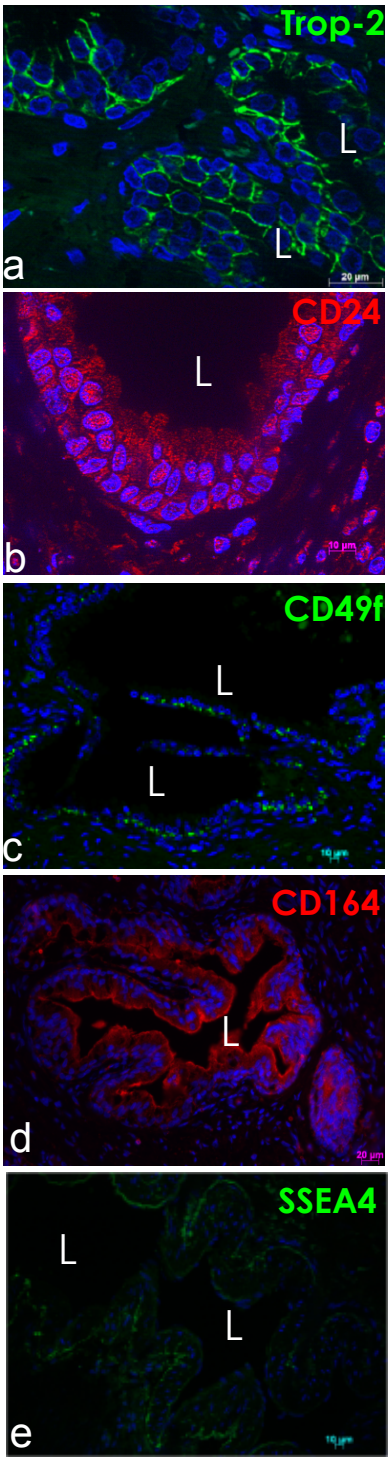

Figure 5.21: Expression of surface markers in human prostate. CD49f is localized in the basal epithelium (a), Trop-2 and CD24 are localized in both basal and luminal compartments (b,c), SSEA-4 was localized in the gland epithelium, in the region between the basal and luminal layers (d), CD164 was expressed strongly in the luminal compartment (d).

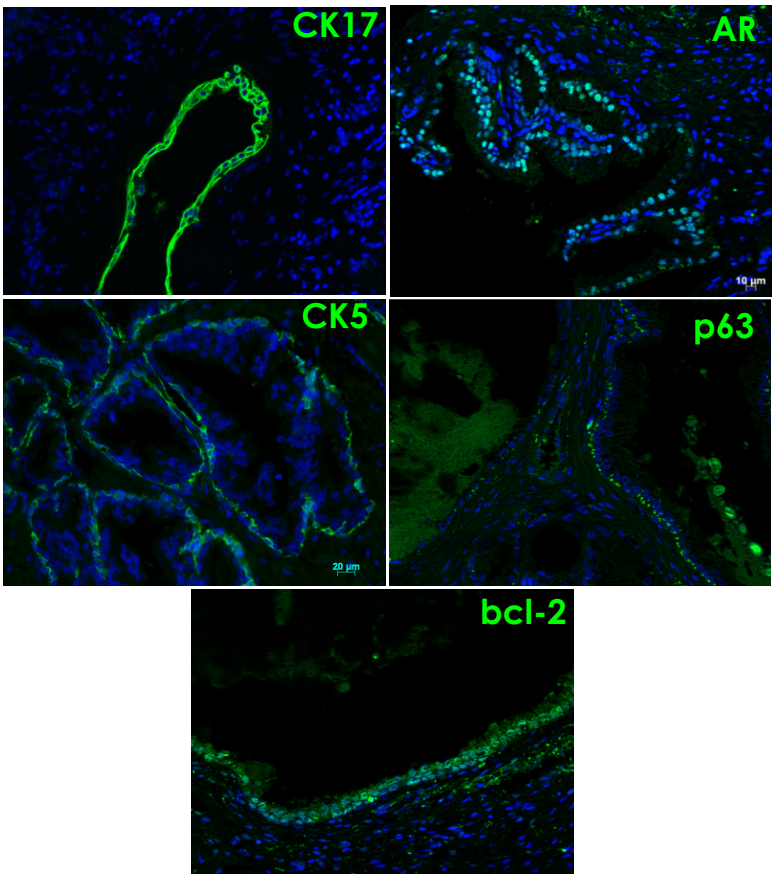

Figure 5.22: Expression of intracellular markers in human prostate. CK17 was a trans-epithelial marker, expressed in both basal and luminal compartments of the prostate epithelium. The markers bcl-2, CK5 and p63 were expressed in the basal layer of the epithelium, while androgen receptor (AR) – in the luminal layer.

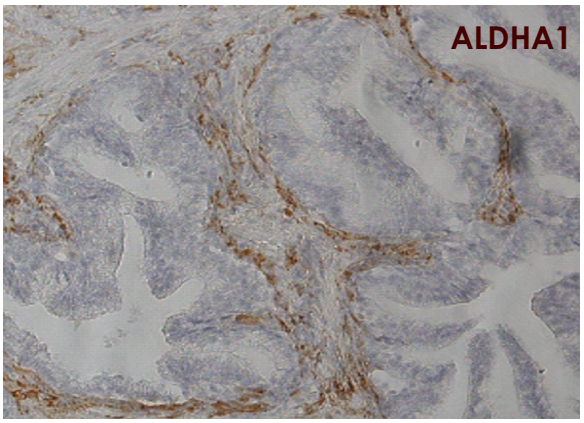

Figure 5.23: ALDHA1 expression in human prostate. ALDHA1 was expressed in the basal layer of the epithelial compartment, as well as in the stromal cells, directly surrounding the epithelial acini.

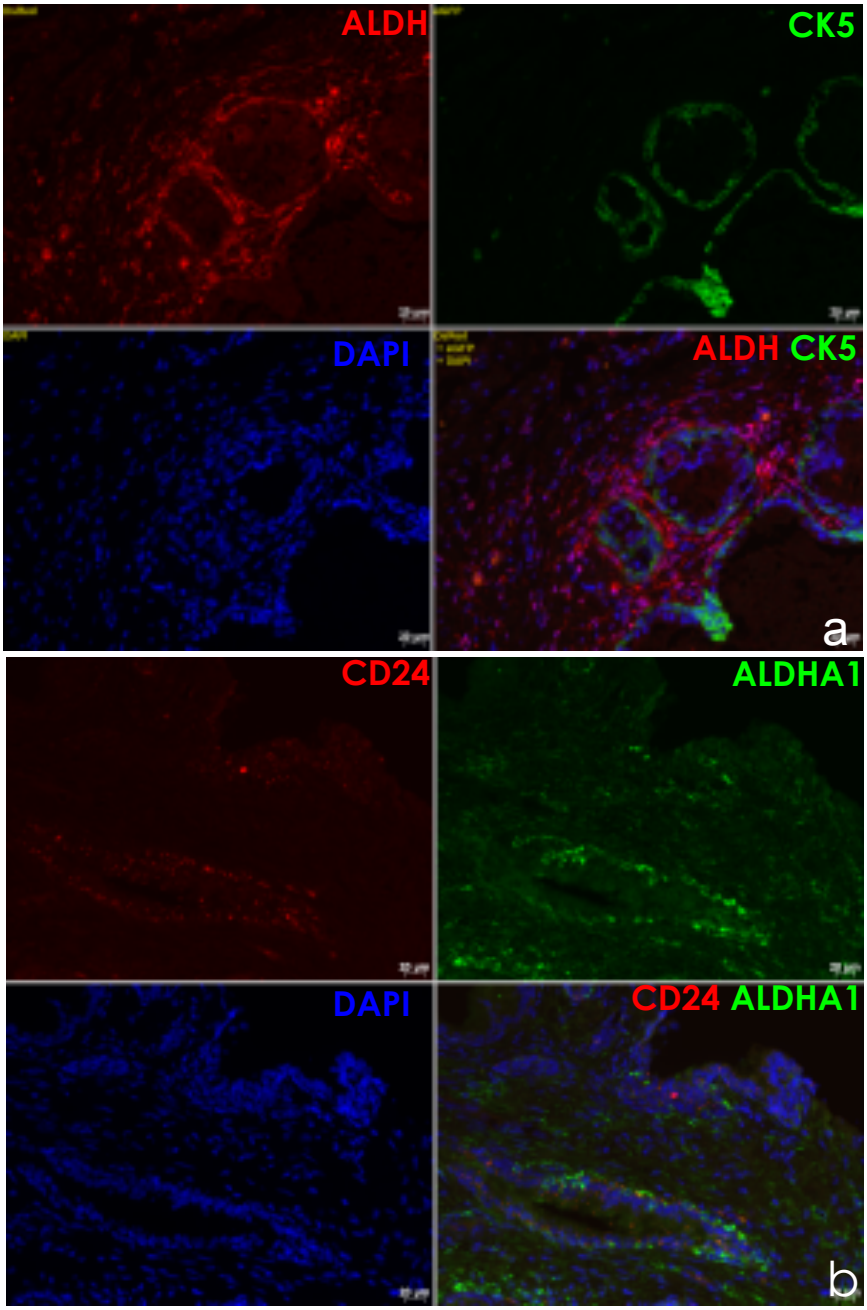

Figure 5.24: ALDHA1 coexpression with CK5(a) and CD24(b). ALDH is not coexpressed exclusively with CK5 and in the epithelium, it is spreaded in the stroma (a). ALDH1 shows coexpression wht CD24 in some cells (b).

croscopically examined on day 14 after cell sorting. Only cells from CD49f$^+$Trop-2$^+$CD24$^-$ and CD49f$^+$Trop-2$^+$CD24$^+$ subsets, but no other subsets, were able to grow and give rise to colonies. In 14 FACS sorted benign samples, clonogenic cells were found in both subsets, whereas in 4 samples colonies grew only from the CD49f$^+$Trop-2$^+$ CD24$^-$ subset.

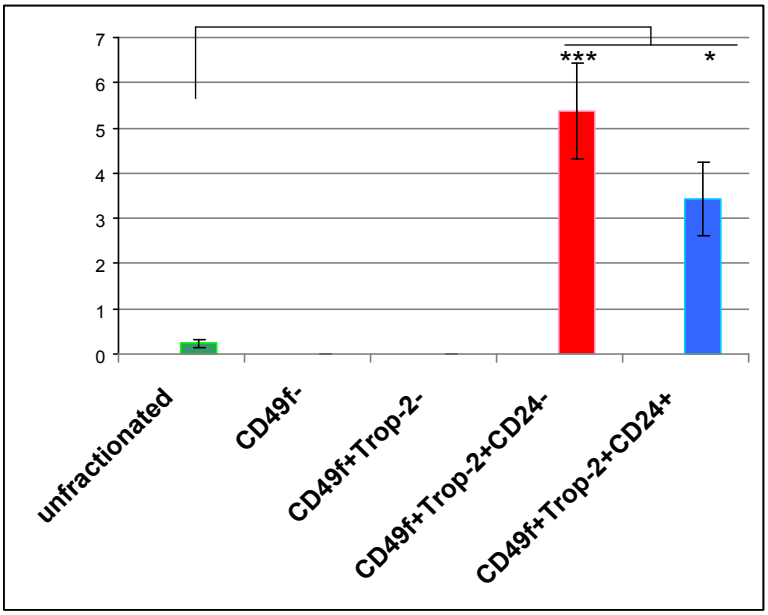

Figure 5.25: Clonogenicity of CD24 sorted cells. Only cells from CD49f$^+$Trop-2$^+$CD24$^-$ and CD49f$^+$Trop-2$^+$CD24$^+$ subsets, but no other subsets, were able to grow and give rise to colonies.

As determined by ANOVA test, the enrichment for colonies in both subsets was statistically significant, when compared with the unfractionated cells (Figure 5.25). On average, colonies were enriched 14.3 times in the CD49f$^+$Trop-2$^+$CD24$^+$ subset and 22.5 times in the CD49f$^+$Trop-2$^+$CD24$^-$ subset. The ANOVA test did not confirm statistical differences in the number of colonies derived from the CD49f$^+$ Trop-2$^+$CD24$^-$ and CD49f$^+$Trop-2$^+$CD24$^+$ subsets. These results demonstrated a tendency that the CD24$^-$ subset was capable of forming more colonies in comparison to the CD24$^+$ subset by a 1.6-fold factor.

CD24$^-$ cells are able to grow into colonies at an approximately 1.6 fold increased proliferation rate compared to the CD24$^+$ cells. Our data are based on the examination of 18 samples from primary BPH. Independently of this high number of samples, we were unable to present reliable statistical measures, but rather a general tendency (Figure 5.26). The data is not directly comparable, due to the existence of confounding factors, such as age and health conditions, as well as systematic errors inherent to the method. The variance between different patient samples might also be influenced by factors such as tissue treatment and handling procedures.

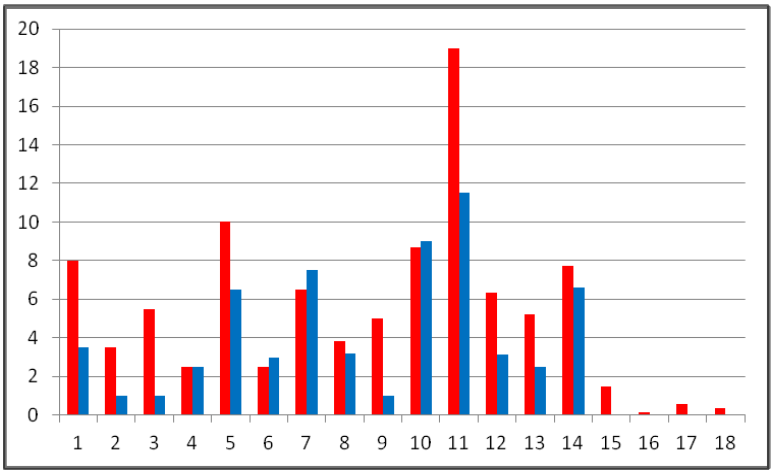

Figure 5.26: Clonogenicity of the two subsets, presented separately for the 18 patient samples. In eight samples the clonogenic potential of the CD49f$^+$Trop-2$^+$CD24$^-$ and CD49f$^+$Trop-2$^+$CD24$^+$ subsets was similar, seven samples cells of the CD49f$^+$Trop-2$^+$CD24$^-$ subset gave rise to increased colony numbers, and in four samples only cells from the CD49f$^+$Trop-2$^+$CD24$^-$ fraction were able to form colonies.

Based on the heterogeneous clonogenic capability of the cells in the CD24$^+$ subsets, three groups in the examined tissue samples could be distinguished. In eight samples the clonogenic potential of the CD49f$^+$Trop-2$^+$CD24$^-$ and CD49f$^+$Trop-2$^+$CD24$^+$ subsets was similar, seven samples cells of the CD49f$^+$Trop-2$^+$CD24$^-$ subset gave rise to increased colony numbers, and in four samples only cells from the CD49f$^+$Trop-2$^+$CD24$^-$ fraction were able to form colonies (Figure 5.27). In contrast to the subsets described above, CD49f$^-$ cells as well as CD49f$^+$Trop-2$^-$CD24$^-$ cells failed to give rise to colonies in all examined samples.

In addition, renewal capacity of the two subsets was examined. Two approaches were used. In the first experiment, single-cell sorting was performed using a 96-well plate, in order to gain a colony from a cell. Alternatively, colonies from the both examined fractions were trypsinized using clonal rings. Next, each cell per colony was replated in another 96-well plate. Further growth was observed in the CD24$^-$ subset only. Moreover, the cells gained from paraclones were not able to grow into colonies, whereas one single cell from the mesoclones was able to grow into another mesoclone. Because of the lower plating rate, holoclones were not able to grow when this approach was used (Table 5.2).

In the second experiment, cells originating from CD49f$^+$Trop-2$^+$CD24$^+$ and CD49f$^+$Trop-2$^+$CD24$^-$ colonies, were continuously replated in order to measure the differences in their growth. The cell count was determined in each passage.

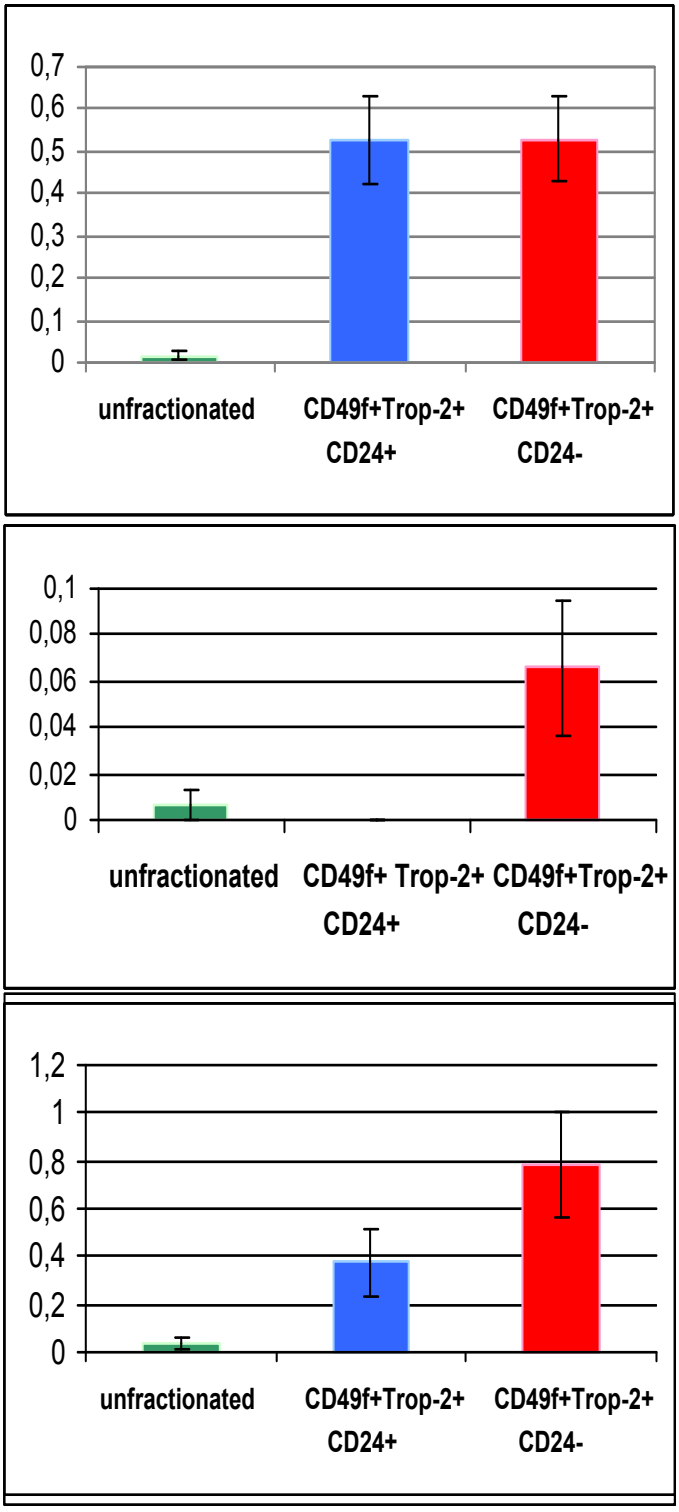

Figure 5.27: Groups of samples based on their clonogenic capability. Three grous were identified: in eight samples the clonogenic potential of the CD49f$^+$Trop-2$^+$CD24$^-$ and CD49f$^+$Trop-2$^+$CD24$^+$ subsets was similar, seven samples cells of the CD49f$^+$Trop-2$^+$CD24$^-$ subset gave rise to increased colony numbers, and in four samples only cells from the CD49f$^+$Trop-2$^+$CD24$^-$ fraction were able to form colonies.

			P0	P1
11.211	$CD24^-$/low	xs	4	-
		s	1	-
		m	1	1
	$CD24^+$	-	-	-
11.228	$CD24^-$/low	xs	2	-
	$CD24^+$	m	1	-
11.285	$CD24^-$/low	s	1	-
	$CD24^+$	xs	1	-
11.282	$CD24^-$/low	s	2	-
		m	1	1
	$CD24^+$	xs	2	-

Table 5.2: Renewal capacity of the $CD24^+$ and $CD24^-$ subsets. $CD49f^+Trop\text{-}2^+CD24^+$ and $CD49f^+Trop\text{-}2^+CD24^-$ colonies, were continuously replated and only the $CD49f^+Trop\text{-}2^+CD24^-$ mesoclones were able to produce new colonies.

The single-cell sorting experiment demonstrated the process of self-renewal. The capability of a single cell per colony to grow into another colony for 14 days was observed. However, this method disregards any aspects of the cell-to-cell interaction. In many experiments with handling prostate epithelial cell cultures in this work, density dependancy of the process of cell growth was observed. This is the motivation for the inclusion of the second experiment.

5.6.2 *$CD24^+$ and $CD24^-$ colonies show a similar basal phenotype*

Cells derived from FACS sorted $CD49f^+Trop\text{-}2^+CD24^-$ and $CD49f^+Trop\text{-}2^+CD24^+$ colonies were examined for expression of trans-epithelial, basal and luminal markers. Firstly, the three types of colonies (holoclones, mesoclones and paraclones) were examined and all of them expressed CK5 strongly and CK18 weakly (Figure 5.28).

Secondly, the cells from both fractions expressed CD24, CD49f, Trop-2 and CD44 at very high levels (90–100% positive cells). Remarkably, the cells derived from the $CD49f^+Trop\text{-}2^+CD24^-$ subset were also positive for CD24 (Figure 5.29). Moreover, flow cytometry analysis revealed that colonies from both subsets exhibit high expression levels of epithelial markers (CD49f, CD49b, Ep-CAM, Trop-2, E-cadherin, Her2 and Her3), low expression of the luminal marker CD26 and lack of expression of the stromal marker CD90 in both subsets (Figure 5.29). CD49f, CD49b, Her2 and CD44 are known to be markers for prostate basal epithelium in human [84]. Therefore, the colonies derived from both subsets demonstrate a basal phenotype.

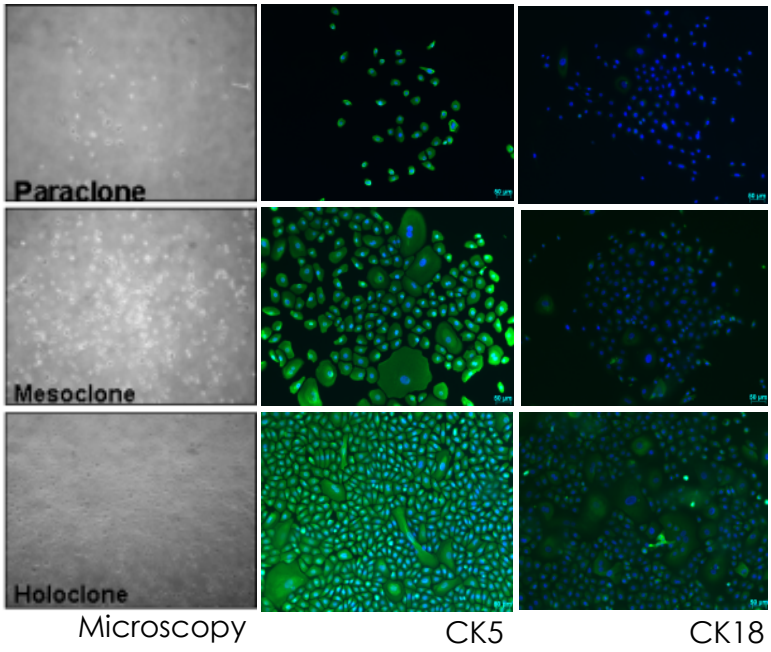

Figure 5.28: Epithelial colonies: paraclones, mesoclones and holoclones. The three types of colonies are defined on the number of cells and showed different size and cell density on microscopy. The three types of colonies showed strong expression of the basal marker CK5 and and weak expression of luminal marker CK18. CK18 was expressed on cells with very long and spindle-shape scattered and rare neuroendocrine cells.

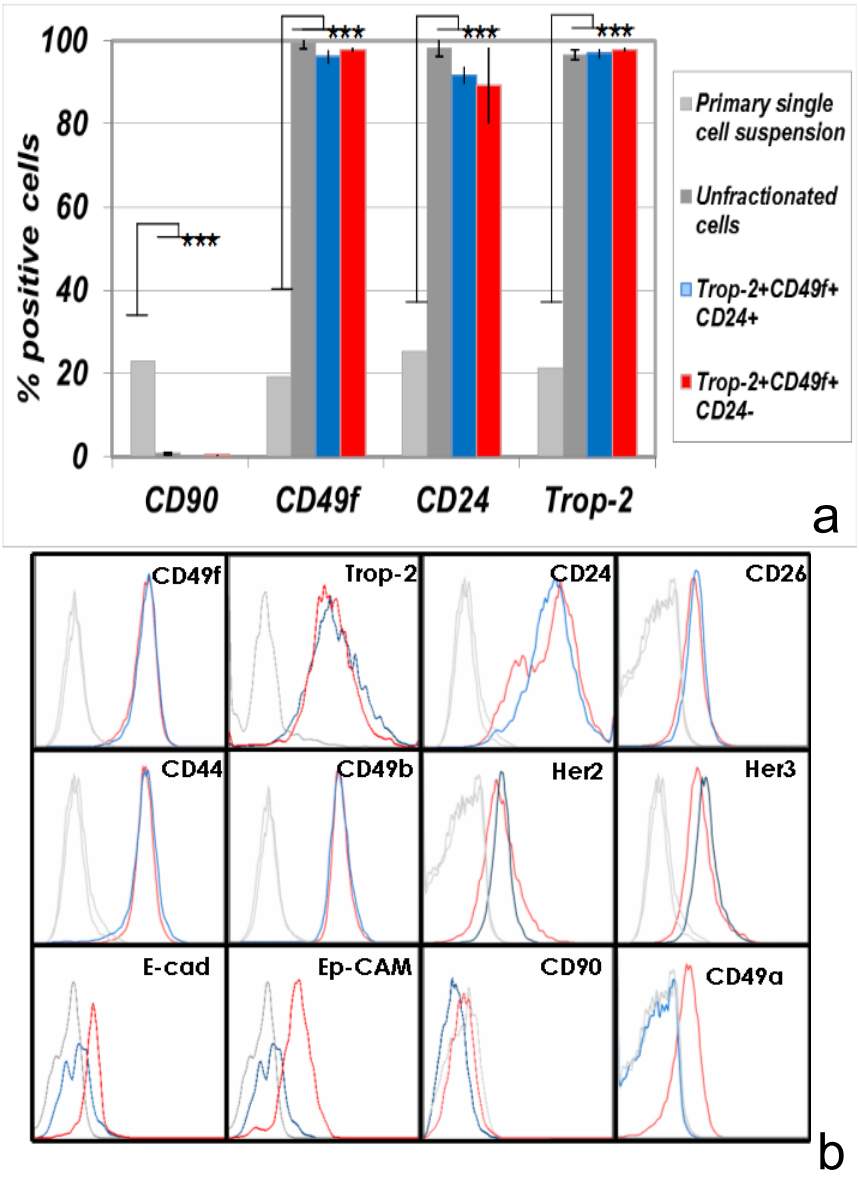

Figure 5.29: Flow cytometry analysis shows that colonies derived from CD49f$^+$Trop-2$^+$CD24$^-$ cells and CD49f$^+$Trop-2$^+$CD24$^+$ cells express high levels of CD49f, Trop-2 and CD24, but are negative for the stromal marker CD90. The expression is compared in primary and unfractionated prostate cells (a). Flow cytometry analysis of colonies derived from CD49f$^+$Trop-2$^+$CD24$^-$ and CD49f$^+$Trop-2$^+$CD24$^+$ cells. Cells of both colonies expressed the epithelial markers Ep-CAM, E-Cadherin, Trop-2, Her3, CD49f, CD49b, CD44, and Her2 (b). FCS is shown on the x-axis.

Real-time PCR analysis of the colonies derived from both subsets confirmed high expression levels of basal markers (cytokeratin 5 (CK5), cytokeratin 14 (CK14), p63, SOX9, bcl2a and bcl2b), low expression of some luminal markers (CK8, CK18, AR), as well as lack of PSA expression (Figure 5.30 and Figure 5.31). As demonstrated by Western blot analysis, high expression of CK5, moderate of p63 and very low expression of CK18 was also detected on protein level in colonies raised from both subsets (Figure 5.30). In addition, cells from both colonies were able to proliferate at similar levels, with relatively higher rate for the CD49f$^+$Trop-2$^+$CD24$^-$ colonies over CD49f$^+$Trop-2$^+$CD24$^+$ (Figure 5.29).

Colonies derived from CD24$^-$ and CD24$^+$ cells were examined for ALDHA1 activity. The results showed that the enzyme-active cells varied in the order of 10–30% (Figure 5.32). ALDHA1-active cells relate to the basal compartment of the human prostate.

5.6.3 *The CD49f$^+$Trop-2$^+$CD24$^+$ subset exhibits higher levels of differentiation than the CD49f$^+$Trop-2$^+$CD24$^-$ subset*

In the search for surface markers able to distinguish between basal stem/progenitor and early intermediate cells in prostate, four epithelial subsets were cell sorted, mRNA was amplified and gene expression analysis using Real-time PCR was performed. The examined subsets were CD49f$^+$Trop-2$^+$CD24$^-$, CD49f$^+$Trop-2$^+$CD24$^+$, CD49f$^-$Trop-2$^+$CD24$^-$ and CD49f$^-$Trop-2$^+$CD24$^-$. As basal markers, CK5 and p63 were utilized, as intermediate markers — PSCA and CK17 and as luminal markers — CK8, CK18, AR and PSA. CK5 is a marker, which is supposed to be expressed at highest levels by the cells at the lowest differentiation stage, whereas p63 is expressed by transit-amplifying and differentiated basal cells, but not by primitive stem/progenitor cells [62].

The results presented on Figure 5.33 confirmed the hypothesis that the CD49f$^+$Trop-2$^+$CD24$^-$ cells were the least differentiated in comparison to the cells from the CD49f$^+$Trop-2$^+$CD24$^+$ subset. CK5 was expressed at the highest levels by the CD49f$^+$Trop-2$^+$CD24$^-$ subset, whereas the differentiation markers (p63, CK8/18, AR) were expressed at the lowest level. Moreover, from the four examined subsets, CD49f$^-$Trop-2$^+$CD24$^+$ showed expression patterns typical for the intermediate luminal phenotype, characterized by the highest expression of luminal markers (CK8, CK18, PSA and AR), as well as more pronounced expression of the intermediate markers CK17 and PSCA (Figure 5.33). The lack of expression of CD49f by this subset shows that it is localized in the luminal layer.

The CD49f$^-$Trop-2$^+$CD24$^-$ subset expressed at highest levels the basal maker p63 as shown on Figure 5.33, indicating that this subset may contain differentiated basal cells. These results suggest that the

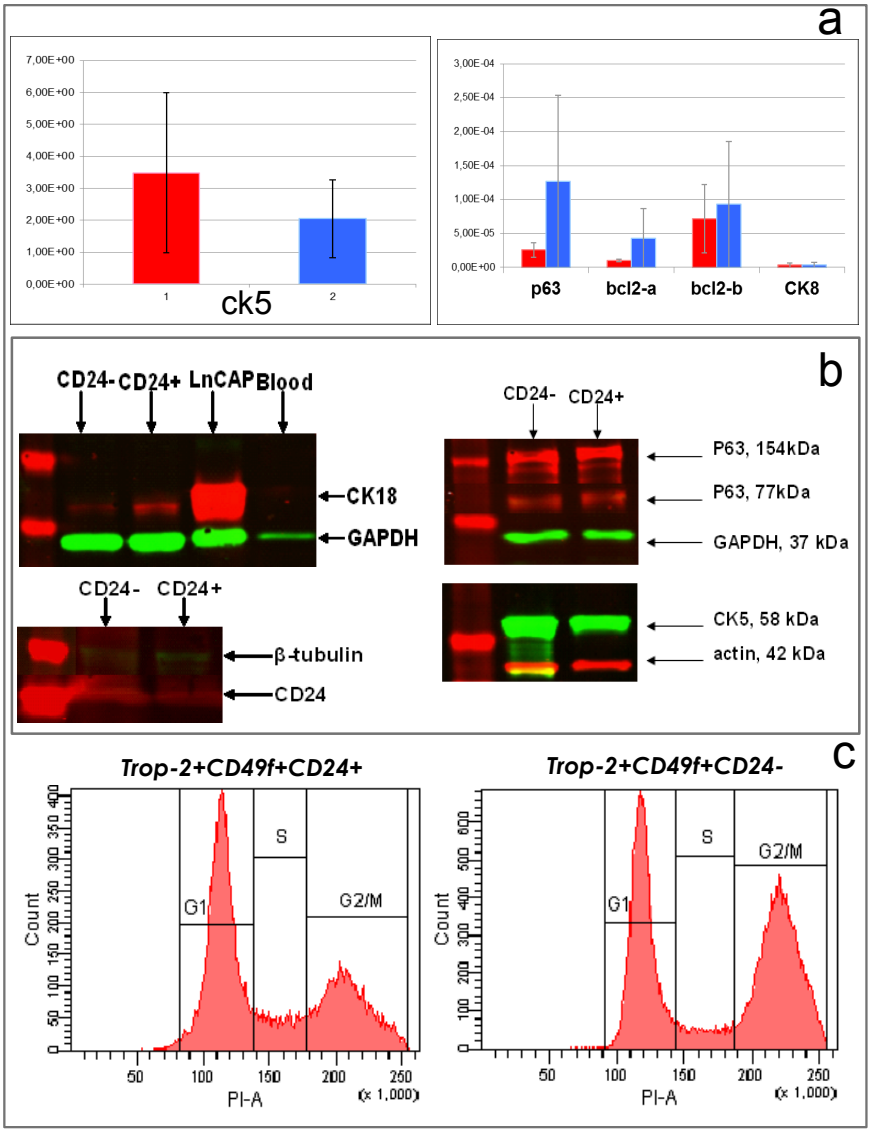

Figure 5.30: qPCR analysis shows that cells of both groups of colonies express at high levels the basal makers CK5, p63, bcl2-a and bcl2-b but low levels of the luminal markers CK8 and CK18 (a). Western blot analysis shows high expression of CK5 and low expression of CK18 within the colonies derived from both fractions. The colonies were positive for p63 and CD24, as the results from PCR (for p63) and flow cytometry (for CD24) show (b). Relatively higher proliferation of the $CD49f^{+}Trop\text{-}2^{+}CD24^{-}$ in comparison to the $CD49f^{+}Trop\text{-}2^{+}CD24^{+}$ colonies (c)

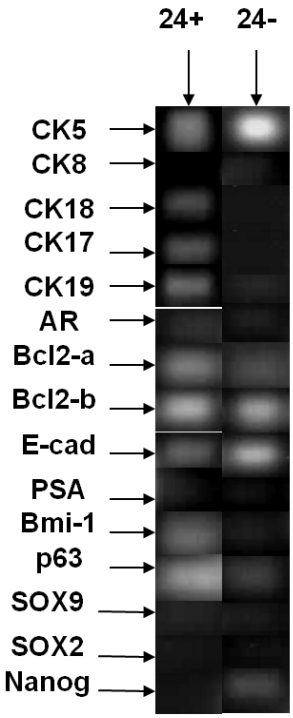

Figure 5.31: PCR analysis shows that cells of both colonies express at high level CK5, bcl2-a, bcl2-b, E-cadherin, p63, low expression of CK18, no expression of PSA, CK8, SOX2, SOX9; the cells from $CD49f^{+}Trop\text{-}2^{+}CD24^{+}$ colonies expressed the TA marker p63 and intermediate markers CK17 and CK19 at higher levels.

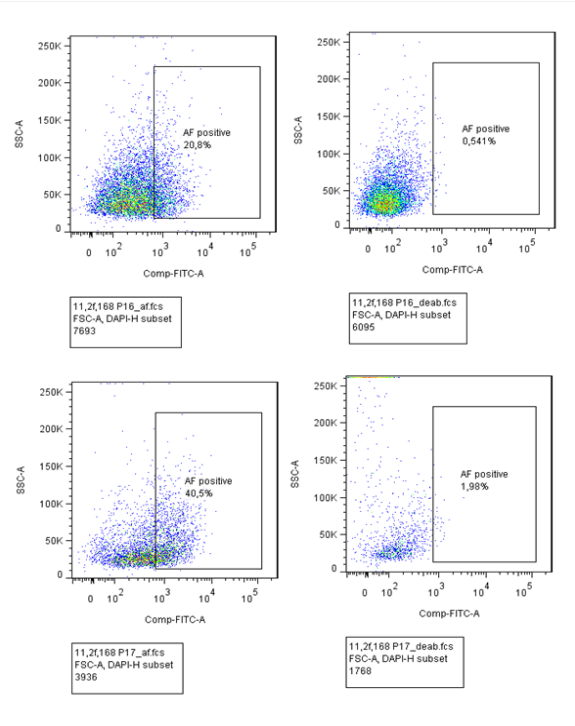

Figure 5.32: ALDHA1 activity of $CD24^+$ and $CD24^-$ colonies. The results showed that the enzyme-active cells were presented in both colonies. The gated controls are visualized on the right.

expression pattern of the $CD49f^+Trop\text{-}2^+CD24^+$ subset is similar to the one of the transit-amplifying/intermediate basal phenotype.

5.6.4 *Localization of CD24 in the human prostate gland*

As shown previously in this chapter, CD24 was found to be localized in both the basal and luminal compartments.

Detailed immunohistochemical studies on different epithelial structures showed that the expression of CD24 differs depending on the structures within the prostate gland. Small glandular buds, typical secretory acini (multi or two layer glands) and main collecting ducts (two layer glands) were examined. These experiments showed that CD24 is expressed in both the center and the periphery of the small glandular buds. Respectively, CD24 is expressed in both basal and luminal epithelium of the glandular acini and only in the luminal layer of the collecting ducts (Figure 5.34).

5.6.5 *CD24 is coexpressed with basal and luminal markers*

In primary tissue, a small subset of ALDHA1-active cells coexpressed CD24, which relates to cells, found to coexpressed CD24 and ALDH1 in basal epithelium (Figure 5.35). Additionally, almost all of the $ALDH^+$

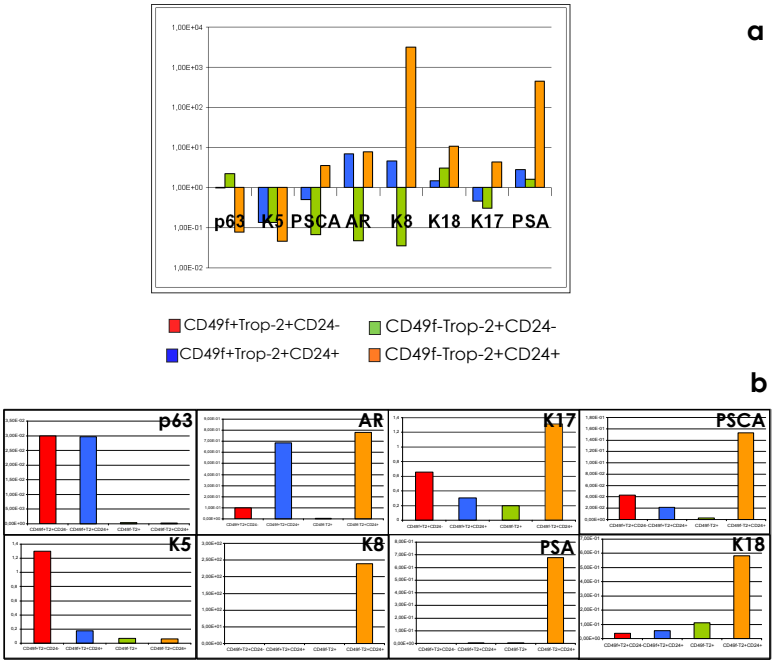

Figure 5.33: Real-time PCR analysis of marker expression in primary prostate: CD49f$^+$Trop-2$^+$CD24$^-$ and CD49f$^-$Trop-2$^+$CD24$^-$ cells showed expression of basal phenotype markers, whereas the CD49f$^+$Trop-2$^+$CD24$^+$ showed a basal intermediate phenotype and the CD49f$^-$Trop-2$^+$CD24$^+$ — a luminal intermediate phenotype (a). The 8 markers are shown separately for the four subsets (b)

cells were positive for CD49f and Trop-2 (Figure 5.35). As CD24 and Trop-2 are regarded as epithelial markers in the prostate, the coexpressed ALDHA1-active cells are therefore localized in the epithelial compartment.

The coexpression of intracellular CK5 and cell surface CD24 in primary BPH and cancer tissues was analyzed. A subset of CD24$^+$ cells showed coexpression of CK5 in all 6 samples (Figure 5.19).

Immunofluorescence analysis of prostate tissues showed coexpression of CD24 and the basal and intermediate marker CK5 in a few cells within the basal epithelium [48, 52] and lack of expression of AR in the basal CD24$^+$ cells Figure 5.38. As previously mentioned in this section, the CD49f$^+$CK5$^+$CD24$^+$ subset contains approximately 1.3$\pm$0.3% of the cells in BPH.

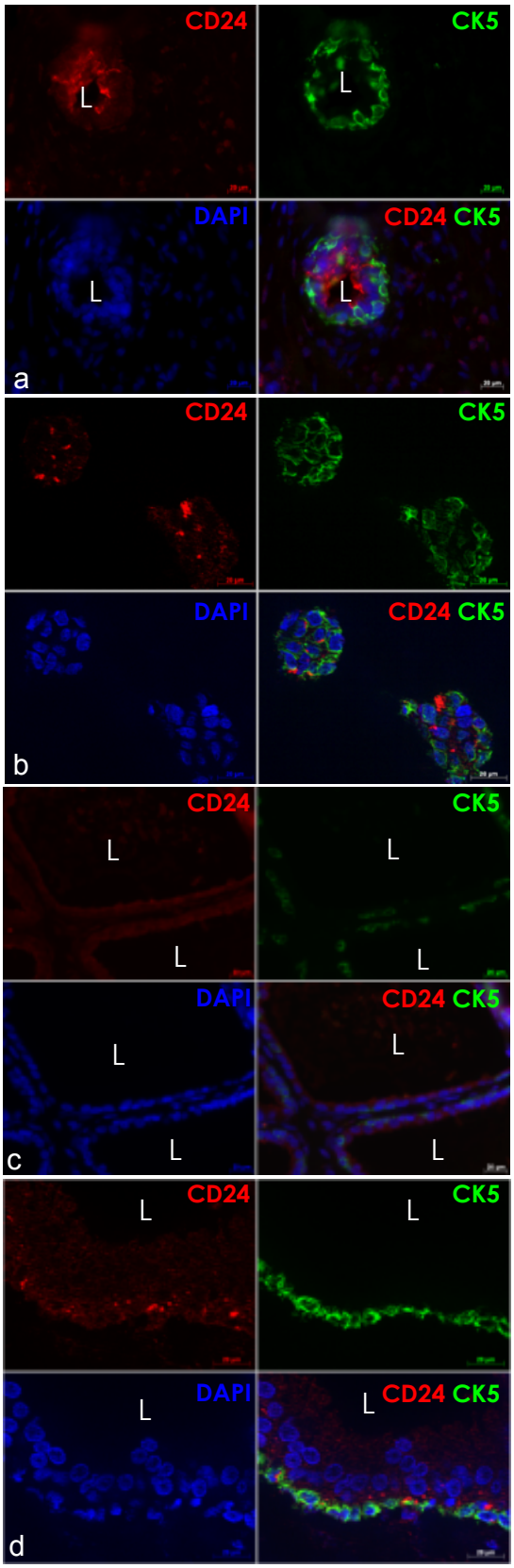

Figure 5.34: Different epithelial structures and CD24 expression. In small glandular buds CD24 is located in the center of the bud or in the basal layer (a,b), in the collecting ducts CD24 is found exclusively in the luminal layer, whereas in the glandular acini CD24 is expressed in both basal and luminal epithelium (d).

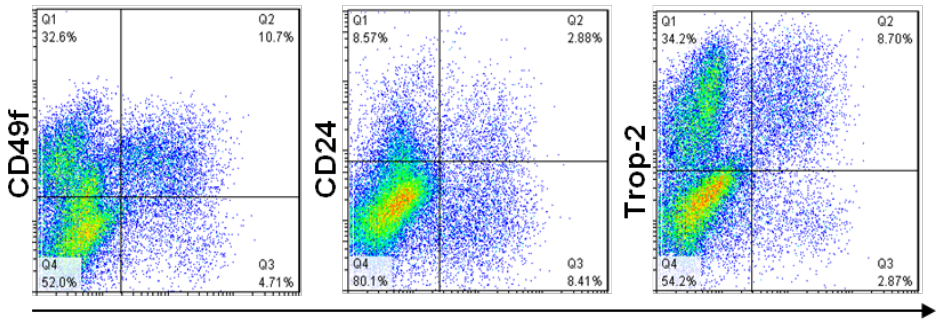

Figure 5.35: ALDH1 expression analysis of defined cellular subsets: subsets of CD49f$^+$, Trop-2$^+$ and CD24$^+$ cells coexpress functionally active ALDH1. Almost all of the ALDH$^+$ cells were positive for CD49f and Trop-2, whereas small subset of ALDHA1-active cells coexpressed CD24.

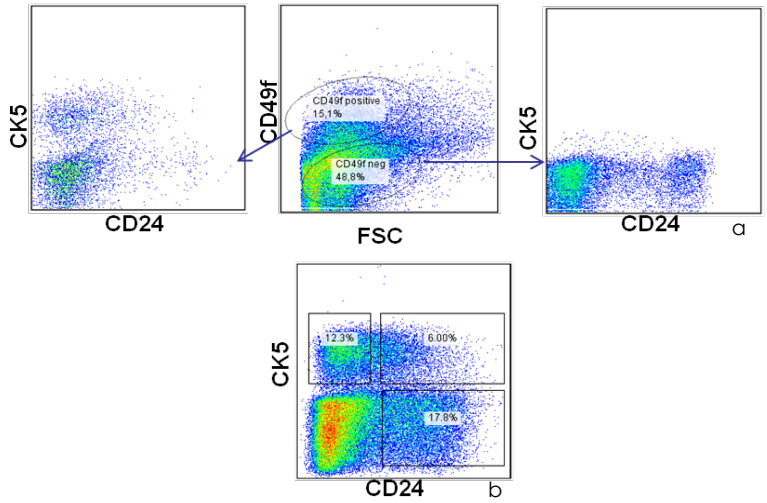

Figure 5.36: CK5 in a coexpression with CD24 in flow cytometry analysis. Gating on CD49f$^+$ cells, CK5 is coexpressed in a subset with CD24 (left), whereas gating on CD49f$^-$ cells, CK5 was not expressed at all (a), experiments showed that CK5 was coexpressed with CD24 within a subset in all the examined 6 samples (b).

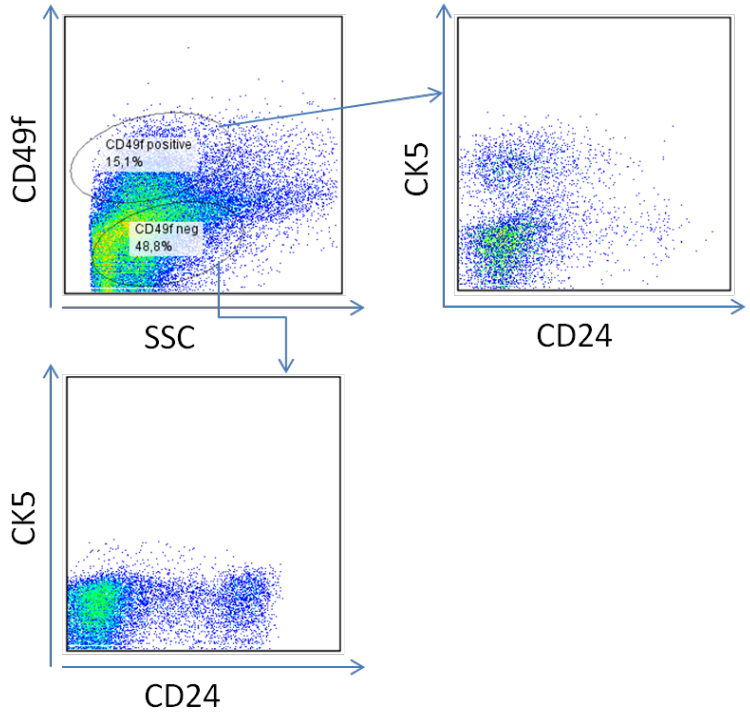

Figure 5.37: CK5 expression pattern of CD49f$^+$ and CD49f$^-$ cells. Gating on CD49f$^+$ cells, CK5 is coexpressed in a subset with CD24 (left), whereas gating on CD49f$^-$ cells, CK5 was not expressed.

5.7 SSEA-4 AS A SURFACE MARKER FOR SUBSETS AT DIFFERENT STAGES OF DIFFERENTIATION

5.7.1 *SSEA-4 is expressed in the prostate epithelium and coexpressed with epithelial markers*

As previously shown in this chapter, the prostate epithelium consists of cells with different differentiation capacities and the basal epithelium layer is heterogeneous. An additional marker which sections the CD49f$^+$Trop-2$^+$ basal subset is SSEA-4. Being utilized as a marker for embryonic stem cells, it is considered to be expressed on cells with low differentiation. However, our results outline that SSEA-4 is expressed by the human prostate epithelium.

5.7.2 *SSEA-4 negative cells enrich basal colonies* in vitro

SSEA-4 is coexpressed with the epithelial marker Trop-2 and it is expressed within the prostate epithelium, as immunohistochemical studies show. Cell sortings of SSEA-4$^+$ and SSEA-4$^-$ cells within the CD49f$^+$Trop-2$^+$ subset show that the SSEA-4$^-$ cells (CD49f$^+$Trop-2$^+$ SSEA-4$^-$) are clonogenic (Figure 5.39). This study is based on FACS sorting of 5 BPH samples, in which experiments 4A2B8 anti-

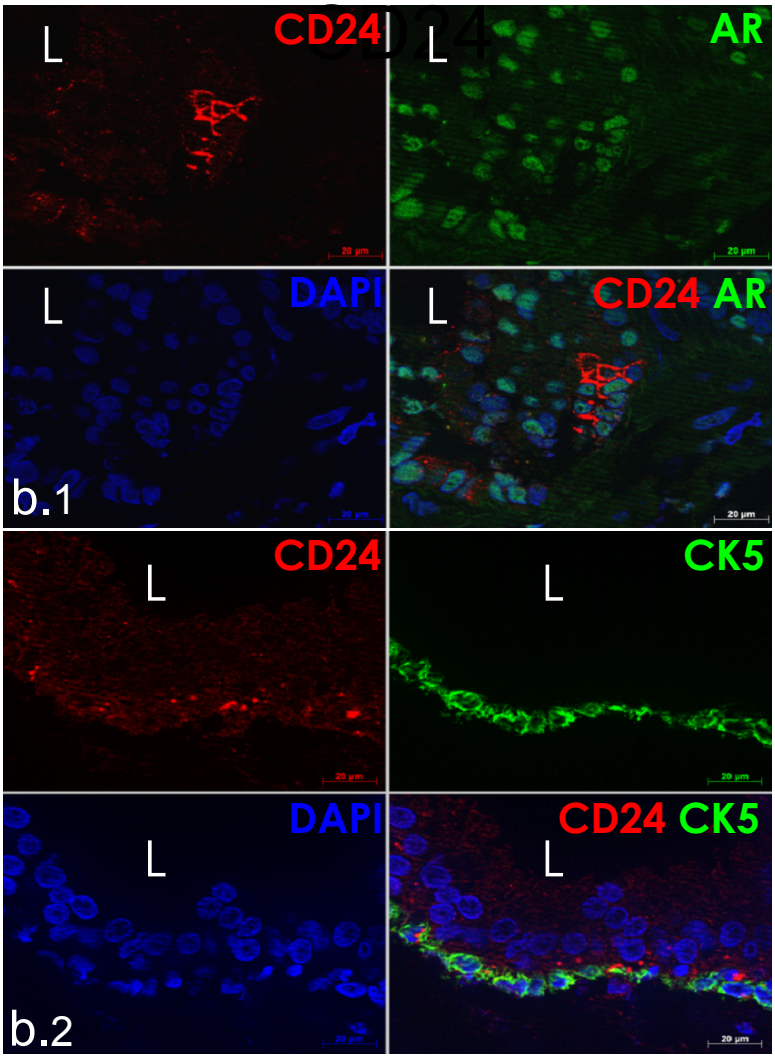

Figure 5.38: Immunostaining of CD24 and AR for coexpression. Coexpression between CD24 and CK5 (b.2) and lack of coexpression of CD24 and AR were observed (b.1) were observed on some cells.

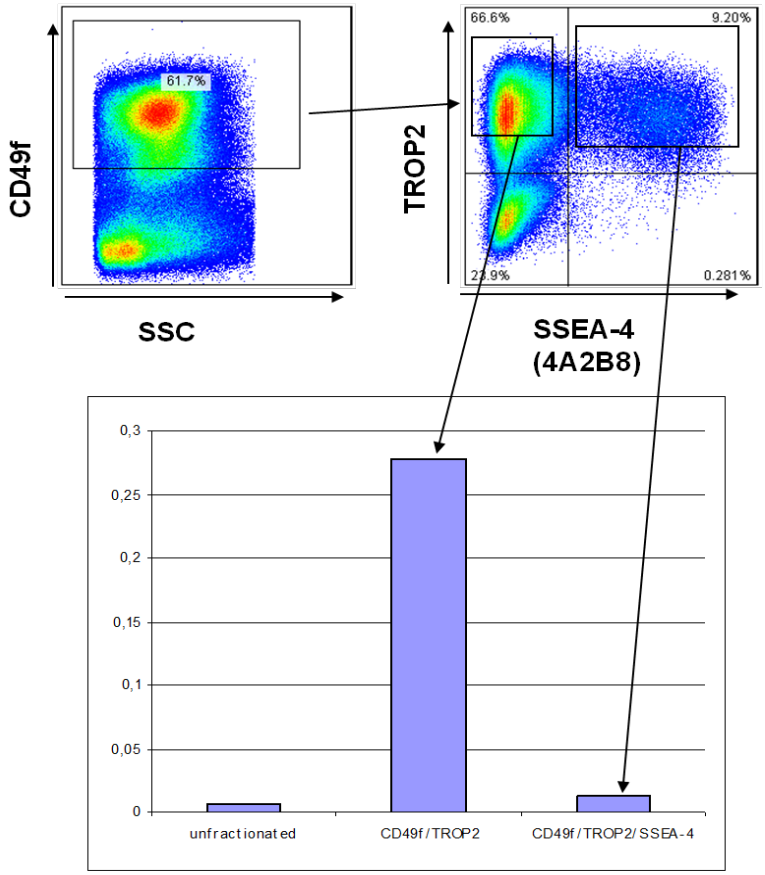

Figure 5.39: Clonogenicity of the SSEA-4 cells.Cell sortings of SSEA-4$^+$ and SSEA-4$^-$ cells within the CD49f$^+$Trop-2$^+$ subset show that the SSEA-4$^-$ cells (CD49f$^+$Trop-2$^+$ SSEA-4$^-$) are clonogenic. The same gating strategy was used – Firstly the CD49f$^+$ were selected and further visualized for Trop-2 and SSEA-4 expression in a separate dot-blot window.

body against SSEA-4 was used. We consider that the 4A2B8 antibody, which is raised against iPS cells, recognizes the epithelial compartment of human prostate.

Additional experiments of FACS sorting of CD49f$^-$SSEA-4$^+$, using the antibody clone MC813-70, show that SSEA-4$^+$ mesenchymal cells exist. Moreover, the CD49f$^-$SSEA-4$^+$ subset was able to give rise to mesenchymal colonies (Figure 5.40).

5.7.3 *SSEA-4 negative cells grow into basal colonies*

As shown on Figure 5.39, SSEA-4$^-$, but not SSEA-4$^+$ cells, were able to grow into epithelial colonies. These colonies were tested for their expression of surface markers, both basal and luminal, as well as the stromal marker CD90. The obtained results underlined the basal character of these colonies: expression of the basal markers CD49f,

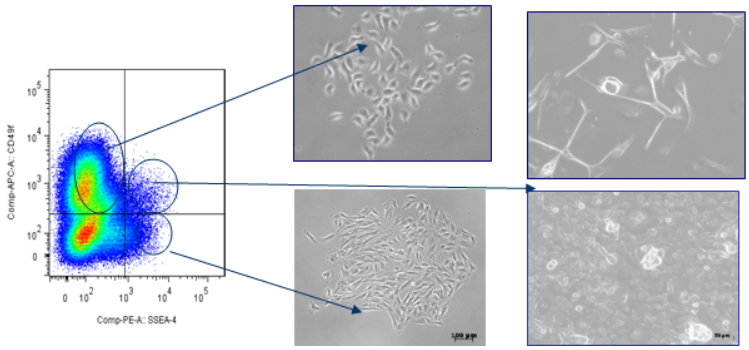

Figure 5.40: Coexpression between CD49f and SSEA-4. Further coexpression analysis and cell sorting, using different SSEA-4 antibody clone (MC813-70), showed that SSEA-4$^+$ cells grew into more mesenchymal-like cells.

CD49b, CD44, Her2, CD24, expression of the epithelial markers Trop-2, E-cadherin, Ep-CAM, Her3 and the lack of expression of CD90.

5.7.4 *Localization of SSEA-4 in the human prostate epithelium*

In addition to the immunohistochemical experiment, SSEA-4 was tested for coexpression with the basal and intermediate marker CK5. The basal cells express CK5 at high levels, whereas the intermediate phenotypes express CK5 with lower intensity. SSEA-4 is expressed within the fraction expressing CK5 at low levels (Figure 5.42).

5.8 SUSD2 AS A SURFACE MARKER TO DISTINGUISH BETWEEN SUBSETS AT DIFFERENT DIFFERENTIATION LEVELS

Cell sorting of the SUSD2$^+$ and SUSD2$^-$ subsets from Du145 and PC-3 cells shows that SUSD2 enriches monolayer colonies.

SUSD2, described as a mesenchymal stem cell marker by Sivasubramaniyan et al., is expressed at high levels by the stromal mesenchymal prostate cells. However, this work demonstrated that SUSD2 is expressed in the prostate epithelium and coexpressed with CD49f, Trop-2 and CD24. Preliminary flow cytometry analysis showed that SUSD2 did not section the CD49f$^+$Trop-2$^+$ subset (Figure 5.13), but when used in a costaining with CD24, a subset of very small size was observed: CD49f$^+$Trop-2$^+$CD24$^+$SUSD2$^+$ (Figure 5.43).

5.9 STUDY ON TNAP (W8B2)

TNAP is a marker expressed in primary prostate tissues and prostate cancer cell lines. TNAP was initially a marker of interest, as it is coexpressed with CD49f. Further cell sortings of the CD49f$^+$TNAP$^+$ and CD49f$^+$TNAP$^-$ subsets, showed that the epithelial colonies grow in

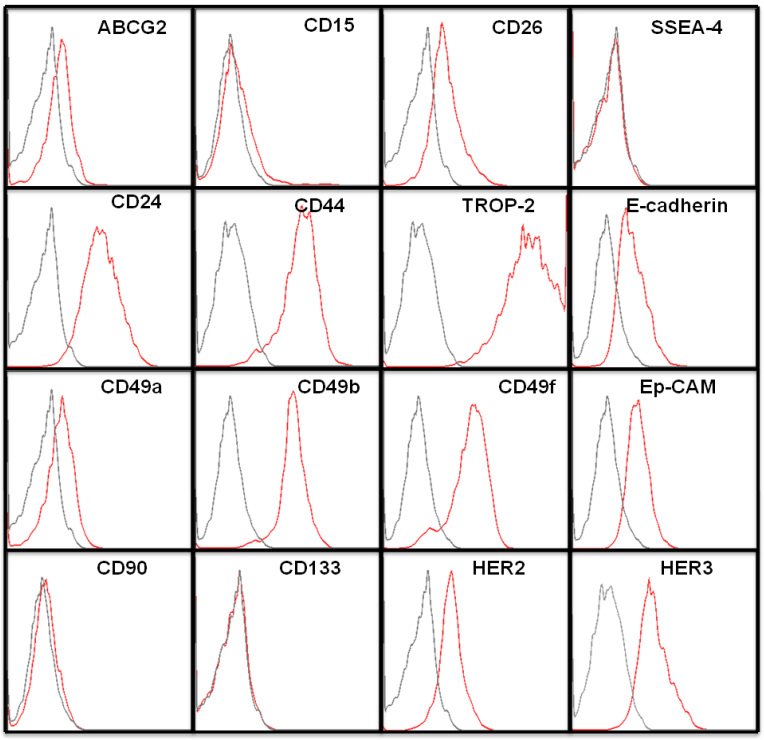

Figure 5.41: The SSEA-4^{-} colonies are basal. Cells from the obtained colonies expressed the basal markers CD49f, CD49b, CD44, Her2, CD24, the trans-epithelial markers Trop-2, E-cadherin, Ep-CAM, Her3 and did not express CD90. FCS is shown on the x-axis.

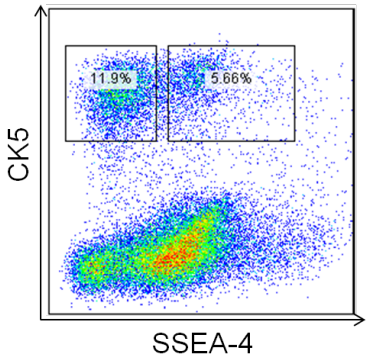

Figure 5.42: Coexpression between CK5 and SSEA-4. A subset of SSEA-4^{+} was expressed within the CK5-positive fraction, those subset expressed SSEA-4 at lower levels in comparison to the CK5^{-}SSEA-4^{+} subset.

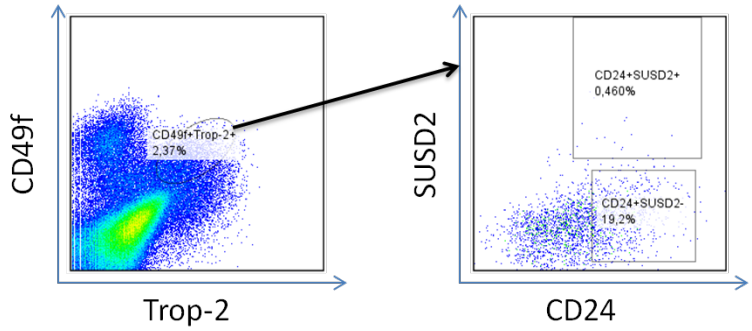

Figure 5.43: Coexpression between SUSD2, CD49f, Trop-2 and CD24. The results show that SUSD2 is coexpressed with CD49f, Trop-2 and CD24. When used in a costaining with CD24, a subset of very small size was observed: $CD49f^{+}Trop\text{-}2^{+}CD24^{+}SUSD2^{+}$.

the $TNAP^{-}$ fraction ($CD49f^{+}TNAP^{-}$). Furthermore, these cells initiated cell division, but their growth has terminated prematurely, due to potential lack of necessary supplements in the medium. Therefore, the cells were sorted in different types of media, combining defined and non-defined conditions. However, none of the used media were suitable. TNAP is not coexpressed with Trop-2 and this observation additionally proves that TNAP is not an epithelial marker.

5.10 EXAMINATION OF CANCER-DERIVED CELL LINES

Human prostate cancer-derived cell lines have been used extensively to study prostate cancer functionally. Different cell lines have been developed from primary prostate carcinomas or prostate cancer lesions. PC-3 is derived from bone marrow metastasis, isolated postmortem from a 62-year-old Caucasian man with poorly differentiated prostate carcinoma (grade IV). Du145 originates from a nervous system lesion of prostate cancer carcinoma of a 69-year-old Caucasian man. LnCAP is another metastatic cell line, derived from a left supraclavicular lymph node metastasis of a prostate carcinoma from a 50-year-old Caucasian male. From the three, only the LnCAP is androgen-sensitive and the least tumorigenic. A set of surface markers, which can potentially distinguish stem/progenitors cells, were tested on them for this purpose. Three adenocarcinoma cell lines are included in this study: PC-3, Du145 and LnCAP.

CD24 was expressed on both PC-3 and Du145, but not expressed on LnCAP cells. SSEA-4 and SUSD2 were expressed in all of the examined cell lines.

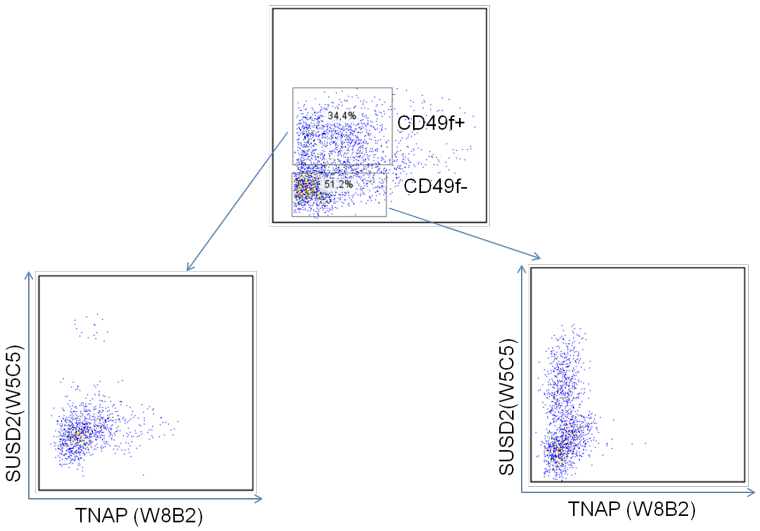

Figure 5.44: Coexpression between CD49f, SUSD2 and TNAP. TNAP and SUSD2 are coexpressed with CD49f in different pattern. When gating on CD49f$^+$ cells, separate subsets of TNAP$^+$ and SUSD2$^+$ cells were observed. The CD49f$^-$ gating revealed SUSD2$^+$, but not TNAP. TNAP and SUSD2 were not coexpressed.

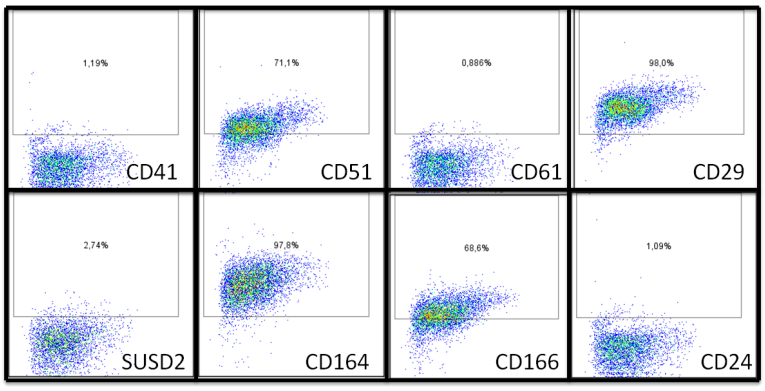

Figure 5.45: Expression of surface markers on LnCAP. The integrins CD51 and CD29 were expressed and the CD41 and CD61 not. CD164 and CD166 were expressed on the LnCAP cells, whereas CD24 and SUSD2 were not expressed. FCS is shown on the x-axis.

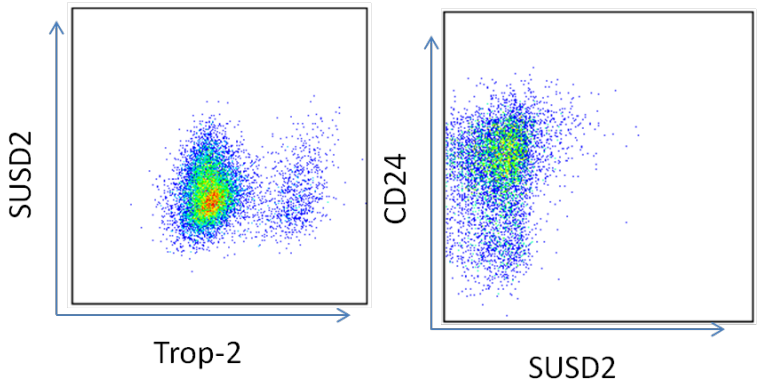

Figure 5.46: PC3 coexpression. CD24 and Trop-2 are expressed on the PC3 cells. Coexpression of these two markers with SUSD2 show that a small subset of TROP-2 and CD24 is coexpressed with SUSD2.

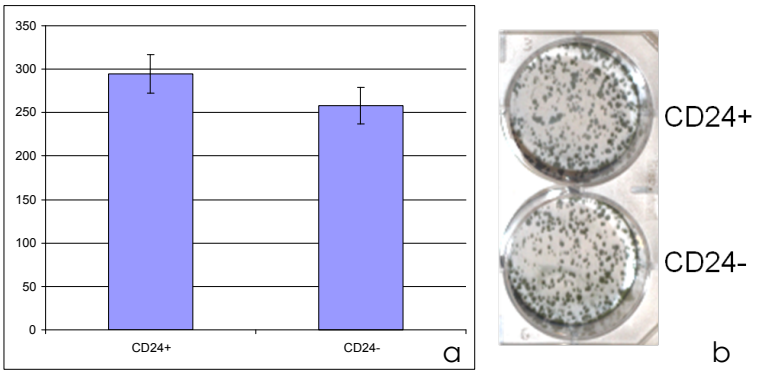

Figure 5.47: Clonogenicity of $CD24^{+}$ and $CD24^{-}$ on Du145. Sorting of the $CD24^{+}$ and $CD24^{-}$ cells on DU145 showed similar colony growth. Both subsets were capable to form colonies, with a small prevalence of the $CD24^{+}$ subset.

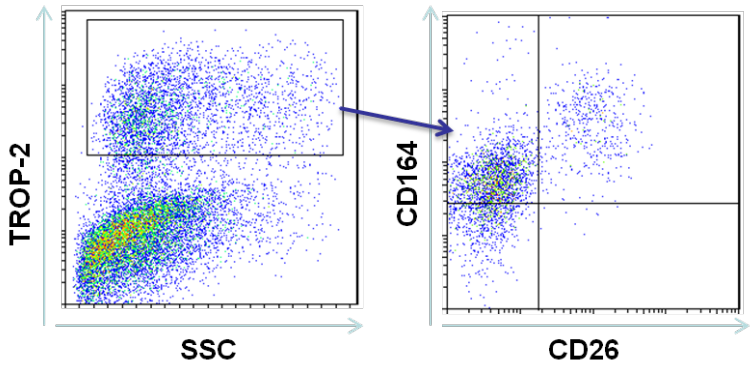

Figure 5.48: CD164 coexpression. CD164 is both epithelial and mesenchymal marker in prostate. Trop-2^{+} subset is coexpressed with CD164. Further analysis of the epithelial cells shows coexpression of CD$164^{h}i$ subset with CD26 (luminal marker), whereas the CD$164^{d}im$ was negative for CD26.

5.11 CD164 AS A MARKER FOR DIFFERENTIATED EPITHELIAL CELLS AND POTENTIAL TUMOR TARGET

Flow cytometry analysis shows that in BPH CD164 is expressed on both epithelial and stromal (mesenchymal) cells. In the epithelium, CD164 was expressed in the luminal compartment of human prostate.

Almost 100% of the prostate cancer cell lines PC-3 and DU-145 expressed CD164, as confirmed by the reactivity of four different anti-CD164 antibodies N6B6, 67D2, 103B2, and 105A5. The strongest signal of CD164 expression was observed when the antibody clone 67D2 was used for the staining. Using this antibody clone, a more pronounced expression of CD164 was observed in cancer in comparison to BPH. PC-3 originates from prostate cancer metastasis in brain and DU-145 — from metastasis in bone. The observation that both cell lines express high levels of CD164 suggests that CD164 is strongly expressed in prostate cancer metastases.

5.12 MESENCHYMAL/STROMAL CELLS OF THE PROSTATE

5.12.1 *Surface marker study to identify stromal cells*

A set of surface markers was tested on primary prostate and on cultivated (unfractionated) cells to identify potential molecules, which could separate mesenchymal stromal cells and stromal progenitor cells.

5.12.2 *Cultivated prostate stromal cells express mesenchymal markers*

After three passages of culturing, the unfractionated cells were analyzed for expression of surface markers using flow cytometry. Fig-

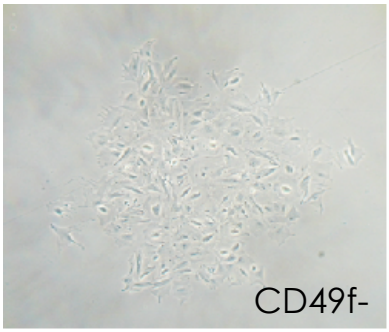

Figure 5.49: The CD49f$^-$ colony. The CD49f$^-$ cells were not capable to grow into epithelial colonies, but when sorted in mesenchymal media, they grew into mesenchymal-like colonies. Cells showed morphology of mesenchymal stem cells with high-spread form and visible actin filaments.

ure 5.11 shows that the cultivated stromal cells were positive for the prostate stromal markers CD90 and CD49a [84, 141] and for the mesenchymal markers CD146, CD44, CD105, CD29 and CD140b [93, 22, 77, 111], but negative for the epithelial markers Ep-CAM, E-cadherin, Trop-2 and CD24. In addition, the stromal cells in culture were positive for TNAP and SUSD2, but negative for SSEA-4. Several antibodies of unknown specificity were also tested to identify specific markers for prostate mesenchymal cells. The results are shown on Figure 5.11.

5.12.3 *Cells of the stromal compartment are present in the CD49f$^-$ subset*

Clonogenic assays performed using CnT52 and CnT12 media revealed that the CD49f$^-$ cells, as well as the CD49f$^+$Trop-2$^-$ cells were not capable of giving rise to epithelial colonies. These data were confirmed in all sorted samples. These two subsets were cell sorted in mesenchymal defined (Knock-out DMEM, supplemented with serum replacement and hFGF) and non-defined complete media (RPMI 1640, supplemented with 10% FCS). Only the CD49f$^-$ cells were able to form stromal colonies at a frequency of 1/10000 (Figure 5.49). The resulting stromal cells were able to grow with lower proliferation capacity in comparison weeks after the examination of the colony forming unit (CFU) capabilities. Furthermore, the cells from the colonies were able to maintain stromal cell mass in many passages without decline of growth, but the growth rate was comparably slow.

After three passages of culture, the sorted cells were analyzed for expression of surface markers using flow cytometry. The obtained results showed an expression profile, very similar to the one of the unfractionated stromal cells. The sorted stromal cells were positive for the prostate stromal and mesenchymal markers, but negative for the epithelial markers Ep-CAM, E-cadherin, Trop-2 and CD24 (Fig-

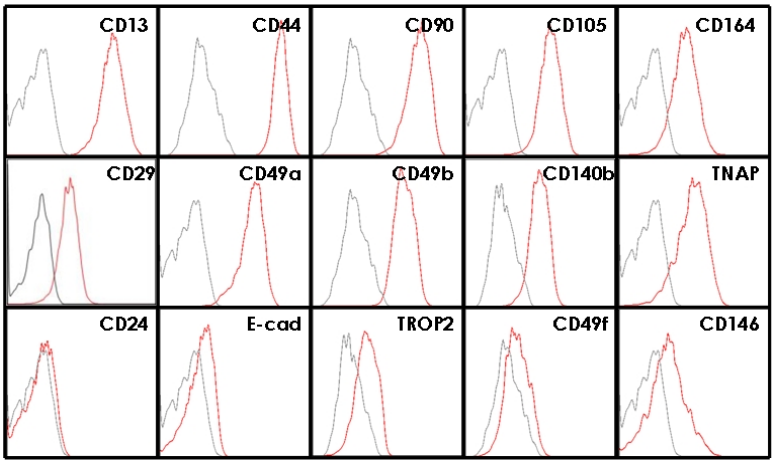

Figure 5.50: Expression pattern of the CD49f$^-$ colonies. The sorted CD49f$^-$ stromal cells were positive for the prostate stromal and mesenchymal markers (CD13, CD44, CD90, CD105, CD164, CD29, CD49a, CD49b, CD140b, TNAP, CD146), but negative for the epithelial markers Ep-CAM, E-cadherin, Trop-2 and CD24. FCS is shown on the x-axis.

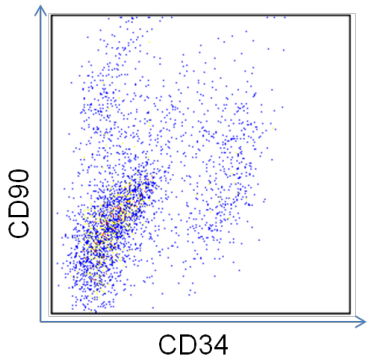

Figure 5.51: Coexpression between CD90 and CD34. CD90 and CD34 were coexpressed in primary prostate and the CD90$^+$CD34$^+$ cells were able to grow into stromal colonies (not shown).

ure 5.50). This is in accordance with the experiments performed on unfractionated cells.

5.12.4 *Cells of the stromal compartment are CD90$^+$ CD34$^+$*

In a set of additional experiments, stromal cells from primary prostate were cell sorted depending on their CD90 and CD34 expression pattern and further plated in non-defined complete media (RPMI-1640, supplemented with 10% FCS). CD90 and CD34 were coexpressed in primary prostate and the CD90$^+$CD34$^+$ cells were able to grow into stromal colonies. CD271-positive and CD271-negative cells were also examined, but stromal colonies were observed in both fractions.

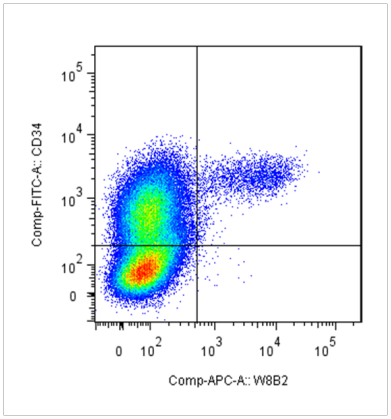

Figure 5.52: CD49a cells were coexpressed with CD34 and TNAP. Moreover, he CD49a^{hi} subpopulation enriches CD34^{+}/TNAP(W8B2)$^{+}$

5.12.5 *Prostate stromal cells were able to differentiate into osteoblasts*

Cultivated stromal cells in the third passage were examined for their capability to perform osteoblastic differentiation. After the 14th day, the cells were positive for alkaline phosphatase and they have excreted calcium hydroxiapatite. These two events are signals for osteoblastic differentiation. The process of differentiation into osteoblasts is typical for the mesenchymal stem cells (MSCs) from bone marrow and many other tissues.

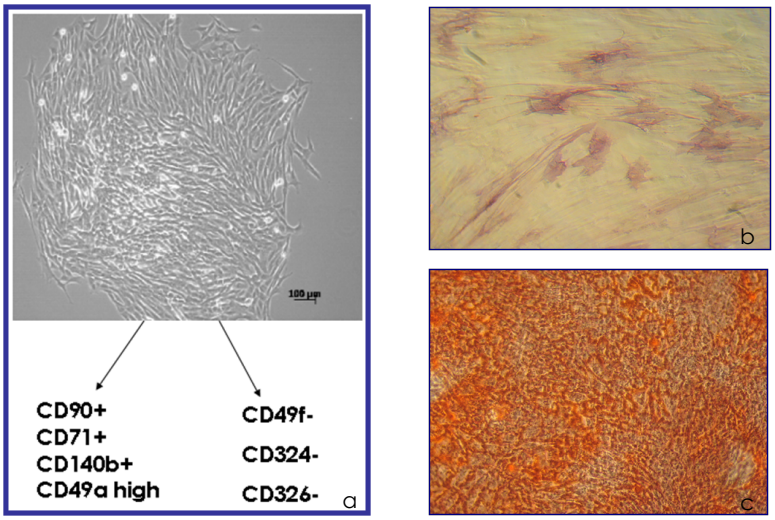

Figure 5.53: Osteoblastic differentiation of the mesenchymal colonies. The prostate stromal mesenchymal cells were able to perform osteoblastic differentiation in a sery of experiments, using alkaline phosphatase assay (b) and hydroxiapatite staining with Alizarin red (c).

6

DISCUSSION

The main goal of this study was to distinguish basal epithelial cell subsets in the human prostate, possessing different stages of differentiation, through the use of novel surface markers.

It is considered that colonies of different size and cardinality originate from cells at specific stages of differentiation. Only putative stem cells are able to give rise to a particular type of clones, termed *holoclones* — the largest colonies with the highest growth capacity and densely packed cells with a count greater than 500. *mesoclones* and *paraclones* are composed of loosely coupled cells and usually originate from transit-amplifying cells (Figure 6.1). The aim of this work is to apply such concepts to analysis of human prostate stem cells and to identify distinct cell subpopulations within the basal epithelium.

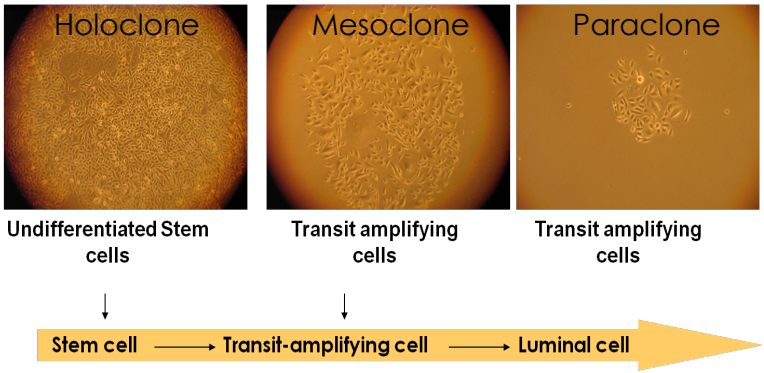

Figure 6.1: The three different epithelial colonies, derived from cells at different stages of differentiation.

Various surface markers have been examined and a significant share of our effort has been directed at the study of adhesion molecules. Based on the results of this study, the conclusion is that appropriate markers for sectioning of cells at different differentiation levels within the prostate basal epithelium are those, which participate in the processes of cell-to-cell and cell-to-matrix adhesion. CD49f was the most suitable cell-to-matrix adhesion molecule for enrichment of epithelial progenitor and stem cells. CD49b was excluded, because of its expression overlap with CD49f. CD49a and CD29 were not found to be appropriate, as CD49a was expressed by the stromal cells and CD29 was expressed by the majority of the cells and did not appear to be a selective marker. CD41, CD51 and CD61 did not lead to a clear subset, eligible for use in further separation. Moreover, CD51 was co-expressed together with CD90, which highlights its expression on the stromal compartment.

As evident from previous reports, the prostate epithelium expresses the epithelial markers E-Cadherin, Ep-CAM and Trop-2 [34, 36]. All of those are cell-to-cell adhesion molecules, typically expressed on epithelial cells, and their function is to keep the epithelial tissue congruent and dense. Additional research efforts attribute the enrichment of prostate epithelial stem cells to Trop-2 and Ep-CAM [34, 36]. However, the combined use of these two markers is unnecessary, as they are both expressed by the entire epithelium compartment. The same applies to E-cadherin as a typical epithelial adhesion molecule, which was expressed by every epithelial cell of the prostate gland and responsible for cell-to-cell adhesion and formation of cell-junctions. Therefore, Trop-2 was selected as a marker for all cells of the epithelium compartment.

As already reported in recent studies, prostate epithelial stem and progenitor cells could be enriched with the combined use of CD49f and Trop-2 [34]. However, this and other previously suggested marker combinations are not sufficient to distinguish the individual differentiation stages of the basal stem/progenitor cells in the course of their development. Several potential markers exist which section the $CD49f^{+}Trop\text{-}2^{+}$ subsets and the most promising were CD24 and SSEA-4 (recognized by the 4A2B8 antibody).

In order to achieve optimal separation, a novel gating strategy was developed and applied to fractionate stem cell/progenitor subsets. It proceeds with gating on CD49f-positive cells and setting coexpression windows in the resulting plot of Trop-2 versus the third marker (CD24, SSEA-4, SUSD2). This gating method has improved significantly the resolution and the separation of the subsets of interest. The original method, which utilizes a combination of CD49f, Trop-2 and CD24, produced only two epithelial subsets. The new gating strategy in contrast allowed us to identify four epithelial subsets, two of which were able to grow into colonies.

Our study shows that CD24 is not an exclusively luminal marker, but also expressed by the basal epithelial cells. Within the basal layer, CD24-positive cells are transit-amplifying (TA) and coexpress Trop-2, CD49f and CK5, but not AR. In line with their TA nature, $CD49f^{+}Trop\text{-}2^{+}CD24+$ cells are able to grow *in vitro* giving rise to basal colonies, which express a large spectrum of basal and transit-amplifying marker proteins (CK5/14, p63, bcl-2a, bcl-2b, CD49f, CD49b, Trop-2, and Her2). Colonies derived from both subsets were able to maintain self-renewal, although with lower renewal capacity compared to the $CD49f^{+}Trop\text{-}2^{+}CD24^{-}$ subset. Considering that some of the CD24-positive cells are able to form colonies, these are most probably the $CD24^{+}CK5^{+}AR^{-}$ cells.

Our results demonstrate that the colonies derived from primary prostate cells (originating from either BPH or prostate cancer samples) consist of a mixture of cells at different stages of differentiation. Most

of those cells acquire a transit-amplifying (basal) phenotype, which can be explained with the expression of many basal markers by all cells and additionally CD24 by the majority of cells. The colonies did not express the other markers of interest, such as SUSD2 and SSEA-4, illustrating that these two molecules are not expressed by transit-amplifying cells, but probably by cells on later or parallel stage of differentiation. In addition, the presence of CK18 at low levels in the colonies suggests that some of the cells have differentiated to ones with intermediate (luminal) phenotype.

The transit-amplifying (TA) progenitor cells are localized in the basal layer, possess limited capacity to grow and renew, express basal markers and do not express luminal markers at all or express them modestly.

$CD24^+$ cells were found to be localized in the basal layer (illustrated on Figure 5.21). A small subset of $CD24^+$ cells are co-expressed with CK5 and not co-expressed with the androgen receptor (Figure 5.36 and Figure 5.38). In addition, $CD24^+$ cells are able to grow in basal/TA colonies (Figure 5.29 and Figure 5.30), which mainly consist of TA cells. $CD49f^+Trop2^+CD24^+$ is a basal subset, because it contains cells capable of growing into colonies (only basal stem/progenitor cells have such capabilities) and moreover, the resulting colonies possess a basal character (Figure 5.29 and Figure 5.30).

In addition, our experiments show that the $CD49f^+Trop2^+CD24^+$ cells are transit-amplifying. They are localized in the basal layer and possess a weaker groth capacity compared to the $CD49f^+Trop2^+CD24^-$ subset. When cultured in a serum-free, calcium-low conditions, prostate epithelial cells grow into colonies, consisting of TA cells predominantly [127, 14, 71, 18]. We prove that these cells possess the phenotype $CD49f^+Trop2^+CD24^+CD49b^+CK5^{++}CK18^{low}$. Interestingly, the observed E-cadherin expression level is low, which is explained by the low-calcium conditions, in which the cells are cultivated, as E-cadherin is calcium dependent [18].

The identification of cell subsets responsible for epithelium lineage differentiation in a mature prostate may provide an insight to understanding the mechanisms of cell differentiation in BPH and prostate cancer.

The experimental results support the concept of a refined discrimination between basal and luminal epithelial cells. The existence of an intermediate subset, responsible for the transition from the basal to the luminal epithelial compartments, is reported. The most commonly used model describing the localization of the prostate stem cells suggests that the ES/P cells reside in the basal cell compartment [20]. These cells divide and amplify, before transitioning to a state of maturation towards terminally differentiated basal progenitors, termed transit-amplifying (TA)/intermediate cells. They are localized within the basal layer, express a basal cell phenotype and

acquire expression patterns of luminal cells [20]. Different developmental models of intermediate cells and their localization exist. Tokar et al. propose a model to distinguish cells of the basal compartment (PS/P cells and mature basal cells) and the luminal compartment (luminal cells and intermediate cells) [120]. According to this view, the most mature basal cells play a crucial role in maintaining the integrity of the prostate and support of luminal cell differentiation [11, 62].

Isaacs propose a model of differentiation, in which putative stem cells divide and differentiate into transit-amplifying (TA) progenitor cells that give rise to intermediate cells of the luminal compartment. These cells possess both basal and luminal characteristics [48]. According to this view, the luminal intermediate cells are the direct progenitors of terminally differentiated secretory luminal cells. Therefore, intermediate cells are expected to reside in both compartments, depending on their differentiation level. The differentiation from the basal to the luminal compartment is associated with the loss of basal markers and the acquisition of luminal markers. The qPCR results presented in our study suggest that the selected surface markers are useful to distinguish between poorly-differentiated progenitors and intermediate basal (transit-amplifying) cells.

It is known that basal, luminal and intermediate cells can be distinguished based on their cytokeratin expression patterns. In this work is shown that the combined use of different surface markers enables the discrimination between subsets of different differentiation stages in prostate basal epithelium. In this study, different combinations were utilized, including CD49f, Trop-2, CD24, SSEA-4. Using the transit-amplifying marker CD24, we show that CD49f$^+$Trop-2$^+$CD24$^-$ and CD49f$^+$Trop-2$^+$CD24$^+$ cells are localized within the basal compartment of human prostate, whereas CD49f$^-$Trop-2$^+$CD24$^+$ cells are localized in the luminal epithelium. Interestingly, CD49f$^-$Trop-2$^+$CD24$^-$ cells express a phenotype, similar to that observed in the basal epithelium.

CD49f$^+$Trop-2$^+$CD24$^+$ and CD49f$^-$Trop-2$^+$CD24$^+$ cells display an expression profile closer to terminal differentiation in comparison to the CD49f$^+$Trop-2$^+$CD24$^-$ cells, as verified by the fact that they express higher AR and CK8/18 levels and lower CK5 levels than CD49f$^+$Trop-2$^+$CD24$^-$ cells. Cells of the CD49f$^+$Trop-2$^+$CD24$^+$ subset express CK5 and are able to give rise to basal colonies. Together with the fact that CD24 is localized in the basal layer of the secretory acini, these data suggest that CD49f$^+$Trop-2$^+$CD24$^+$ cells are localized within the basal layer. Moreover, *in vitro* cultivation of these cells, as well as cells of the CD49f$^+$Trop-2$^+$CD24$^+$ subset, generates colonies whose cells predominantly exhibit the CD49f$^+$Trop-2$^+$CD24$^+$ phenotype. The composite phenotype of this cell subset resembles the phenotype of the transit-amplifying cells, which are localized in the basal layer, but are characterized by lower clonogenic and

proliferative properties and lower levels of CK5 expression. In contrast to CD49f$^+$Trop-2$^+$CD24$^-$ cells, CD49f$^-$Trop-2$^+$CD24$^+$ cells displayed properties closer to intermediate cells, which are localized in the luminal layer. These traits include the expression of the luminal markers CK8/18, the expression of CK17 and PSCA, as well as the absence of any proliferative capacity. Cells of the non-clonogenic CD49f$^-$Trop-2$^-$CD24$^-$ subset expressed low levels of luminal markers and high levels of the basal marker p63, a molecule which is not expressed in the epithelial stem cells. This indicates that this subset consists of mature basal cells. More experiments need to be performed to confirm that observation and to examine this subset further. Lack of expression of CD49f by the cells of this subset is a major drawback in concluding its definite basal localization. Based on the findings in this study, it is proposed that the CD49f$^+$Trop-2$^+$CD24$^+$ and CD49f$^-$Trop-2$^-$CD24$^-$ subsets originate from the more primitive CD49f$^+$Trop-2$^+$CD24$^-$ subset, which is characterized by cells with the highest clonogenic capacity and the strictest basal phenotype (Figure 6.2) [92].

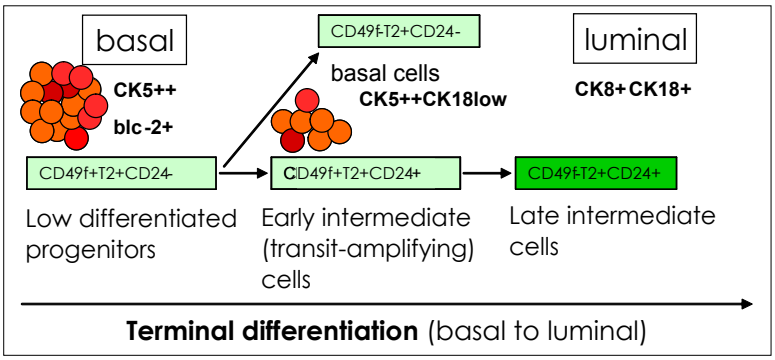

Figure 6.2: Model of the human prostate epithelial lineage development, based on differential surface marker expression.

The CD49f$^+$Trop-2$^+$CD24$^+$ cells in human BPH and cancer have colony-forming and proliferative potential [92], which raises the question about the function and ontogeny of these cells within human prostate epithelium. The role of CD24 in benign diseases has not been identified. In prostate and breast cancer CD44$^+$CD24$^-$ subset shows phenotype typical for stem cells. Nevertheless, CD24$^+$ cells are associated with poor prognosis in prostate cancer [61], breast cancer [2, 81] and other epithelial malignancies [60]. Moreover, recent studies identified CD24$^+$ tumor-initiating cells in solid tumor cancers [30], colorectal cancer [138], liver cancer [67] and pancreatic cancer [69].

As CD24 expression was detected in the basal and luminal layers, it is likely that the acquisition of CD24 in the basal layer reflects the onset of differentiation into luminal cells. However, CD24$^+$ cells that reside in the basal layer show a less pronounced clonogenic capacity compared to CD24$^-$ basal cells. These features, together with the

distinct expression profiles of key markers, indicate that $CD24^+$ cells in the basal layer are the transit-amplifying cells that are localized at the interface between stem and luminal cells. CD24 is an adhesion molecule, which alters cell adhesion and stimulates migration and proliferation. This molecule may participate in the process of migration of cells from the basal to luminal layer. In agreement with this concept is the fact that CD24 increases the motility of tumor cells [8]. However, the physiological function of CD24 in normal and benign epithelium remains unknown.

The function of SSEA-4 on epithelial cells and tissues has not been studied sufficiently. SSEA-4 is reported to be highly expressed on the differentiated corneal epithelium and it is a negative marker for human limbal stem/progenitor cells [123]. Similar results are here reported for human prostate, regarding its epithelial stem/progenitor cells. Our work shows that SSEA-4 is expressed on human prostate epithelium, as well as that SSEA-4^+ cells are not clonogenic and expressed between the basal and luminal layer. This suggest that this marker is expressed by a subset of intermediate cells, which are passing through luminal differentiation. These cells are not able to grow into colonies, but still do coexpress CD49f and Trop-2.

In this project, no correlation and statistically significant difference between BPH and prostate cancer was found concerning surface marker expression and clonogenicity. All examined markers were expressed in both diseases and their expression levels varied on a tissue basis. Prostate cancer is a heterogeneous disease and a correlation between the expression of surface markers and cancer development is difficult to assess.

Epithelial-mesenchymal transition (EMT) is regarded to play an important role in the development of BPH and prostate cancer. It is also considered to be linked to the stem cell signatures in prostate. EMT involves the participation of adhesion molecules, therefore study of these molecules within basal layer is beneficial. CD24 is a cell-to-cell adhesion molecule, which may functionally participate in the epithelial development of normal human prostate, as well as in BPH and prostate cancer.

In addition to the epithelial markers, many mesenchymal ones have been expressed on human prostate cells. CD90 was reported to be expressed on the reactive stroma of human prostate cancer [141]. However, it is expressed by the mesenchymal stroma of the normal and prostate BPH as well. In this work, it is shown that the mesenchymal stromal colonies grow from the $CD49f^-$ subset, but not from the $CD49f^+$. In line with this observation, the $CD49f^+TNAP^+$ subset failed to grow into mesenchymal colonies in several media, even though some cells have initiated a couple of divisions. These cells were suggested to be endothelial progenitors, but they were out of scope of the project and were not examined further. Comparing

these data to the results for the epithelial subsets, these were the $CD49f^{+}Trop\text{-}2^{-}CD24^{-}$ cells ($CD49f^{+}Trop\text{-}2^{-}CD24^{-}TNAP^{+}$), which were not able to grow into mesenchymal colonies.

The findings in this study indicate a hierarchy of cells with various differentiation capacities within the adult prostate gland, in which developmentally distinct and prospectively separable stem and differentiated progenitors are involved. The ability to isolate these distinct populations provides a new basis to investigate the prostate epithelial stem/progenitor cell differentiation and to study the precise stage, at which aberrant BPH and prostate cancer cells preferentially develop.

7 OUTLOOK

Future research on the function of CD24 and SSEA-4 in human prostate could open up interesting opportunities and bring an insight on the potential mechanisms of development of BPH and prostate cancer. Trivial targeting and downregulation of markers expressed on both normal and cancerous prostate tissues would not prevent the disease from developing; rather, it might reveal previously unknown mechanisms. This prompts the need to explore the underlying mechanisms which govern the development of the disease.

The process of epithelial-mesenchymal transition (EMT) is regarded to take an important role in benign prostate hyperplasia and prostate cancer development, because EMT is directly linked to the stem cell signatures in prostate cancer. Therefore, it is important to investigate potential EMT markers as possible therapeutic targets. It has been known that adhesion markers are involved in the development of EMT. Various adhesion molecules have been studied in this work and the knowledge of their expression pattern in human benign prostate and prostate cancer will contribute to future EMT research efforts. Further studies on the role of these markers in EMT and their exact function are required.

This project lays the groundwork for future research in the field of prostate cancer stem cell biology and prostate oncology. Further experiments with cancer cell lines and primary prostate cancer tissues are planned. These studies will focus on several aspects of prognostic and therapeutic relevance. One goal is to distinguish normal and cancer stem cells according to differential surface marker expression and to define prospective clinical and diagnostic markers. Another important aim is to discriminate between benign and tumor stem cells by their phenotype and propose candidate antibodies, designed to target cancer stem cells specifically. Such antibodies may either directly eliminate the cancer cells, or may be effective after optimization of their Fc regions and emerge as promising candidates for therapy. An additional aspect of future research efforts will be the identification of surface markers for monitoring of the epithelial-mesenchymal transition process.

PUBLICATIONS

Some ideas and figures have previously appeared in the following publications:

Publications

- *Petkova N*, Hennenlotter J, Sobiesiak M, Todenhöfer T, Scharpf M, Stenzl A, Bühring HJ, Schwentner C. Surface CD24 distinguishes between low differentiated and transit-amplifying cells in the basal layer of human prostate. *The Prostate*. 2013.
  - Text and figures from this manuscript appear in Chapter 5 and Chapter 6.
- Sivasubramaniyan K, Daniela L, Ghazanfari R, Sobiesiak M, Harichandan A, Mortha E, *Petkova N*, Grimm S, Cerabona F, de Zwart P, Abele H, Aicher WK, Faul C, Kanz L, Bühring HJ. Phenotypic and functional heterogeneity of human bone marrow- and amnion-derived MSC subsets. *Annals of the New York Academy of Sciences*. 2012.
  - Text and figures from this manuscript appear in Chapter 2

Posters

- *Petkova N*, Hennenlotter J, Grimm S, Cerabona F, Stenzl A, Bühring HJ. Isolation and surface marker characterization of epithelial and stromal stem cells in benign prostate tissue. Biostar Congress, 2010. Published in: *Tissue Engineering Part A. Vol. 17*. 2011.
  - Text and figures from this poster appear in Chapter 5
- *Petkova N*, Hennenlotter J, Schwentner C, Todenhöfer T, Grimm S, Cerabona F, Schilling D, Stenzl A, Bühring HJ. Differential isolation and surface marker characterization of epithelial and stromal stem cells in benign prostate tissue. European Association of Urology Congress, 2011. Published in: *European Urology Supplements*. 2011.
  - Text and figures from this poster appear in Chapter 5
- *Petkova N*, Hennenlotter J, Todenhöfer T, Sobiesiak M, Aufderklamm S, Scharpf M, Stenzl A, Bühring HJ, Schwentner C. 899 Surface CD24 distinguishes undifferentiated from transit-amplifying cells in the basal layer of the human prostate. Uropean Association of Urology Congress, 2013. Published in: *European Urology Supplements*. 2013.

– Text and figures from this poster appear in Chapter 2

BIBLIOGRAPHY

[1] J M Adams and S Cory. The Bcl-2 protein family: arbiters of cell survival. *Science*, 281(5381):1322–1326, 1998.

[2] Mohamed A H Ahmed, Mohammed A Aleskandarany, Emad A Rakha, Radwa Z A Moustafa, Ahmed Benhasouna, Christopher Nolan, Andrew R Green, Mohammad Ilyas, and Ian O Ellis. A CD44(-)/CD24 (+) phenotype is a poor prognostic marker in early invasive breast cancer. *Breast Cancer Research and Treatment*, 133(3):979–95, 2011. ISSN 15737217. doi: 10.1007/s10549-011-1865-8.

[3] K Aigner, B Dampier, L Descovich, M Mikula, A Sultan, M Schreiber, W Mikulits, T Brabletz, D Strand, P Obrist, W Sommergruber, N Schweifer, A Wernitznig, H Beug, R Foisner, and A Eger. The transcription factor ZEB1 (deltaEF1) promotes tumour cell dedifferentiation by repressing master regulators of epithelial polarity. *Oncogene*, 26(49):6979–6988, 2007.

[4] S Aigner, C L Ramos, A Hafezi-Moghadam, M B Lawrence, J Friederichs, P Altevogt, and K Ley. CD24 mediates rolling of breast carcinoma cells on P-selectin. *The FASEB journal official publication of the Federation of American Societies for Experimental Biology*, 12(12):1241–1251, 1998.

[5] Paloma Alonso-Magdalena, Clemens Brössner, Angelika Reiner, Guojun Cheng, Nobuhiro Sugiyama, Margaret Warner, and Jan-Ake Gustafsson. A role for epithelial-mesenchymal transition in the etiology of benign prostatic hyperplasia. *Proceedings of the National Academy of Sciences of the United States of America*, 106(8):2859–2863, 2009.

[6] Wendy W Barclay, Ralph D Woodruff, M Craig Hall, and Scott D Cramer. A system for studying epithelial-stromal interactions reveals distinct inductive abilities of stromal cells from benign prostatic hyperplasia and prostate cancer. *Endocrinology*, 146(1):13–18, 2004.

[7] Perrine Barraud, Simon Stott, Kjeld Mø llgård, Malin Parmar, and Anders Björklund. In vitro characterization of a human neural progenitor cell coexpressing SSEA4 and CD133. *Journal of Neuroscience Research*, 85(2):250–259, 2007.

[8] Petra Baumann, Natascha Cremers, Frans Kroese, Gertraud Orend, Ruth Chiquet-Ehrismann, Toshi Uede, Hideo Yagita,

and Jonathan P Sleeman. CD24 expression causes the acquisition of multiple cellular properties associated with tumor growth and metastasis. *Cancer Research*, 65(23):10783–10793, 2005.

[9] Petra Baumann, Wilko Thiele, Natascha Cremers, Santoshi Muppala, Justyna Krachulec, Markus Diefenbacher, Olivier Kassel, Giridhar Mudduluru, Heike Allgayer, Margaret Frame, and Jonathan P Sleeman. CD24 interacts with and promotes the activity of c-src within lipid rafts in breast cancer cells, thereby increasing integrin-dependent adhesion. *Cellular and molecular life sciences CMLS*, pages 1–14, 2011. ISSN 14209071. doi: 10.1007/s00018-011-0756-9.

[10] S. T. Boesch, S. Corvin, J. Zhang, H. Rogatsch, G. Bartsch, and H. Klocker. Modulation of the differentiation status of cultured prostatic smooth muscle cells by an alpha1-adrenergic receptor antagonist. *Prostate*, 39(4):226–233, Jun 1999.

[11] H Bonkhoff and T Fixemer. Neuroendocrine differentiation in prostate cancer. An unrecognized and therapy-resistant phenotype. *Der Urologe Ausg A*, 43(7):836–842, 2004.

[12] H Bonkhoff, U Stein, and K Remberger. The proliferative function of basal cells in the normal and hyperplastic human prostate. *The Prostate*, 24(3):114–118, 1994.

[13] D Bonnet and J E Dick. Human acute myeloid leukemia is organized as a hierarchy that originates from a primitive hematopoietic cell. *Nature Medicine*, 3(7):730–737, 1997.

[14] Patrick Bühler, Philipp Wolf, Arndt Katzenwadel, Wolfgang Schultze-Seemann, Ulrich Wetterauer, Nikolaus Freudenberg, and Ursula Elsässer-Beile. Primary prostate cancer cultures are models for androgen-independent transit amplifying cells. *Oncology Reports*, 23(2):465–470, 2010.

[15] A T Collins, P A Berry, C Hyde, M J Stower, and N J Maitland. Prospective identification of tumorigenic prostate cancer stem cells. *Cancer Research*, 65(23):10946–10951, 2005.

[16] Anne T Collins, Fouad K Habib, Norman J Maitland, and David E Neal. Identification and isolation of human prostate epithelial stem cells based on α 2 β 1 -integrin expression. *Journal of Cell Science*, 114(Pt 21):3865–72, 2001. ISSN 00219533.

[17] Carlton R Cooper, Christopher H Chay, James D Gendernalik, Hyung-Lae Lee, Jasmine Bhatia, Russell S Taichman, Laurie K McCauley, Evan T Keller, and Kenneth J Pienta. Stromal factors involved in prostate carcinoma metastasis to bone. *Cancer*, 97(3 Suppl):739–747, 2003.

[18] Susan Dalrymple, Lizamma Antony, Yi Xu, Aarti R Uzgare, Julia T Arnold, Jurga Savaugeot, Lori J Sokoll, Angelo M De Marzo, and John T Isaacs. Role of notch-1 and E-cadherin in the differential response to calcium in culturing normal versus malignant prostate cells. *Cancer Research*, 65(20):9269–9279, 2005.

[19] T L Davis, A E Cress, B L Dalkin, and R B Nagle. Unique expression pattern of the alpha6beta4 integrin and laminin-5 in human prostate carcinoma. *The Prostate*, 46(3):240–248, 2001.

[20] A M De Marzo, W G Nelson, A K Meeker, and D S Coffey. Stem cell features of benign and malignant prostate epithelial cells. *The Journal of Urology*, 160(6 Pt 2):2381–2392, 1998.

[21] Gregor B Deutsch, Elisabeth M Zielonka, Daniel Coutandin, Tobias A Weber, Birgit Schäfer, Jens Hannewald, Laura M Luh, Florian G Durst, Mohamed Ibrahim, Jan Hoffmann, Frank H Niesen, Aycan Sentürk, Hana Kunkel, Bernd Brutschy, Enrico Schleiff, Stefan Knapp, Amparo Acker-Palmer, Manuel Grez, Frank McKeon, and Volker Dötsch. DNA Damage in Oocytes Induces a Switch of the Quality Control Factor TAp63α from Dimer to Tetramer. *Cell*, 144(4):566–576, 2011.

[22] M Dominici, K Le Blanc, I Mueller, I Slaper-Cortenbach, Fc Marini, Ds Krause, Rj Deans, A Keating, Dj Prockop, and Em Horwitz. Minimal criteria for defining multipotent mesenchymal stromal cells. The International Society for Cellular Therapy position statement. *Cytotherapy*, 8(4):315–317, 2006.

[23] Lei Du, Hongyi Wang, Leya He, Jingyu Zhang, Biyun Ni, Xiaohui Wang, Haijing Jin, Nathalie Cahuzac, Maryam Mehrpour, Youyong Lu, and Quan Chen. CD44 is of functional importance for colorectal cancer stem cells. *Clinical Cancer Research*, 14(21):6751–6760, 2008.

[24] H F English, J R Drago, and R J Santen. Cellular response to androgen depletion and repletion in the rat ventral prostate: autoradiography and morphometric analysis. *The Prostate*, 7(1): 41–51, 1985.

[25] H F English, R J Santen, and J T Isaacs. Response of glandular versus basal rat ventral prostatic epithelial cells to androgen withdrawal and replacement. *The Prostate*, 11(3):229–242, 1987.

[26] Xianfeng Fang, Pan Zheng, Jie Tang, and Yang Liu. CD24: from A to Z. *Cellular molecular immunology*, 7(2):100–103, 2010.

[27] D Fong, P Moser, C Krammel, J M Gostner, R Margreiter, M Mitterer, G Gastl, and G Spizzo. High expression of TROP2 correlates with poor prognosis in pancreatic cancer. *British Journal of Cancer*, 99(8):1290–1295, 2008.

[28] Dominic Fong, Gilbert Spizzo, Johanna M Gostner, Guenther Gastl, Patrizia Moser, Clemens Krammel, Stefan Gerhard, Michael Rasse, and Klaus Laimer. TROP2: a novel prognostic marker in squamous cell carcinoma of the oral cavity. *Modern pathology an official journal of the United States and Canadian Academy of Pathology Inc*, 21(2):186–191, 2008.

[29] Eun J Gang, Darko Bosnakovski, Camila A Figueiredo, Jan W Visser, and Rita C R Perlingeiro. SSEA-4 identifies mesenchymal stem cells from bone marrow. *Blood*, 109(4):1743–1751, 2007.

[30] M-Q Gao, Y-P Choi, S Kang, J H Youn, and N-H Cho. CD24+ cells from hierarchically organized ovarian cancer are enriched in cancer stem cells. *Oncogene*, 29(18):2672–2680, 2010.

[31] Isla P Garraway, Wenyi Sun, Chau P Tran, Sven Perner, Bao Zhang, Andrew S Goldstein, Scott A Hahm, Maahum Haider, Christian S Head, Robert E Reiter, Mark A Rubin, and Owen N Witte. Human prostate sphere-forming cells represent a subset of basal epithelial cells capable of glandular regeneration in vivo. *The Prostate*, 70(5):491–501, 2010.

[32] Chiara Gentili and Ranieri Cancedda. Cartilage and bone extracellular matrix. *Current Pharmaceutical Design*, 15(12):1334–1348, 2009. ISSN 13816128.

[33] Filippo G Giancotti and Guido Tarone. Positional control of cell fate through joint integrin/receptor protein kinase signaling. *Annual Review of Cell and Developmental Biology*, 19(1):173–206, 2003.

[34] Andrew S Goldstein, Devon A Lawson, Donghui Cheng, Wenyi Sun, Isla P Garraway, and Owen N Witte. Trop2 identifies a subpopulation of murine and human prostate basal cells with stem cell characteristics. *Proceedings of the National Academy of Sciences of the United States of America*, 105(52):20882–20887, 2008.

[35] Andrew S Goldstein, Justin M Drake, Daina L Burnes, David S Finley, Hong Zhang, Robert E Reiter, Jiaoti Huang, and Owen N Witte. Purification and direct transformation of epithelial progenitor cells from primary human prostate. *Nature Protocols*, 6 (5):656–667, 2011.

[36] Changyong Guo, Haibo Liu, Bao-Hui Zhang, Radu M Cadaneanu, Aqila M Mayle, and Isla P Garraway. Epcam, CD44, and CD49f distinguish sphere-forming human prostate basal cells from a subpopulation with predominant tubule initiation capability. *PloS one*, 7(4):e34219, January 2012. ISSN 1932-6203. doi: 10.1371/journal.pone.0034219.

[37] Natalia Guzmán-Ramírez, Maureen Völler, Antoinette Wetterwald, Markus Germann, Neil A Cross, Cyrill A Rentsch, Jack Schalken, George N Thalmann, and Marco G Cecchini. In vitro propagation and characterization of neoplastic stem/progenitor-like cells from human prostate cancer tissue. *The Prostate*, 69(15):1683–1693, 2009.

[38] Myoung-Eun Han, Tae-Yong Jeon, Sun-Hwi Hwang, Young-Suk Lee, Hyun-Jung Kim, Hye-Eun Shim, Sik Yoon, Sun-Yong Baek, Bong-Seon Kim, Chi-Dug Kang, and Sae-Ock Oh. Cancer spheres from gastric cancer patients provide an ideal model system for cancer stem cell research. *Cellular and molecular life sciences CMLS*, 68(21):3589–605, 2011. ISSN 14209071. doi: 10.1007/s00018-011-0672-z.

[39] J. Hansson and P. A. Abrahamsson. Neuroendocrine differentiation in prostatic carcinoma. *Scand J Urol Nephrol Suppl*, (212): 28–36, 2003.

[40] S M Harman, E J Metter, J D Tobin, J Pearson, and M R Blackman. Longitudinal effects of aging on serum total and free testosterone levels in healthy men. Baltimore Longitudinal Study of Aging. *The Journal of Clinical Endocrinology & Metabolism*, 86(2):724–731, 2001.

[41] AM Havens, Y Jung, YX Sun, J Wang, RB Shah, HJ Bühring, KJ Pienta, and RS Taichman. The role of sialomucin CD164 (MGC-24v or endolyn) in prostate cancer metastasis. *BMC Cancer*, 6:195, 2006.

[42] J K Henderson, J S Draper, H S Baillie, S Fishel, J A Thomson, H Moore, and P W Andrews. Preimplantation human embryos and embryonic stem cells show comparable expression of stage-specific embryonic antigens. *Stem Cells*, 20(4):329–337, 2002.

[43] Gabriella Honeth, Pär-Ola Bendahl, Markus Ringnér, Lao H Saal, Sofia K Gruvberger-Saal, Kristina Lövgren, Dorthe Grabau, Må rten Fernö, Å ke Borg, and Cecilia Hegardt. The CD44+/CD24- phenotype is enriched in basal-like breast tumors. *Breast cancer research BCR*, 10(3):R53, 2008.

[44] D L Hudson, M O'Hare, F M Watt, and J R Masters. Proliferative heterogeneity in the human prostate: Evidence for epithelial stem cells. *Laboratory investigation a journal of technical methods and pathology*, 80(8):1243–1250, 2000.

[45] D L Hudson, A T Guy, P Fry, M J O'Hare, F M Watt, and J R Masters. Epithelial cell differentiation pathways in the human prostate: Identification of intermediate phenotypes by keratin expression. *The Prostate*, 49(2):271–278, 2001.

[46] E M Hurt, B T Kawasaki, G J Klarmann, S B Thomas, and W L Farrar. CD44+CD24- prostate cells are early cancer progenitor/stem cells that provide a model for patients with poor prognosis. *British Journal of Cancer*, 98(4):756–765, 2008.

[47] Kenneth A Iczkowski. Cell adhesion molecule CD44: its functional roles in prostate cancer. *American journal of translational research*, 3(1):1–7, 2010.

[48] John T Isaacs. Prostate stem cells and benign prostatic hyperplasia. *The Prostate*, 68(9):1025–1034, 2008.

[49] D F Jarrard, R Paul, A Van Bokhoven, S H Nguyen, G S Bova, M J Wheelock, K R Johnson, J Schalken, M Bussemakers, and W B Isaacs. P-Cadherin is a basal cell-specific epithelial marker that is not expressed in prostate cancer. *Clinical Cancer Research*, 3(11):2121–2128, 1997.

[50] B V Kallakury, F Yang, J Figge, K E Smith, S J Kausik, N J Tacy, H A Fisher, R Kaufman, H Figge, and J S Ross. Decreased levels of CD44 protein and mRNA in prostate carcinoma. Correlation with tumor grade and ploidy. *Cancer*, 78(7):1461–1469, 1996.

[51] R Kannagi, N A Cochran, F Ishigami, S Hakomori, P W Andrews, B B Knowles, and D Solter. Stage-specific embryonic antigens (SSEA-3 and -4) are epitopes of a unique globo-series ganglioside isolated from human teratocarcinoma cells. *the The European Molecular Biology Organization Journal*, 2(12):2355–2361, 1983.

[52] Susan Kasper. Exploring the origins of the normal prostate and prostate cancer stem cell. *Stem Cell Reviews*, 4(3):193–201, 2008.

[53] Noriaki Kawanabe, Satoko Murata, Hiroaki Fukushima, Yoshihito Ishihara, Takeshi Yanagita, Emmy Yanagita, Mitsuaki Ono, Hiroshi Kurosaka, Hiroshi Kamioka, Tomoo Itoh, Takuo Kuboki, and Takashi Yamashiro. Stage-specific embryonic antigen-4 identifies human dental pulp stem cells. *Experimental Cell Research*, 318(5):2–5, 2012. ISSN 10902422. doi: 10.1016/j.yexcr.2012.01.008.

[54] R Kay, P M Rosten, and R K Humphries. CD24, a signal transducer modulating B cell activation responses, is a very short peptide with a glycosyl phosphatidylinositol membrane anchor. *The Journal of Immunology*, 147(4):1412–1416, 1991.

[55] P Kellokumpu-Lehtinen. Correlation of embryonic development and adult neoplastic changes of human prostate. *European Urology*, 16(5):386–390, 1989.

[56] P J Koelink, C F M Sier, D W Hommes, C B H W Lamers, and H W Verspaget. Clinical significance of TROP2 expression in colorectal cancer. *British Journal of Cancer*, 101(5):765–773, 2009.

[57] Gero Kramer and Michael Marberger. Could inflammation be a key component in the progression of benign prostatic hyperplasia? *Current Opinion in Urology*, 16(1):25–29, 2006.

[58] S Krishnamurthy and J E Nör. Head and Neck Cancer Stem Cells. *Journal of Dental Research*, 91(4):334–40, 2011. ISSN 15440591. doi: 10.1177/0022034511423393.

[59] G Kristiansen, K Schlüns, Y Yongwei, C Denkert, M Dietel, and I Petersen. CD24 is an independent prognostic marker of survival in nonsmall cell lung cancer patients. *British Journal of Cancer*, 88(2):231–236, 2003.

[60] G Kristiansen, M Sammar, and P Altevogt. Tumour biological aspects of CD24, a mucin-like adhesion molecule. *Journal of Molecular Histology*, 35(3):255–262, 2004.

[61] Glen Kristiansen, Christian Pilarsky, Janja Pervan, Burkhard Stürzebecher, Carsten Stephan, Klaus Jung, Stefan Loening, Andre Rosenthal, and Manfred Dietel. CD24 expression is a significant predictor of PSA relapse and poor prognosis in low grade or organ confined prostate cancer. *The Prostate*, 58(2):183–192, 2004.

[62] Takeshi Kurita, Roanna T Medina, Alea A Mills, and Gerald R Cunha. Role of p63 and basal cells in the prostate. *Development Cambridge England*, 131(20):4955–4964, 2004.

[63] N Kyprianou and J T Isaacs. Activation of programmed cell death in the rat ventral prostate after castration. *Endocrinology*, 122(2):552–562, 1988.

[64] U. K. Laemmli. Cleavage of structural proteins during the assembly of the head of bacteriophage T4. *Nature*, 227(5259):680–685, Aug 1970.

[65] D A Lawson, L Xin, R Lukacs, Q Xu, D Cheng, and O N Witte. Prostate stem cells and prostate cancer. *Cold Spring Harbor Symposia on Quantitative Biology*, 70(187-196):187–196, 2005.

[66] Devon A Lawson, Li Xin, Rita U Lukacs, Donghui Cheng, and Owen N Witte. Isolation and functional characterization of murine prostate stem cells. *Proceedings of the National Academy of Sciences of the United States of America*, 104(1):181–186, 2007.

[67] Terence Kin Wah Lee, Antonia Castilho, Vincent Chi Ho Cheung, Kwan Ho Tang, Stephanie Ma, and Irene Oi Lin Ng.

CD24(+) liver tumor-initiating cells drive self-renewal and tumor initiation through STAT3-mediated NANOG regulation. *Cell stem cell*, 9(1):50–63, 2011. doi: 10.1016/j.stem.2011.06.005.

[68] Kevin G Leong, Bu-Er Wang, Leisa Johnson, and Wei-Qiang Gao. Generation of a prostate from a single adult stem cell. *Nature*, 456(7223):804–808, 2008.

[69] Chenwei Li, David G Heidt, Piero Dalerba, Charles F Burant, Lanjing Zhang, Volkan Adsay, Max Wicha, Michael F Clarke, and Diane M Simeone. Identification of pancreatic cancer stem cells. *Cancer Research*, 67(3):1030–1037, 2007.

[70] Ting Li, Yun Su, Yuping Mei, Qixin Leng, Bingjie Leng, Zhenqiu Liu, Sanford A Stass, and Feng Jiang. ALDH1A1 is a marker for malignant prostate stem cells and predictor of prostate cancer patients' outcome. *Laboratory investigation a journal of technical methods and pathology*, 90(2):234–244, 2010.

[71] Ivan V Litvinov, Donald J Vander Griend, Yi Xu, Lizamma Antony, Susan L Dalrymple, and John T Isaacs. Low-calcium serum-free defined medium selects for growth of normal prostatic epithelial stem cells. *Cancer Research*, 66(17):8598–8607, 2006.

[72] A Y Liu and D M Peehl. Characterization of cultured human prostatic epithelial cells by cluster designation antigen expression. *Cell and Tissue Research*, 305(3):389–397, 2002.

[73] Alvin Y Liu, Martine P Roudier, and Lawrence D True. Heterogeneity in primary and metastatic prostate cancer as defined by cell surface CD profile. *The American journal of pathology*, 165(5): 1543–1556, 2004.

[74] Ronan M Long, Colm Morrissey, John M Fitzpatrick, and R William G Watson. Prostate epithelial cell differentiation and its relevance to the understanding of prostate cancer therapies. *Clinical science London England 1979*, 108(1):1–11, 2005.

[75] A. Lunacek, J. Oswald, C. Schwentner, B. Schlenck, W. Horninger, H. Fritsch, S. Longato, C. Sergi, G. Bartsch, and C. Radmayr. Growth curves of the fetal prostate based on three-dimensional reconstructions: a correlation with gestational age and maternal testosterone levels. *BJU Int.*, 99(1): 151–156, Jan 2007.

[76] A. Lunacek, C. Schwentner, J. Oswald, H. Fritsch, C. Sergi, L. N. Thomas, R. S. Rittmaster, H. Klocker, H. Neuwirt, G. Bartsch, and C. Radmayr. Fetal distribution of 5alpha-reductase 1 and 5alpha-reductase 2, and their input on human prostate development. *J. Urol.*, 178(2):716–721, Aug 2007.

[77] Manas K Majumdar, Michele Keane-Moore, Diana Buyaner, Wayne B Hardy, Mark A Moorman, Kevin R McIntosh, and Joseph D Mosca. Characterization and functionality of cell surface molecules on human mesenchymal stem cells. *Journal of Biomedical Science*, 10(2):228–241, 2003.

[78] T Matsui, N Kurosawa, K Hibi, S Akiyama, Y Kasai, J Sakamoto, K Ito, A Nakao, and T Muramatsu. The ratio of splicing variants of MGC-24/CD164, a sialomucin, correlates with the metastatic potential of colorectal carcinomas. *Journal of Biochemistry*, 127(6): 1103–1107, 2000.

[79] J. E. McNeal. Regional morphology and pathology of the prostate. *Am. J. Clin. Pathol.*, 49(3):347–357, Mar 1968.

[80] G Moreno-Bueno, F Portillo, and A Cano. Transcriptional regulation of cell polarity in EMT and cancer. *Oncogene*, 27(55): 6958–6969, 2008.

[81] Eleni Mylona, Ioanna Giannopoulou, Emmanouil Fasomytakis, Alexandros Nomikos, Christina Magkou, Panagiotis Bakarakos, and Lydia Nakopoulou. The clinicopathologic and prognostic significance of CD44+/CD24(-/low) and CD44-/CD24+ tumor cells in invasive breast carcinomas. *Human Pathology*, 39(7): 1096–1102, 2008.

[82] J C Nickel, J Downey, I Young, and S Boag. Asymptomatic inflammation and/or infection in benign prostatic hyperplasia. *BJU International*, 84(9):976–981, 1999.

[83] Mayuko Okabe, Yuko Tsukahara, Minoru Tanaka, Kaori Suzuki, Shigeru Saito, Yoshiko Kamiya, Tohru Tsujimura, Koji Nakamura, and Atsushi Miyajima. Potential hepatic stem cells reside in EpCAM+ cells of normal and injured mouse liver. *Development Cambridge England*, 136(11):1951–1960, 2009.

[84] Laura E Pascal, Lawrence D True, David S Campbell, Eric W Deutsch, Michael Risk, Ilsa M Coleman, Lillian J Eichner, Peter S Nelson, and Alvin Y Liu. Correlation of mRNA and protein levels: Cell type-specific gene expression of cluster designation antigens in the prostate. *BMC Genomics*, 9(1):246, 2008.

[85] L Patrawala, T Calhoun, R Schneider-Broussard, H Li, B Bhatia, S Tang, J G Reilly, D Chandra, J Zhou, K Claypool, L Coghlan, and D G Tang. Highly purified CD44+ prostate cancer cells from xenograft human tumors are enriched in tumorigenic and metastatic progenitor cells. *Oncogene*, 25(12):1696–1708, 2006.

[86] L Patrawala, T Calhoun, R Schneider-Broussard, H Li, B Bhatia, S Tang, J G Reilly, D Chandra, J Zhou, K Claypool, L Coghlan,

and D G Tang. Highly purified CD44+ prostate cancer cells from xenograft human tumors are enriched in tumorigenic and metastatic progenitor cells. *Oncogene*, 25(12):1696–1708, 2006.

[87] Lubna Patrawala, Tammy Calhoun-Davis, Robin Schneider-Broussard, and Dean G Tang. Hierarchical organization of prostate cancer cells in xenograft tumors: the CD44+alpha2beta1+ cell population is enriched in tumor-initiating cells. *Cancer Research*, 67(14):6796–6805, 2007.

[88] Lubna Patrawala, Tammy Calhoun-Davis, Robin Schneider-Broussard, and Dean G Tang. Hierarchical organization of prostate cancer cells in xenograft tumors: the CD44+alpha2beta1+ cell population is enriched in tumor-initiating cells. *Cancer Research*, 67(14):6796–6805, 2007.

[89] Lubna Patrawala, Tammy Calhoun-Davis, Robin Schneider-Broussard, and Dean G Tang. Hierarchical organization of prostate cancer cells in xenograft tumors: the CD44+alpha2beta1+ cell population is enriched in tumor-initiating cells. *Cancer Research*, 67(14):6796–6805, 2007.

[90] Héctor Peinado, David Olmeda, and Amparo Cano. Snail, Zeb and bHLH factors in tumour progression: an alliance against the epithelial phenotype? *Nature Reviews Cancer*, 7(6):415–428, 2007.

[91] A Peralta Soler, K A Knudsen, H Salazar, A C Han, and A A Keshgegian. P-cadherin expression in breast carcinoma indicates poor survival. *Cancer*, 86(7):1263–1272, 1999.

[92] N. Petkova, J. Hennenlotter, M. Sobiesiak, T. Todenhofer, M. Scharpf, A. Stenzl, H. J. Buhring, and C. Schwentner. Surface CD24 distinguishes between low differentiated and transit-amplifying cells in the basal layer of human prostate. *Prostate*, Jul 2013.

[93] M F Pittenger. Multilineage Potential of Adult Human Mesenchymal Stem Cells. *Science*, 284(5411):143–147, 1999. ISSN 00368075. doi: 10.1126/science.284.5411.143.

[94] Gavin D Richardson, Craig N Robson, Shona H Lang, David E Neal, Norman J Maitland, and Anne T Collins. CD133, a novel marker for human prostatic epithelial stem cells. *Journal of Cell Science*, 117(Pt 16):3539–3545, 2004.

[95] G David Roodman. Mechanisms of bone metastasis. *Discovery Medicine*, 4(8 Suppl):1546–1556, 2004.

[96] Sarah N Salm, Patricia E Burger, Sandra Coetzee, Ken Goto, David Moscatelli, and E Lynette Wilson. TGF-beta maintains

dormancy of prostatic stem cells in the proximal region of ducts. *The Journal of Cell Biology*, 170(1):81–90, 2005.

[97] M Schostak, H Krause, K Miller, M Schrader, S Weikert, F Christoph, C Kempkensteffen, and J Kollermann. Quantitative real-time RT-PCR of CD24 mRNA in the detection of prostate cancer. *BMC Urology*, 6:7, 2006.

[98] Seema Sethi, Jill Macoska, Wei Chen, and Fazlul H Sarkar. Molecular signature of epithelial-mesenchymal transition (EMT) in human prostate cancer bone metastasis. *American journal of translational research*, 3(1):90–99, 2010.

[99] Michael M Shen and Cory Abate-Shen. Molecular genetics of prostate cancer: new prospects for old challenges. *Genes & Development*, 24(18):1967–2000, 2010.

[100] D Sheppard. Epithelial integrins. *BioEssays*, 18(8):655–660 ST – Epithelial integrins, 1996. ISSN 02659247. doi: 10.1002/bies.950180809.

[101] M F Shi, J Jiao, W G Lu, F Ye, D Ma, Q G Dong, and X Xie. Identification of cancer stem cell-like cells from human epithelial ovarian carcinoma cell line. *Cellular and molecular life sciences CMLS*, 67(22):3915–3925, 2010.

[102] X. Shi, J. Gipp, and W. Bushman. Anchorage-independent culture maintains prostate stem cells. *Dev. Biol.*, 312(1):396–406, Dec 2007.

[103] Sabina Signoretti, David Waltregny, James Dilks, Beth Isaac, Douglas Lin, Levi Garraway, Annie Yang, Rodolfo Montironi, Frank McKeon, and Massimo Loda. p63 is a prostate basal cell marker and is required for prostate development. *The American journal of pathology*, 157(6):1769–1775, 2000.

[104] Sabina Signoretti, Maira M Pires, Meghan Lindauer, James W Horner, Chiara Grisanzio, Sonya Dhar, Pradip Majumder, Frank McKeon, Philip W Kantoff, William R Sellers, and Massimo Loda. p63 regulates commitment to the prostate cell lineage. *Proceedings of the National Academy of Sciences of the United States of America*, 102(32):11355–11360, 2005.

[105] Kavitha Sivasubramaniyan, Abhishek Harichandan, Susanne Schumann, Malgorzata Sobiesiak, Claudia Lengerke, Andreas Maurer, Hubert Kalbacher, and Hans-Jörg Bühring. Prospective Isolation of Mesenchymal Stem Cells from Human Bone Marrow Using Novel Antibodies Directed Against Sushi Domain Containing 2. *Stem cells and development*, 00(00), March 2013. ISSN 1557-8534. doi: 10.1089/scd.2012.0584.

[106] Eva Slabáková, Zuzana Pernicová, Eva Slavíčková, Andrea Staršíchová, Alois Kozubík, and Karel Souček. TGF-β1-induced EMT of non-transformed prostate hyperplasia cells is characterized by early induction of SNAI2/Slug. *The Prostate*, 71(12): 1332–1343, 2011. doi: 10.1002/pros.21350.

[107] Katherine E Sleeman, Howard Kendrick, Alan Ashworth, Clare M Isacke, and Matthew J Smalley. CD24 staining of mouse mammary gland cells defines luminal epithelial, myoepithelial/basal and non-epithelial cells. *Breast Cancer Research*, 8 (1):R7, 2006.

[108] P. Smith, N. P. Rhodes, Y. Ke, and C. S. Foster. Influence of the alpha1-adrenergic antagonist, doxazosin, on noradrenaline-induced modulation of cytoskeletal proteins in cultured hyperplastic prostatic stromal cells. *Prostate*, 38(3):216–227, Feb 1999.

[109] Verónica R Sobrado, Gema Moreno-Bueno, Eva Cubillo, Liam J Holt, M Angela Nieto, Francisco Portillo, and Amparo Cano. The class I bHLH factors E2-2A and E2-2B regulate EMT. *Journal of Cell Science*, 122(Pt 7):1014–1024, 2009.

[110] A P Soler, G D Harner, K A Knudsen, F X McBrearty, E Grujic, H Salazar, A C Han, and A A Keshgegian. Expression of P-cadherin identifies prostate-specific-antigen-negative cells in epithelial tissues of male sexual accessory organs and in prostatic carcinomas. Implications for prostate cancer biology. *The American journal of pathology*, 151(2):471–478, 1997.

[111] Antonio Sorrentino, Manuela Ferracin, Germana Castelli, Mauro Biffoni, Giada Tomaselli, Marta Baiocchi, Alessandro Fatica, Massimo Negrini, Cesare Peschle, and Mauro Valtieri. Isolation and characterization of CD146+ multipotent mesenchymal stromal cells. *Experimental Hematology*, 36(8):1035–1046, 2008.

[112] Simone Spaderna, Otto Schmalhofer, Mandy Wahlbuhl, Arno Dimmler, Katja Bauer, Aneesa Sultan, Falk Hlubek, Andreas Jung, Dennis Strand, Andreas Eger, Thomas Kirchner, Jürgen Behrens, and Thomas Brabletz. The transcriptional repressor ZEB1 promotes metastasis and loss of cell polarity in cancer. *Cancer Research*, 68(2):537–544, 2008.

[113] T Springer, G Galfrè, D S Secher, and C Milstein. Monoclonal xenogeneic antibodies to murine cell surface antigens: identification of novel leukocyte differentiation antigens. *European Journal of Immunology*, 8(8):539–551, 1978.

[114] I Stefanová, V Horejsí, I J Ansotegui, W Knapp, and H Stockinger. GPI-anchored cell-surface molecules complexed to protein tyrosine kinases. *Science*, 254(5034):1016–1019, 1991.

[115] Delisha A Stewart, Carlton R Cooper, and Robert A Sikes. Changes in extracellular matrix (ECM) and ECM-associated proteins in the metastatic progression of prostate cancer. *Reproductive biology and endocrinology RBE*, 2(1):2, 2004.

[116] Yuting Sun, Bu-Er Wang, Kevin G Leong, Peng Yue, Li Li, Suchit Jhunjhunwala, Darrell Chen, Kyounghee Seo, Zora Modrusan, Wei-Qiang Gao, Jeffrey Settleman, and Leisa Johnson. Androgen Deprivation Causes Epithelial-Mesenchymal Transition in the Prostate: Implications for Androgen-Deprivation Therapy. *Cancer Research*, 72(2):527–536, 2012. ISSN 15387445. doi: 10.1158/0008-5472.CAN-11-3004.

[117] Shugo Suzuki, Satoru Takahashi, Seishiro Takahashi, Kentaro Takeshita, Atsuya Hikosaka, Toshiaki Wakita, Naoki Nishiyama, Tamio Fujita, Takehiko Okamura, and Tomoyuki Shirai. Selective expression of CD44, a putative prostate cancer stem cell marker, in neuroendocrine tumor cells of human prostate cancer. *The Prostate*, 66(7):787–798, 2006.

[118] M Takeichi. Cadherin cell adhesion receptors as a morphogenetic regulator. *Science*, 251(5000):1451–1455, 1991.

[119] Renea A Taylor, Roxanne Toivanen, Mark Frydenberg, John Pedersen, Laurence Harewood, Australian Prostate Cancer Bioresource, Anne T Collins, Norman J Maitland, and Gail P Risbridger. Human Epithelial Basal Cells Are Cells of Origin of Prostate Cancer, Independent of CD133 Status. *Stem cells Dayton Ohio*, 30(6):1087–96, 2012. ISSN 15494918. doi: 10.1002/stem.1094.

[120] Erik J Tokar, Brooke B Ancrile, Gerald R Cunha, and Mukta M Webber. Stem/progenitor and intermediate cell types and the origin of human prostate cancer. *Differentiation*, 73(9-10):463–473, 2005. ISSN 03014681. doi: 10.1111/j.1432-0436.2005.00047.x.

[121] H. Towbin, T. Staehelin, and J. Gordon. Electrophoretic transfer of proteins from polyacrylamide gels to nitrocellulose sheets: procedure and some applications. *Proc. Natl. Acad. Sci. U.S.A.*, 76(9):4350–4354, Sep 1979.

[122] Chau P Tran, Connie Lin, Joyce Yamashiro, and Robert E Reiter. Prostate stem cell antigen is a marker of late intermediate prostate epithelial cells. *Molecular cancer research MCR*, 1(2):113–121, 2002.

[123] Thuy T Truong, Kyle Huynh, Martin N Nakatsu, and Sophie X Deng. SSEA4 Is a Potential Negative Marker for the Enrichment of Human Corneal Epithelial Stem / Progenitor Cells. *Investigative Ophthalmology*, 52(9):1–6, 2011. ISSN 15525783. doi: 10.1167/iovs.11-7518.

[124] Akira Tsujimura, Yasuhiro Koikawa, Sarah Salm, Tetsuya Takao, Sandra Coetzee, David Moscatelli, Ellen Shapiro, Herbert Lepor, Tung-Tien Sun, and E Lynette Wilson. Proximal location of mouse prostate epithelial stem cells: a model of prostatic homeostasis. *The Journal of Cell Biology*, 157(7):1257–65, 2002. ISSN 00219525. doi: 10.1083/jcb.200202067.

[125] Sylvester Tumusiime, Manish K Rana, Swapnil S Kher, Vinodh B Kurella, Kelly A Williams, Jessie J Guidry, David K Worthylake, and Rebecca A Worthylake. CD24 induces localization of beta1 integrin to lipid raft domains. *Biochemical and Biophysical Research Communications*, 365(3):393–396, 2008.

[126] T S Udayakumar, D A Jeyaraj, M Rajalakshmi, and R S Sharma. Culture of prostate epithelial cells of the rhesus monkey on extracellular matrix substrate: influence of steroids and insulin-like growth factors. *The Journal of endocrinology*, 162(3):443–450, 1999.

[127] Aarti R Uzgare, Yi Xu, and John T Isaacs. In vitro culturing and characteristics of transit amplifying epithelial cells from human prostate tissue. *Journal of Cellular Biochemistry*, 91(1):196–205, 2004.

[128] Geert J L H Van Leenders and Jack A Schalken. Epithelial cell differentiation in the human prostate epithelium: implications for the pathogenesis and therapy of prostate cancer. *Critical reviews in oncologyhematology*, 46 Suppl:S3–S10, 2003.

[129] A P Verhagen, F C Ramaekers, T W Aalders, H E Schaafsma, F M Debruyne, and J A Schalken. Colocalization of basal and luminal cell-type cytokeratins in human prostate cancer. *Cancer Research*, 52(22):6182–6187, 1992.

[130] Xianhui Wang, Mingzhe Zheng, Gang Liu, Weiya Xia, Paula J McKeown-Longo, Mien-Chie Hung, and Jihe Zhao. Krüppel-like factor 8 induces epithelial to mesenchymal transition and epithelial cell invasion. *Cancer Research*, 67(15):7184–7193, 2007.

[131] S M Watt, H J Bühring, I Rappold, J Y Chan, J Lee-Prudhoe, T Jones, A C Zannettino, P J Simmons, R Doyonnas, D Sheer, and L H Butler. CD164, a novel sialomucin on CD34(+) and erythroid subsets, is located on human chromosome 6q21. *Blood*, 92(3):849–866, 1998.

[132] Chan JY Watt SM. CD164–a novel sialomucin on CD34+ cells. *Leuk Lymphoma*, 37(1-2):1–25, 2000.

[133] Kai-Yu Xu and Jin Gu. Expression of TROP2 mRNA in left-sided and right-sided colon cancer and its clinical significance. *Zhonghua wei chang wai ke za zhi Chinese journal of gastrointestinal surgery*, 12(3):285–289, 2009.

[134] Hidekazu Yamamoto, John R Masters, Prokar Dasgupta, Ashish Chandra, Rick Popert, Alex Freeman, and Aamir Ahmed. CD49f Is an Efficient Marker of Monolayer- and Spheroid Colony-Forming Cells of the Benign and Malignant Human Prostate. *PloS one*, 7(10):e46979, January 2012. ISSN 1932-6203. doi: 10.1371/journal.pone.0046979.

[135] Jing Yang and Robert A Weinberg. Epithelial-mesenchymal transition: at the crossroads of development and tumor metastasis. *Developmental Cell*, 14(6):818–829, 2008.

[136] M. Yao, R. A. Taylor, M. G. Richards, P. Sved, J. Wong, D. Eisinger, C. Xie, R. Salomon, G. P. Risbridger, and Q. Dong. Prostate-regenerating capacity of cultured human adult prostate epithelial cells. *Cells Tissues Organs (Print)*, 191 (3):203–212, 2010.

[137] Hisataka Yasuda, Nobuyuki Shima, Nobuaki Nakagawa, Kyoji Yamaguchi, Masahiko Kinosaki, Shin-ichi Mochizuki, Akihiro Tomoyasu, Kazuki Yano, Masaaki Goto, Akihiko Murakami, Eisuke Tsuda, Tomonori Morinaga, Kanji Higashio, Nobuyuki Udagawa, Naoyuki Takahashi, and Tatsuo Suda. Osteoclast differentiation factor is a ligand for osteoprotegerin/osteoclastogenesis-inhibitory factor and is identical to TRANCE/RANKL. *Proceedings of the National Academy of Sciences of the United States of America*, 95(7):3597–3602, 1998.

[138] Trevor M Yeung, Shaan C Gandhi, Jennifer L Wilding, Ruth Muschel, and Walter F Bodmer. Cancer stem cells from colorectal cancer-derived cell lines. *Proceedings of the National Academy of Sciences of the United States of America*, 107(8):3722–3727, 2010.

[139] J. Zhang, M. W. Hess, M. Thurnher, A. Hobisch, C. Radmayr, M. V. Cronauer, A. Hittmair, Z. Culig, G. Bartsch, and H. Klocker. Human prostatic smooth muscle cells in culture: estradiol enhances expression of smooth muscle cell-specific markers. *Prostate*, 30(2):117–129, Feb 1997.

[140] Y Zhang, J Wei, H Wang, X Xue, Y An, D Tang, Z Yuan, F Wang, J Wu, J Zhang, and Y Miao. Epithelial mesenchymal transition correlates with CD24+CD44+ and CD133+ cells in pancreatic

cancer. *Oncology Reports*, 27(5):1599–1605, 2012. ISSN 17912431. doi: 10.3892/or.2012.1681.

[141] Hongjuan Zhao and Donna M Peehl. Tumor-promoting phenotype of CD90hi prostate cancer-associated fibroblasts. *The Prostate*, 69(9):991–1000, 2009.

COLOPHON

This document was typeset using the typographical look-and-feel `classicthesis` developed by André Miede. The style was inspired by Robert Bringhurst's seminal book on typography "*The Elements of Typographic Style*". `classicthesis` is available for both LaTeX and LyX:

http://code.google.com/p/classicthesis/